UC Berkeley
UC Berkeley Electronic Theses and Dissertations

Title
Effective Field Theory Techniques for Resummation in Jet Physics

Permalink
https://escholarship.org/uc/item/9p7949fh

Author
Dunn, Nicholas Daniel

Publication Date
2012

Peer reviewed|Thesis/dissertation

eScholarship.org Powered by the California Digital Library
University of California

Effective Field Theory Techniques for Resummation in Jet Physics

by

Nicholas Daniel Dunn

A dissertation submitted in partial satisfaction of the

requirements for the degree of

Doctor of Philosophy

in

Physics

in the

Graduate Division

of the

University of California, Berkeley

Committee in charge:

Christian W. Bauer, Co-Chair

Professor Lawrence J. Hall, Co-Chair

Professor Yasunori Nomura

Professor Leo Blitz

Spring 2012

Effective Field Theory Techniques for Resummation in Jet Physics

Copyright 2012
by
Nicholas Daniel Dunn

Abstract

Effective Field Theory Techniques for Resummation in Jet Physics

by

Nicholas Daniel Dunn

Doctor of Philosophy in Physics

University of California, Berkeley

Christian W. Bauer, Co-Chair

Professor Lawrence J. Hall, Co-Chair

In this thesis, we present several new techniques for the resummation of observables relevant to jet physics at the LHC using effective field theory techniques. Specifically, we first derive the factorization theorem and calculate the generic soft function for N-jet threshold resummation. This allows for dynamic threshold resummation at hadron colliders, where parton distribution functions may enhance threshold effects. Then we develop a new metric to gauge the importance of threshold resummation in a process-independent manner. This also allows us to determine the relevant scales for threshold resummation without the introduction of an arbitrary procedure. Next, we present a new subtraction technique for the calculation of soft functions with complex phase space boundaries. This technique is especially useful in calculations involving $\eta - \phi$ jet algorithms, which are common at hadron colliders. Finally, we discuss a new regularization scheme for real emission diagrams and present an example of said scheme.

Chapter 1

Introduction

The goal of particle physics is to discover the fundamental particles of nature and accurately predict their interactions. In this endeavor, the Standard Model [103, 116, 74, 76, 99] has been phenomenally (and phenomenologically) successful. Experiments place strong limits on the possibility of substructure for the (current) list of fundamental particles, suggesting they may actually be nature's smallest building blocks. Similarly, every experiment to date is consistent with the $SU(3)_c \times SU(2)_L \times U(1)_Y$ gauge theory of particle interactions. Hundreds of precision measurements from several experiments around the globe done over dozens of years all confirm (or at the very least, do not disprove) that the Standard Model is indeed the correct theory of particle physics at currently accessible energies. For more details on current measurements constraining deviations from the Standard Model, see [98] and the references therein.

In spite of all this, we have very compelling reasons to believe that the Standard Model is not the whole story. It depends on the existence of at least one particle (the Higgs boson) that has not yet been observed (though this may change in the very near future). It does not provide an explanation for either dark matter or dark energy, both of which are experimental certainties at this juncture (see [102] for a review on dark matter and dark energy). There are also more aesthetic concerns. The so-called hierarchy problem [117], which stems from a desire for theoretical niceness rather than consistency with experimental evidence, drives much of our current research, both theoretically and experimentally.

Without any new physics, the Standard Model provides a consistent theory of particles an their interactions up to a scale of $\mathcal{O}(10^{18})$ GeV. However, as it stands this consistency is predicated upon cancellations between (potentially) unrelated quantities of 1 part per $\mathcal{O}(10^{32})$. New physics at the TeV scale could eliminate (or at the very least greatly reduce) this "unnatural" cancellation. New physics at the GeV scale would also work, but this has been experimentally excluded. Along with discovering the Standard Model's missing ingredient, experimentalist at the LHC hope to find new TeV-scale physics to solve the hierarchy problem.

The search for new physics at the LHC is complicated by the fact that other experiments have yet to find any evidence of discrepancy with the Standard Model (cosmological experiments providing evidence for dark matter and dark energy excepted). New physics events, if they are produced at all at the LHC, will be extremely rare. This leads us to two facts which have guided this research: First, that any new physics at the LHC will most likely be discovered in conjunction with one or more particles that are charged under $SU(3)_c$. Due to the nature of the experiment (proton-on-proton collisions), final states with strongly-interacting particles are produced at a much higher rate than color-neutral final states. This enhancement in production will almost certainly be necessary in order to distinguish new physics from Standard Model background. Second, that we need predictions that are both accurate and precise, in order to be sure we are seeing new physics, rather than simply misunderstanding the Standard Model.

1.1 Quantum Chromodynamics

Quantum Chromodynamics (QCD) is the theory of strongly-interacting or colored (hence the name) particles. It is an unbroken SU(3) Yang-Mills gauge theory with two major defining features: asymptotic freedom and confinement. Asymptotic freedom is the property that, at high energies, the theory tends towards non-interaction. The flip side of this, confinement, is the observation that at large distances (and therefore low energies) there are no particles charged under QCD. The is consistent with experimental evidence that the particles directly observed in detectors, protons, neutrons, pions, and kaons, are color-neutral, despite being composed of strongly-interacting quarks and gluons.

In terms of predictions for experiments such as the LHC, QCD presents a unique challenge. Calculations in 4D quantum field theory are generally done using perturbation theory. The theory is solved exactly in the limit of no interactions, and then perturbed around this limit. In the case of QCD, this is clearly useful in the high energy regime, where the coupling constant (the common measure of the strength of the interaction) is small, due to asymptotic freedom. However, in any real experiment, any strongly-interacting particles produced at high energies eventually must confine into color-neutral objects. As this process occurs, the theory enters the regime in which naive perturbation theory is no longer reliable. The goal of much current research in QCD is to provide a way of calculating observables relevant to current experiments that avoid this issue.

1.2 Jet Observables

An observable is some quantity calculated from information about the final state. A simple example is the number of electrons. This is theoretically easy to calculate,

since the emission of electrons in the Standard Model is perturbative (ignoring the contribution from decays). It's also fairly easy to measure (assuming any issues involving conversion of photons into electrons and vice-versa can be experimentally disentangled).

In QCD, an analogous observable, the number of pions, is much less straightforward. While it is still relatively easy to measure, it is effectively impossible to calculate. The hadronization of quarks and gluons into color-neutral hadrons involves the details of low energy QCD, where standard perturbative methods do not work. The question then becomes, what *can* we calculate?

To avoid the complications of confinement, we want to calculate observables that are completely (or mostly) determined by high energy dynamics, where the coupling constant of QCD is small. The most common way of doing this is to group final state hadrons into jets, usually with a jet algorithm. The goal of this is that the resulting jets will roughly correspond to the high energy partons (quarks and gluons) initially produced in the collision, such that corrections from the low energy evolution from partons into hadrons are small.

Once hadrons have been grouped into jets, one can calculate observables based on the jets, rather than their constituent hadrons. Building on our earlier example, the number of jets in the final state is both theoretically tractable (assuming a reasonable jet algorithm is used) and experimentally feasible.

Jet observables, however, come with their own set of issues. Take for example jet thrust, defined as

$$\tau_0 = \frac{1}{2E_{\text{jet}}} \sum_{i \in \text{jet}} n_{\text{jet}} \cdot p_i \,. \tag{1.1}$$

Here the sum is over all particles in the jet and $n_{\text{jet}} = (1, \mathbf{n}_{\text{jet}})$, where $\mathbf{n}_{\text{jet}}$ is the direction of the jet. Since the naive emission probability of a parton radiating energy goes like

$$\mathrm{P}_{\text{emission}}(p) \propto \frac{1}{n_{\text{parton}} \cdot p} \,, \tag{1.2}$$

there is a divergence in the perturbative cross section of the form

$$\frac{\mathrm{d}\sigma}{\mathrm{d}\tau_0} \sim \sum_{n=1}^{\infty} \alpha_{\mathrm{s}}^n \frac{\ln^{2n-1}\tau_0}{\tau_0} \,. \tag{1.3}$$

As $\tau_0 \to 0$, there is a region where $\alpha_{\mathrm{s}} \ln^2 \tau_0$ is $\mathcal{O}(1)$ and the perturbative expansion breaks down. This breakdown, along with naive divergence of the cross section, presents a problem for calculating this (and other) jet observables.

1.3 Resummation and the Effective Field Theory Approach

The solution to this problem is resummation. By re-expressing the cross section as an expansion in a different variable (in this case $\alpha_s \ln \tau_0$), we can restore perturbativity and perform a meaningful calculation. While there are several different techniques for resummation in QCD (see [111] for a review of QCD resummation methods), in this thesis we will focus on effective field theory methods. Specifically, we will work in the framework of soft-collinear effective theory (SCET) [23, 25, 31, 30].

Using the definition of $n_{\rm jet}$ above, we can decompose a generic four-vector p into components given by

$$\begin{aligned} p &= \bar{n}_{\rm jet}\cdot p\,\frac{n_{\rm jet}}{2} + n_{\rm jet}\cdot p\,\frac{\bar{n}_{\rm jet}}{2} + p_\perp \\ &= (\bar{n}_{\rm jet}\cdot p, n_{\rm jet}\cdot p, p_\perp) = (p^-, p^+, p_\perp) \end{aligned} \tag{1.4}$$

Here, $\bar{n}_{\rm jet} = (1, -\mathbf{n}_{\rm jet})$ and $p_\perp$ is defined implicitly. In these coordinates, collinear momenta scale like

$$p_c \sim (1, \lambda^2, \lambda)\,, \tag{1.5}$$

while soft momenta have scaling given by

$$p_s \sim (\lambda^2, \lambda^2, \lambda^2)\,, \tag{1.6}$$

where λ^2 is taken to be some small number. In the example above, if we assume jet thrust to be small (say, $\mathcal{O}(\lambda^2)$), then at leading order in τ_0 these are the only allowed on-shell modes. SCET is approximation to QCD in the limit only soft and collinear modes are present, with λ as the relevant expansion parameter.

In order to make this expansion more formal, we first divide momenta p into two components

$$p = \widetilde{p} + k\,, \tag{1.7}$$

where $\widetilde{p}$ contains the $\mathcal{O}(1)$ and $\mathcal{O}(\lambda)$ parts of p, while the residual momentum k is strictly $\mathcal{O}(\lambda^2)$. We then divide the quark field $\psi(x)$ into collinear piece, $\psi_n(x)$ and a soft piece, $\psi_s(x)$ such that

$$\psi(x) = \psi_n(x) + \psi_s(x)\,. \tag{1.8}$$

We further redefine the collinear quark field

$$\psi_n(x) = \sum_{\widetilde{p}} e^{-i\widetilde{p}\cdot x}\psi_{n,p}\,. \tag{1.9}$$

The new field $\psi_{n,p}$ only contains residual momentum, such that derivatives ∂^μ acting on $\psi_{n,p}$ are $\mathcal{O}(\lambda^2)$. We can also separate the four-component spinor $\psi_{n,p}$ into two two-component using projection operators defined as

$$1 = \frac{\not{n}\bar{\not{n}}}{4} + \frac{\bar{\not{n}}\not{n}}{4} = P_n + P_{\bar{n}}\,. \tag{1.10}$$

The relevant two component spinors are then

$$\xi_{n,p} = P_n \psi_{n,p} \tag{1.11}$$
$$\xi_{\bar{n},p} = P_{\bar{n}} \psi_{n,p} \tag{1.12}$$

Writing the collinear quark Lagrangian in terms of these spinors gives

$$\mathcal{L}_\xi = \sum_{\widetilde{p},\widetilde{p}'} \Bigg[\bar{\xi}_{n,p'} \frac{\bar{\not{n}}}{2} \left(in\cdot D\right) \xi_{n,p} + \bar{\xi}_{\bar{n},p'} \frac{\not{n}}{2} \left(\bar{n}\cdot p + i\bar{n}\cdot D\right) \xi_{\bar{n},p} \tag{1.13}$$
$$+ \bar{\xi}_{n,p'} \left(\not{p}_\perp + i\not{D}_\perp\right) \xi_{\bar{n},p} + \bar{\xi}_{\bar{n},p'} \left(\not{p}_\perp + i\not{D}_\perp\right) \xi_{n,p} \Bigg]\,.$$

Because derivatives acting on $\xi_{n,p}$ and $\xi_{\bar{n},p}$ are suppressed in λ relative to label momenta, we can drop the derivatives from the second, third, and fourth terms, leaving.

$$\mathcal{L}_\xi = \sum_{\widetilde{p},\widetilde{p}'} \Bigg[\bar{\xi}_{n,p'} \frac{\bar{\not{n}}}{2} \left(in\cdot D\right) \xi_{n,p} + \bar{\xi}_{\bar{n},p'} \frac{\not{n}}{2} \left(\bar{n}\cdot p\right) \xi_{\bar{n},p} \tag{1.14}$$
$$+ \bar{\xi}_{n,p'} \left(\not{p}_\perp\right) \xi_{\bar{n},p} + \bar{\xi}_{\bar{n},p'} \left(\not{p}_\perp\right) \xi_{n,p} \Bigg]\,.$$

Clearly, at leading order in λ, $\xi_{\bar{n},p}$ is not a dynamical field and can be integrated out. Applying the equation of motion

$$\left(\bar{n}\cdot p + i\bar{n}\cdot D\right) \xi_{\bar{n},p} = \left(\not{p}_\perp + i\not{D}_\perp\right) \frac{\bar{n}}{2} \xi_{n,p}\,, \tag{1.15}$$

leaves

$$\mathcal{L}_\xi = \sum_{\widetilde{p},\widetilde{p}'} e^{-i(\widetilde{p}-\widetilde{p}')\cdot x} \bar{\xi}_{n,p'} \left[in\cdot D + \left(\not{p}_\perp + i\not{D}_\perp\right) \frac{1}{\bar{n}\cdot p + i\bar{n}\cdot D} \left(\not{p}_\perp + i\not{D}_\perp\right) \right] \frac{\bar{n}}{2} \xi_{n,p}\,. \tag{1.16}$$

At this point, it is useful to define an operator $\mathcal{P}$, such that

$$\mathcal{P}\xi_{n,p} = \widetilde{p}\,\xi_{n,p}\,. \tag{1.17}$$

We will also divide the gluon field $A(x)$ into soft and collinear components, such that

$$A(x) = A_n(x) + A_s(x)\,. \tag{1.18}$$

Using these definitions gives

$$\mathcal{L}_\xi = \bar{\xi}_n \left(in\cdot D + i\not{D}_\perp \frac{1}{i\bar{n}\cdot D} i\not{D}_\perp \right) \frac{\not{\bar{n}}}{2} \xi_n \,, \tag{1.19}$$

where we have absorbed $\mathcal{P}$ into D, used the equality

$$i\partial \sum_p e^{-ip\cdot x} \xi_{n,p} = e^{-i\mathcal{P}\cdot x} \left(\mathcal{P} + i\partial\right) \xi_n \,, \tag{1.20}$$

and omitted the phase factor $e^{-i\mathcal{P}\cdot x}$. Note that, at leading order in λ,

$$i\bar{n}\cdot\mathcal{D} = \bar{n}\cdot\mathcal{P} + g\,\bar{n}\cdot A_n \,. \tag{1.21}$$

If we now define the collinear Wilson line W_n as

$$W_n = \sum_{\text{permutations}} \exp\left(-g \frac{1}{\bar{n}\cdot\mathcal{P}} \bar{n}\cdot A_n \right) \,, \tag{1.22}$$

we can further simply the collinear quark Lagrangian to

$$\mathcal{L}_\xi = \bar{\xi}_n \left(in\cdot D + i\not{D}_\perp W_n^\dagger \frac{1}{i\bar{n}\cdot\mathcal{P}} W_n i\not{D}_\perp \right) \frac{\not{\bar{n}}}{2} \xi_n \tag{1.23}$$

A similar expansion can be done for the gluon Lagrangian. Since the derivation is identical, here we will just quote the result. Defining

$$i\mathcal{D} = \mathcal{P} + gA_n + \frac{\bar{n}}{2}\left(in\cdot\partial + g\,n\cdot A_s\right) \tag{1.24}$$

and noting that, at leading order in λ, $iD = i\mathcal{D}$, we find that the collinear gluon Lagrangian is given by

$$\begin{aligned} \mathcal{L}_{A_n} =& \frac{1}{2g^2}\mathrm{Tr}\left([i\mathcal{D}, i\mathcal{D}]\right)^2 + \tau\,\mathrm{Tr}\left\{ \left(\left[\mathcal{P} + \frac{\bar{n}}{2}\left(in\cdot\partial + g\,n\cdot A_s\right), A_n \right] \right)^2 \right\} \\ &+ 2\,\mathrm{Tr}\left(\bar{c}_n \left[\left[\mathcal{P} + \frac{\bar{n}}{2}\left(in\cdot\partial + g\,n\cdot A_s\right), [i\mathcal{D}, c_n \right] \right] \right) \,. \end{aligned} \tag{1.25}$$

All together, at leading order in λ, the SCET Lagrangian can be written as

$$\mathcal{L}_{\text{SCET}} = \mathcal{L}_\xi + \mathcal{L}_{A_n} + \mathcal{L}_{\text{QCD}}^{\text{soft}} = \mathcal{L}_{\text{QCD}} + \mathcal{O}(\lambda) \,. \tag{1.26}$$

Here $\mathcal{L}_{\text{QCD}}^{\text{soft}}$ is the full QCD Lagrangian, but only containing soft quark and gluon fields.

It is important to note that in both $\mathcal{L}_\xi$ and $\mathcal{L}_{A_n}$, the soft gluon field A_s only appears in terms that go like $n\cdot A_s$. If we define the soft Wilson line Y as

$$Y(x) = \mathrm{P}\exp\left(ig \int_{-\infty}^{x} \mathrm{d}s\, n\cdot A_s^a(ns) T^a \right) \tag{1.27}$$

we can make the field redefinitons

$$\xi_{n,p} = Y\,\xi^{(0)}_{n,p} \tag{1.28}$$

$$A_{n,p} = Y\,A^{(0)}_{n,p}\,Y^\dagger \tag{1.29}$$

$$c_{n,p} = Y\,c^{(0)}_{n,p}\,Y^\dagger\,, \tag{1.30}$$

and completely remove all interactions between soft and collinear modes at leading order. This is a defining feature of SCET.

By separating the various energy scales (Q for hard radiation, $Q\lambda$ for collinear radiation, and $Q\lambda^2$ for soft radiation), the effective theory allows us to simplify the calculation by working with the only the degrees of freedom relevant at each scale. Resummation then naturally arises as a consequence of renormalization group evolution between the various scales.

This thesis is organized as follows. In Chapter 2, we will explore threshold resummation, which is necessary in situations where the mass of a produced particle is near the limit allowed by the experiment. We will derive the form of the general threshold soft function in SCET, which is applicable not only in traditional threshold situations (hadronic threshold), but also when some other factor is forcing additional radiation to be suppressed (partonic threshold). In Chapter 3, we develop a useful metric to determine when dynamic threshold resummation is necessary in the case of proton-(anti-)proton collisions. This metric depends only on the form of the parton distribution functions (pdfs) and the mass of the produced object and is independent of the dynamics of the interaction. In Chapter 4, we present a method that allows us to calculate the soft function for a wide range of jet observables and algorithms. This extends previous work, which was restricted to a small class of jet algorithms. In Chapter 5, we discuss some calculational techniques for observables that are not symmetric about the jet access. Finally, in Chapter 6 we conclude. Note that some of this work has been presented previously in [19, 20, 21].

Chapter 2

The Soft Function for Threshold Resummation

2.1 Introduction

Explicit applications of factorization theorems for processes at hadron colliders near the hadronic endpoint have largely focused on simple final states with either no jets (e.g., Drell-Yan) or one inclusive jet (e.g., deep inelastic scattering and prompt photon production). Factorization for the former type of process gives rise to a soft function that depends on timelike momenta, whereas the soft function for the latter type depends on null momenta. Here, we derive in soft-collinear effective theory a factorization theorem that allows for an arbitrary number of jets, where the jets are defined with respect to a jet algorithm, together with any number of non-strongly interacting particles. We find that the soft function in general depends on the null components of the soft momenta inside the jets and on a timelike component of the soft momentum outside of all jets. This generalizes and interpolates between the soft functions for the cases of no jets and one inclusive jet. We verify consistency of our factorization theorem to $\mathcal{O}(\alpha_s)$ for any number of jets. While we demonstrate consistency only near the hadronic endpoint, we keep the kinematics general enough (in particular allowing for nonzero boost) to allow for an extension to partonic threshold resummation away from the hadronic endpoint.

Factorization of cross sections is the basis of every theoretical prediction at hadron colliders. In its simplest form, factorization states the measured hadronic cross section σ can be obtained by convolving a perturbatively calculable cross section $\hat{\sigma}$ with nonperturbative parton distribution functions (pdfs) [60, 56],

$$\sigma = f \otimes f \otimes \hat{\sigma}\,. \tag{2.1}$$

The pdfs are universal, and can therefore be extracted from one process and used to make predictions in another. Moreover, $\hat{\sigma}$ will in general depend on a hard scale Q

(for example, the partonic center-of-mass energy $\sqrt{\hat{s}}$), while the pdfs depend on the scale at which they are measured, say Q_0. The evolution of the pdfs between these two scales resums logarithms of Q/Q_0. This basic paradigm illustrates the two main uses of factorization: separation of universal, nonperturbative contributions to a cross section from perturbatively calculable contributions, and resummation of logarithms of ratios of scales to which each contribution is sensitive.

When $\hat{\sigma}$ depends only on a single scale, Equation (2.1) is the end of the story. The situation is more involved when $\hat{\sigma}$ itself depends on multiple, widely disparate scales. For example, in many collider physics processes involving jets, $\hat{\sigma}$ can depend on mass scales associated with the jets such as M_J, hard scales like $\sqrt{\hat{s}}$, and seesaw scales like $M_J^2/\sqrt{\hat{s}}$. In such cases large logarithms of ratios of these scales can spoil the convergence of the fixed order perturbative expansion of $\hat{\sigma}$. One must further factorize $\hat{\sigma}$ in order to resum these large logarithms and, perhaps, to separate out any other nonperturbative physics that is not captured in the pdfs [57, 58, 87, 86]. The general structure of resummation, at the level of next-to-leading logarithms, has been previously investigated in [42].

In this section we will focus on so-called threshold logarithms. When a process approaches its kinematical threshold, there is limited phase space available for radiation. This gives rise to an incomplete cancellation between real and virtual diagrams, resulting in large logarithmic terms. This is common in situations where the invariant mass of the final state is near the maximum available energy, which limits the amount of energy that can go into excess radiation. Examples of this type of resummation can be found for Drell-Yan, deep-inelastic scattering (DIS), B meson decay, and top production [6, 110, 109, 48, 49, 61, 41, 69, 88, 91, 4, 40, 86, 94, 23, 95, 34, 53]. It has been suggested [13, 51] that a similar effect occurs at hadron colliders away from hadronic endpoint due to the steepness of parton luminosities, and this effect was explored more quantitatively in [35]. In this section, we will concentrate on hadronic threshold and assume that the invariant mass of the final state is near the maximum allowed by the collider. However, we will derive a factorization theorem that can be applied away from hadronic threshold without loss of information.

An extremely useful tool to prove factorization is effective field theory. In the case of jet physics, soft-collinear effective theory [23, 25, 31, 30] is the relevant effective field theory that can be used to derive factorization in many hard scattering processes [24]. The SCET Lagrangian is constructed by integrating out all modes of QCD except for soft modes and collinear modes with respect to some fixed number of directions n_i. Matching QCD onto SCET gives rise to a hard function that contains the physics of the hard scales in the problem, and matrix elements of the remaining soft and collinear fields give rise to soft and jet functions, respectively.

The first applications of SCET involved cases with particularly simple jet definitions, such as in Drell-Yan [82, 35] where there are no jets, hemisphere jets in event shapes [29, 27, 92, 93, 70, 105, 71, 22, 36, 81, 80], or completely inclusive jets as in $B \to X_s\gamma$ [23], DIS [95, 34, 53], and prompt photon production [37]. Factoriza-

tion of jets defined with more generic algorithms was considered in [26] and two-jet rates defined with jet algorithms were computed using SCET in [27, 115, 54]. A study of various different jet algorithms and the dependence on the jet parameters in the framework of SCET was discussed in [54]. More recently, an NLL analysis of jet shapes in multijet events using modern jet algorithms in e^+e^- collisions was performed in [65, 66].

The goal of this section is to derive a factorization formula for an arbitrary number of jets in the presence of any number of non-strongly interacting particles in the threshold limit. We allow for a nonzero total rapidity and calculate the ingredients of this formula to allow resummation of threshold logarithms at NLL accuracy. This is conceptually distinct from the case of a single final state jet, which can be measured indirectly by simply demanding that a non-strongly interacting particle is produced with nonzero p_{T}. When there is more than one final state jet, jet algorithms must be used to identify jets, and so the technology of incorporating jet algorithms into a factorization formula, developed in [26] and applied to e^+e^- collisions in [66, 65], must be employed. The consistency of this factorization (that is, the fact that the cross section is independent of the factorization scale μ) is only demonstrated here in the true hadronic endpoint. However, we will show in Chapter 3 that, under the correct conditions, this factorization is consistent away from hadronic threshold..

Throughout this thesis, we will assume that Glauber modes do not contribute at leading order in the power counting. This cancellation has only been formally proven at the level of cross sections for simple processes, e.g. [59]. While Glauber modes could potentially spoil our factorization theorem, we assume that for sufficiently inclusive observables the argument in [59] generalizes. We also assume that pdfs can always be factorized from the partonic cross section, i.e. that

$$\frac{\mathrm{d}\sigma}{\mathrm{d}\mathcal{O}} = f \otimes f \otimes \frac{\mathrm{d}\hat{\sigma}}{\mathrm{d}\mathcal{O}}\,. \tag{2.2}$$

is always valid. This has also not been proven to be generically true, but is phenomenologically valid for a wide range of observables.

The organization of this section is as follows. In Section 2.2, we define precisely what we mean by threshold production of N jets and discuss the corresponding kinematics. In Section 2.3, we discuss how the definition of threshold affects the logarithmic structure of the result and how, in particular, our definition should not introduce so-called non-global logarithms. In Section 2.4, we briefly discuss different classes of jet algorithms used at hadron colliders. We then derive our factorization theorem in Section 2.5, beginning for notational simplicity with the case of a single (quark or gluon) final state jet, then extending these results to the case of N jets. We derive the anomalous dimensions for the objects that appear in our N-jet factorization formula in Section 2.6 and use these in Section 2.7 to show that our factorization theorem is formally consistent, at least in the hadronic endpoint region.

2.2 Kinematics of Threshold Resummation

To explain our approach to threshold resummation, how it includes both the cases of Drell-Yan and direct gauge boson production as limiting cases, and how it is extendable to arbitrary N-jet production, we first discuss the kinematics. By demanding that the final state contains N jets each with fixed transverse momentum $p_{\rm T}$ and pseudorapidity η, together with some number of non-strongly interacting particles with total 4-momentum q, we are requiring that there is a minimum partonic center-of-mass energy

$$\hat{s}_{\rm min} = \left(q + \sum_i^N p_J^i\right)^2 , \tag{2.3}$$

where p_J^i is the momentum of the ith jet. This momentum is defined in terms of the $p_J^{\rm T}$ and η_J of the jet as

$$p_J \equiv (p_J^{\rm T} \cosh\eta_J, \mathbf{p}_J^{\rm T}, p_J^{\rm T} \sinh\eta_J) . \tag{2.4}$$

Of course, the actual partonic center-of-mass energy $\hat{s}$ typically exceeds this minimum value, and in general can be as large as the available machine center-of-mass energy s. Therefore, the dimensionless variable z, defined as

$$z \equiv \frac{\hat{s}_{\rm min}}{\hat{s}} , \tag{2.5}$$

can range from

$$\tau \leq z \leq 1 , \qquad \text{with} \qquad \tau \equiv \frac{\hat{s}_{\rm min}}{s} . \tag{2.6}$$

Going to hadronic threshold ($\tau \to 1$) forces $z \to 1$, such that the only emissions kinematically allowed are collinear radiation off the hard partons that form jets, as well as soft radiation. Radiation collinear to one of the jets with momentum scaling as $E_{\rm cm}(1, \lambda^2, \lambda)$ (in the light-cone coordinates of the jet) and soft radiation scaling as $E_{\rm cm}(\lambda^2, \lambda^2, \lambda^2)$, each contribute an equal amount to $\hat{s}$, where $\lambda \sim \sqrt{1-z}$ is a small, dimensionless parameter. In this limit of restricted radiation, partonic momentum conservation can be written as

$$p_I = q + k_s + \sum_i^N p_c^i , \tag{2.7}$$

where p_I is the total initial-state (partonic) momentum, k_s is the total soft momentum, and p_c^i is the momentum carried by collinear fields in the direction of jet i. The total momentum can be separated into two components: the first is the minimum momentum needed to create N jets of fixed $p_{\rm T}$ and η together with the non-strongly interacting particles of total momentum q, while the second brings the invariant mass of the final state above its minimum value $\hat{s}_{\rm min}$. To do this, we note that an arbitrary

four-vector p can be written as the sum of a massless four-vector which characterizes the transverse momentum and pseudorapidity of p and a purely timelike four-vector with a magnitude equal to the +-component of p in light-cone coordinates about $n = (1, \mathbf{p}/|\mathbf{p}|)$ (i.e., $p^+ \equiv p^0 - |\mathbf{p}|$), which characterizes the off-shellness of p. That is, for any four-vector p, we can write

$$p^\mu = p_J^\mu + p^+ v^\mu \,, \tag{2.8}$$

where $v^\mu = (1, \mathbf{0})$ and p_J is given in Equation (2.4) with p_J^{T} and η_J the transverse momentum and pseudorapidity of p, respectively. We want to apply this relation to the total 4-momentum in each of the jets. To do this, we note that the jet algorithm will group some of the soft momentum k_s into parts that belong to jet i, k_i, and a part that is not included in any of the jets, k_{out},

$$k_s = \sum_i^N k_i + k_{\mathrm{out}} \,. \tag{2.9}$$

Using this together with the relation Equation (2.8) and the fact that

$$(p_c^i + k_i)^+ \equiv p_c^{i,0} + k_i^0 - |\mathbf{p}_c^i + \mathbf{k}_i| = p_c^{i+} + k_i^+ + \mathcal{O}(\lambda^4) \,, \tag{2.10}$$

where on the right-hand side, k_i^+ is plus with respect to p_J and p_c^{i+} is plus with respect to p_c, we can write momentum conservation Equation (2.7) at leading order in λ as

$$p_I^\mu = q^\mu + k_{\mathrm{out}}^\mu + \sum_i^N p_J^\mu + v^\mu \Big[\sum_i^N (p_i^+ + k_i^+) \Big] \,. \tag{2.11}$$

Here, we have also used that out-of-jet collinear radiation is power suppressed [66].

Given these definitions, we can write

$$\begin{aligned} 1 - z &= \frac{2}{\hat{s}} p_I \cdot \left(k_{\mathrm{out}} + v \Big[\sum_i^N (p_i^+ + k_i^+) \Big] \right) + \mathcal{O}(\lambda^4) \\ &= \frac{2}{\hat{s}} \Big(p_I \cdot k_{\mathrm{out}} + p_I^0 \sum_i^N (p_i^+ + k_i^+) \Big) + \mathcal{O}(\lambda^4) \,, \end{aligned} \tag{2.12}$$

where $\hat{s} = p_I^2$. We see that since p_I is timelike, $1 - z$ depends on the timelike component of the soft momentum outside of the jets and on the null component of the momentum within the jets.

So far, we have discussed the kinematics in the hadronic endpoint defined as $\tau \to 1$, which is the main focus of this paper. However, z can be forced close to 1 not only in this hadronic endpoint, but also in the limit of steeply falling parton luminosities. In this case, final states with small values of $\hat{s}$ are preferred, giving again $z \to 1$. Our

analysis is independent of the precise mechanism which guarantees that $1-z$ can be regarded as a small quantity, and can therefore be used away from the true hadronic endpoint.

We are now in a position to discuss how our parametrization of $1-z$ reduces to the standard variable in the case of Drell-Yan and cases when there is one inclusive jet, such as $B \to X_s\gamma$, DIS, and direct gauge boson production. As we will see in Section 2.5, Equation (2.12) implies the soft function in general depends on the timelike component of k_{out} and on the null components (with respect to the corresponding jet directions) of the soft momenta in each of the jets k_i. In Drell-Yan, there are no jets in the final state and so the entire soft momentum k_s is just k_{out}. This is why the soft function in Drell-Yan depends only on the timelike component of the total soft momentum. For a single inclusive jet (i.e., defined with a jet algorithm that includes all of the hadronic momentum), all the soft momentum is included in the jet, such that $k_s = k_1$. This explains why the soft function in this latter type of process only depends on the null component of the total soft momentum. In Ref. [86], on the other hand, threshold resummation for dijet production was considered and it was found that the soft function only depended on the timelike component of momentum outside of the jets. This apparent discrepancy is due to the fact that the limit of small jet size $R \to 0$ was taken and the contribution of in-jet soft particles vanishes in this limit.[1] From the discussion above, the soft function will have dependence on the null component of in-jet momentum for jets of finite size.

2.3 Non-global Logarithms and Our Definition of Threshold

In Ref. [86], two definitions of z were defined for the case of two final state jets, which we denote here as z_a and z_b,

$$\begin{aligned} z_a &\equiv \frac{(p_1+p_2)^2}{\hat{s}} \\ z_b &\equiv \frac{2p_1\cdot p_2}{\hat{s}}\,, \end{aligned} \tag{2.13}$$

where $p_{1,2}$ are the *total* 4-momenta of the jets . Note that, unlike p_J (cf. Equation (2.4)), $p_{1,2}$ can not be defined by the jet direction and energy alone, so both definitions of z are indirectly sensitive to the jet mass. To lowest order, $1-z_{a,b}$ can

[1] Note that double counting is avoided in [86] by removing collinear modes from the soft function ("eikonal subtractions"), which, for $R \sim \lambda$, removes any dependence on the soft momentum inside of jets, at leading order in the power counting.

be written as

$$1 - z_a = \frac{2k^0_{\text{out}}}{M_{JJ}} + \mathcal{O}(\lambda^4)$$
$$1 - z_b = \frac{2k^0_{\text{out}}}{M_{JJ}} + \frac{p_1^2 + p_2^2}{M_{JJ}^2} + \mathcal{O}(\lambda^4)\,, \tag{2.14}$$

where on the right-hand side, M_{JJ}^2 can be set to $(p_1 + p_2)^2$ for both $z_{a,b}$ to order λ^4.

It is well-known that jet observables which have an energy scale of radiation inside of a jet that is widely disparate from the scale outside the jet give rise to non-global logarithms [62]. This is due to the fact that in this case, real emission corrections to radiation inside the jet can be vetoed when one of the daughter particles escapes the jet, and this leads to an incomplete cancellation of real and virtual corrections, an effect which is stronger for radiation near the jet boundary (the so-called "buffer region"). As has been pointed out in the literature (see, e.g., Ref. [17]), z_a introduces non-global logarithms, whereas z_b does not. This is clear because the limit $1 - z_a \ll 1$ only restricts radiation outside of the jet and, for a jet size $R \sim 1$, the radiation within the jet is not restricted in the hadronic endpoint $\tau \to 1$. On the other hand, the scaling of in-jet and out-of-jet radiation is correlated with z_b (in particular, in both cases soft radiation has momentum components that scale as $M_{JJ}(1 - z_b)$) such that no non-global logarithms should arise.

Notice that for a two-jet final state in the hadronic endpoint ($\tau \to 1$), the definition of z given in Equation (2.5) reduces to

$$1 - z \xrightarrow{\tau \to 1} \frac{2k^0_{\text{out}}}{M_{JJ}} + 2\frac{p_1^2 + p_2^2}{M_{JJ}^2} + \mathcal{O}(\lambda^4)\,, \tag{2.15}$$

where we used Equation (2.12) and that, to $\mathcal{O}(\lambda^2)$, $p_I = (\sqrt{\hat{s}}, \mathbf{0}) = (M_{JJ}, \mathbf{0})$ in the $\tau \to 1$ limit. Thus, our definition of z restricts radiation both inside and outside of the jet, similarly to z_b in this limit and should correspondingly not introduce non-global logarithms for $R \sim 1$. (This is also clear directly from Equation (2.12) which is valid away from the hadronic endpoint, provided another mechanism enforces $1 - z \ll 1$, such as the steepness of pdfs.)

2.4 Jet Algorithms at Hadron Colliders

Perturbative calculations require a precise definition of the phase space boundaries imposed by the jet algorithms. Any jet algorithms needs to be infrared safe; otherwise, it leads to infrared divergent results when calculated in perturbation theory. There are two general types of jet algorithms: cone algorithms and cluster algorithms. Cone algorithms decide on which particles belong to a given jet based on cones of fixed size R, while cluster algorithms group particles together into jets based on a relative

measure of their distance. These jet algorithms act on the entire set of particles in the final state to decide how many jets are contained in a given event and which particles belong to which jet. Almost all jet algorithms depend on a jet size R, and a distance $\Delta\mathcal{R}_{ij}$ that measures the distance between two particles in $\eta - \phi$ space

$$\Delta\mathcal{R}_{ij} = \sqrt{(\Delta\eta_{ij})^2 + (\Delta\phi_{ij})^2}\,. \tag{2.16}$$

As discussed in the previous section, the relevant degrees of freedom in jet production close to $z = 1$ are collinear and soft particles. To perform perturbative calculations in this region we therefore need a restriction on these degrees of freedom to decide whether they belong to a given jet or not. Collinear particles in a given direction all belong to the same jet. This is in contrast with soft particles, which can either belong to a jet or not. Note that the treatment of jet algorithms in SCET is only correct to leading order in the power counting parameter λ. Therefore, we assume that all jets have energy much in excess of their mass, and that all jets are widely separated.

Standard cone algorithms, such as SISCone, are quite simple. The restrictions they impose on each particle to belong to a given jet are independent of other particles in the event, and only depend on the angular distance from the jet direction. The restriction for both soft and collinear particles to be in a jet j with direction n is therefore

$$\hat{\Theta}^R_{\text{soft},j} = \hat{\Theta}^R_{\text{coll},j} = \prod_i \Theta(\Delta\mathcal{R}_{i,n} < R)\,. \tag{2.17}$$

For the purposes of this paper, we only need results at relative order α_s, and therefore only have to consider one extra particle in the final state. The restrictions therefore simplify, and for the extra particle i we can write

$$\hat{\Theta}^R_{\text{soft},j} = \hat{\Theta}^R_{\text{coll},j} = \Theta(\Delta\mathcal{R}_{i,n} < R)\,. \tag{2.18}$$

Cluster algorithms iterate a process of calculating a distance measure d_{ij} for all pairs of particles and a distance d_i for each jet and, if a d_i is smallest, removing particle i, or, if a d_{ij} is smallest, merging jets i and j. In general , d_{ij} is defined as $d_{ij} = \min\{d_i, d_j\}\Delta\mathcal{R}_{ij}/D$, where D is a fixed parameter that characterizes the size of a jet and the precise definition of d_i depends on the choice of algorithm.[2] This makes the action of the jet algorithm considerably more complicated. As explained above, all collinear particles in a given direction have to end up in the same jet, which allows us to write a generic restriction for the action of a cluster algorithm on a set of collinear particles in a given direction as

$$\hat{\Theta}^R_{\text{coll},j} = \prod_{k=0}^{N-1} \Theta(\Delta\mathcal{R}^{N-k}_{\min} < R)\,. \tag{2.19}$$

[2] An example for such a distance measure is $d_i = p_{\text{T}}^i$ for the k_{T} algorithm.

Here, N denotes the total number of collinear particles in the direction of the jet n_j. $\Delta\mathcal{R}_{\min}^{N-k}$ denotes the $\Delta\mathcal{R}_{ij}$ between the pair of collinear particles in the set of $N-k$ remaining particles with the smallest d_{ij}. For soft particles, such a generic formula is not possible (at least analytically), since different soft particles can end up in different jets, and the restriction on a given particle depends on all other soft particles in the event. At relative order α_s, however, the restrictions Θ_i^R for cluster algorithms simplify and are given by

$$\hat{\Theta}_{\text{soft},j}^R = \Theta(\Delta\mathcal{R}_{i,n} < R) \tag{2.20}$$

for soft particles and by

$$\hat{\Theta}_{\text{coll},j}^R = \Theta(\Delta\mathcal{R}_{k,l} < R) \tag{2.21}$$

for collinear particles, where k and l label the new particles after the collinear splitting. For more information about jet algorithms in SCET, see [66].

2.5 N-Jet Factorization Theorem

In this section, we present the factorization theorem for the cross section to produce N jets, defined with respect to a jet algorithm, differential in the 3-momentum (p_{T} and pseudorapidity η) of each jet and of the non-strongly interacting particles. To keep the notation simple, we begin in Section 2.5.1 by discussing the case of a single jet produced via the channel $q\bar{q} \to g$. We then discuss the differences between this derivation and the one needed for the channel $qg \to q$. It will be clear from these derivations that, aside from the promotion of the hard and soft functions to matrices which arise from mixing of operators in color space, there is nothing conceptually or technically new for arbitrary N-jet production in our approach. This allows us to generalize our results to the N-jet factorization formula in Section 2.5.2.

In writing down a factorization theorem, we first assume that we can match QCD onto operators in SCET containing $N+2$ distinct collinear fields. This is valid when a (direct or indirect) measurement constrains the final state to be N-jet like. In our case, this is ensured by the fact that we take the variable $1-z$ to be small, together with the assumption that the jets are well separated from each other and from the beams (with the latter requirement ensuring that the probability of initial-state collinear radiation to produce a jet is power suppressed relative to the probability of the jet arising from the hard interaction). Our derivation is agnostic as to the cause of $1-z \ll 1$, and in Chapter 3 we explore in greater detail in what regimes the steepness of parton luminosities allow the factorization theorem we derive here to be applied away from the hadronic endpoint. We will assume in this section that the reader has some familiarity with SCET. For details, we refer the reader to the original SCET literature [23, 25, 31, 30].

2.5.1 Case of a Single Jet

Working to leading order in the electroweak coupling constant, we first write the full theory matrix element mediating the partonic interaction as

$$\langle qX|O|P_1P_2\rangle = \sum_i M_i^{\alpha\beta\mu} T_{ab}^A \langle X|\bar{\psi}_a^\alpha \psi_b^\beta A_\mu^A|P_1P_2\rangle\,. \tag{2.22}$$

Here, $|q\rangle$ represents the non-strongly interacting final state of total momentum q, $|P_1\rangle$ and $|P_2\rangle$ are the incoming hadrons with the corresponding momentum, and $|X\rangle$ represents the hadronic final state. The index i labels Dirac structures. This equation defines the $M_i^{\alpha\beta\mu}$. Note that we have used the fact that there is only one color singlet in the decomposition of $3\otimes\bar{3}\otimes 8$.

In terms of M_i, the matching of QCD onto the fields of SCET takes the form

$$\begin{aligned} M_i^{\alpha\beta\mu}\mathcal{Q}^{\alpha\beta\mu}(x) &\equiv M_i^{\alpha\beta\mu}\big[\bar{\psi}_a^\alpha \psi_b^\beta A_\mu^A\big](x) \\ &= \sum_j M_j^{\alpha\beta\mu} \sum_{\{\tilde{p}\}} C_{ij}(\{\tilde{p}\}) e^{i(\tilde{p}_1+\tilde{p}_2-\tilde{p}_3)\cdot x}\big[(\bar{\chi}_{-\tilde{p}_1})_a^\alpha (\chi_{\tilde{p}_2})_b^\beta (B_{-\tilde{p}_3})_\mu^A\big](x)\,, \end{aligned} \tag{2.23}$$

where $\tilde{p}_i$ is the label momentum carried by the field. At tree level, we have

$$C_{ij}(\{\tilde{p}\}) = \delta_{ij}\,. \tag{2.24}$$

The matching condition in momentum space takes the form

$$\begin{aligned} M_i^{\alpha\beta\mu}\mathcal{Q}^{\alpha\beta\mu}(k) &\equiv M_i^{\alpha\beta\mu}\int \mathrm{d}^4x\, e^{-ik\cdot x}\mathcal{Q}^{\alpha\beta\mu}(x) \\ &= \sum_j M_j^{\alpha\beta\mu}\bigg(\prod_{i=1}^3 \int \!\!\!\!\!\!- \,\mathrm{d}^4p_i\bigg) C_{ij}(\{\tilde{p}\})\big[\bar{\chi}_b^\beta(-p_1)\,\chi_a^\alpha(p_2)\,B_\mu^A(-p_3)\big] \\ &\quad\times (2\pi)^4\delta^4(p_1+p_2-p_3-k)\,, \end{aligned} \tag{2.25}$$

where we turned the sums over labels and integrals over residual momenta into integrals over the full d^4p_i and used the shorthand notation

$$\int \!\!\!\!\!\!- \,\mathrm{d}^4p \equiv \int \frac{\mathrm{d}^4p}{(2\pi)^4}\,. \tag{2.26}$$

Using this matching condition, we can write the cross section differential in the jet pseudorapidity η_J and transverse momentum p_J^{T} as

$$\begin{aligned} \frac{\mathrm{d}\sigma}{\mathrm{d}^2p_J^{\mathrm{T}}\mathrm{d}\tanh\eta_J\mathrm{d}\Phi_q} &= \frac{1}{2E_{\mathrm{cm}}^2}\sum_X^{\text{rest.}} |\langle qX|O|P_1P_2\rangle|^2_{\text{spin avg.}}\delta(\eta_J-\eta(X))\delta^2(\mathbf{p}_J^{\mathrm{T}}-\mathbf{p}^{\mathrm{T}}(X)) \\ &\quad\times(2\pi)^4\delta^4(P_1+P_2-q-p_X) \end{aligned} \tag{2.27}$$

$$= \frac{1}{2E_{\rm cm}^2} \sum_X^{\rm rest.} \sum_{\substack{i,j,i',j',\\ \rm spin}} M_j^{\alpha\beta\mu} \overline{M}_{j'}^{\bar\beta\bar\alpha\bar\mu} \frac{T_{ab}^A T_{\bar b\bar a}^{\bar A}}{4C_A^2} \Big(\prod_{k=1}^{3} \int \not{\mathrm{d}}^4 p_k \not{\mathrm{d}}^4 p_k' \Big) C_{ij}(\{\tilde p_k\}) C_{i'j'}^*(\{\tilde p_k'\})$$
$$\times \langle P_1 P_2 | \bar\chi_{\bar b}^{\bar\beta}(p_2') \, \chi_{\bar a}^{\bar\alpha}(-p_1') B_{\bar\mu}^{\dagger \bar A}(-p_3') | X \rangle \langle X | \bar\chi_a^\alpha(-p_1) \, \chi_b^\beta(p_2) B_\mu^A(-p_3) | P_1 P_2 \rangle$$
$$\times \, \delta(\eta_J - \eta(X)) \delta^2(\mathbf{p}_J^\perp - \mathbf{p}^\perp(X)) \, (2\pi)^4 \delta^4(p_1 + p_2 - p_3 - q) \,. \tag{2.28}$$

Here, we defined $\mathrm{d}\Phi_q$ as the phase space measure of the m non-strongly interacting final-state particles,

$$\mathrm{d}\Phi_q \equiv \prod_k^m \frac{\not{\mathrm{d}}^3 q_k}{2E_k} \,, \tag{2.29}$$

where we have omitted symmetry factors coming from identical particles in Φ_q. The restriction on the sum over final states X ("rest.") is that they include exactly one jet as defined by the jet algorithm and the delta functions that fix $\eta(X)$ and $\mathbf{p}^{\rm T}(X)$ act on the part of X identified to be the jet, which we assume to be sufficiently separated from the beams such that contributions from collinear initial-state radiation are power suppressed. We also define $\overline{M} \equiv \gamma^0 M^\dagger \gamma^0$. To arrive at this equation, we used the hadronic momentum-conserving delta function in the first line to shift the operator $O^\dagger$ to the point x, applied the matching condition Equation (2.25), and then integrated over x which resulted in the partonic momentum-conserving delta function on the last line.

We can simplify Equation (2.27) using the following observations. First, we can use the BPS field redefinition [30] to decouple soft and collinear modes to $\mathcal{O}(\lambda^2)$,

$$\chi_n(x) \to Y_n(x) \chi_n(x) \tag{2.30a}$$
$$\bar\chi_n(x) \to \bar\chi_n(x) Y_n^\dagger(x) \tag{2.30b}$$
$$B_n(x) \to \mathcal{Y}_n(x) B_n(x) = Y_n^\dagger(x) B_n(x) Y_n(x) \,, \tag{2.30c}$$

where Y_n is a soft Wilson line, for which we adopt the conventions[3]

$$Y_n^{\rm in}(x) = P \, \exp\left[\mathrm{i} g_s \int_{-\infty}^0 \mathrm{d}s \, n \cdot A_s(x + sn) \right] , \tag{2.31a}$$

for an incoming particle (where P denotes path ordering) and

$$Y_n^{\rm out\,\dagger}(x) = P \exp\left[\mathrm{i} g_s \int_0^\infty \mathrm{d}s \, n \cdot A_s(x + s\, n) \right] , \tag{2.31b}$$

for an outgoing particle. In momentum space, the field redefinition in Equation (2.30) induces the shift $p_c \to p_c + k_s$, where k_s is the total soft momentum carried by the Wilson lines.

[3]For a discussion of the various conventions for incoming and outgoing Wilson lines and how they are related see, for example, Ref. [14]. There is also a nice discussion of how soft Wilson lines arise in the path integral formulation of SCET in Appendix C of Ref. [35].

Second, we can implement the restriction on the final state X that there is one jet at the operator level to all orders by using the jet algorithm operator $\hat{\Theta}_i^R$, defined in Section 2.4. This allows us to complete the sum over X and factorize the collinear and soft matrix elements from one another.

The final state collinear matrix element can be written as

$$\begin{aligned}\big\langle 0\big|B_\mu^{\dagger A}(-p_3')\,\hat{\Theta}^R_{\mathrm{coll},3}\delta(\eta_J-\hat{\eta})\delta^2(\mathbf{p}_J^{\mathrm{T}}-\hat{\mathbf{p}}^{\mathrm{T}})\,B_\nu^B(-p_3)\big|0\big\rangle = \\ -E_J(2\pi)^4\delta^4(p_3'-p_3)\delta^{AB}g_{\mu\nu}^{\perp 3}J_\omega^g(p_3)\,,\end{aligned} \tag{2.32}$$

which defines the gluon jet function $J_w^g(p)$. Integrating Equation (2.32) over the full p_3 and p_3', which contain integrals over residual momentum and sums over the labels ω and n_3 of the $B_\perp$ field, fixes the labels to be $n_3=(1,\mathbf{p}_J^{\mathrm{T}}/|\mathbf{p}_J^{\mathrm{T}}|\cosh\eta_J,\tanh\eta_J)$ and $\omega=2p_J^{\mathrm{T}}\cosh\eta_J$. The label "3" on $\hat{\Theta}_R^3$ and on $g_{\mu\nu}^{\perp 3}$ indicates these are defined with respect to the direction n_3 of the jet. Note that this jet function depends on the choice of the jet algorithm.

For an algorithm that is inclusive over collinear initial-state radiation, the initial-state collinear matrix elements give rise to pdfs from the relations [24, 26]

$$\begin{aligned}\int\!\!\!\!\!\!-\,\mathrm{d}^4p\int\!\!\!\!\!\!-\,\mathrm{d}^4p'\langle P|\bar{\chi}_{a'}^{\alpha'}(p')\chi_a^\alpha(p)|P\rangle_{\text{spin avg.}} &= E_{\mathrm{cm}}\delta_{aa'}\Big(\frac{\bar{n}\!\!\!/}{2}\Big)^{\alpha\alpha'}\int_0^1\mathrm{d}x\,f_q(x)\\ \int\!\!\!\!\!\!-\,\mathrm{d}^4p\int\!\!\!\!\!\!-\,\mathrm{d}^4p'\langle P|\chi_{a'}^{\alpha'}(-p')\bar{\chi}_a^{\alpha}(-p)|P\rangle_{\text{spin avg.}} &= E_{\mathrm{cm}}\delta_{aa'}\Big(\frac{n\!\!\!/}{2}\Big)^{\alpha'\alpha}\int_0^1\mathrm{d}x\,f_{\bar{q}}(x)\,,\end{aligned} \tag{2.33}$$

with $p_{1,2}$ set to $x_{1,2}E_{\mathrm{cm}}\frac{n_{1,2}}{2}=\frac{1}{2}\omega_{1,2}\,n_{1,2}$ (where $n_1\equiv n$ and $n_2\equiv\bar{n}$) and $p_{1,2}'=p_{1,2}$.

The color structure in the matrix elements Equations (2.32) and (2.33) leads to a trace over the color structure of the Wilson lines in the soft function. We can write the soft function in terms of the variables of interest k_{out} and k_3 (the out-of-jet and in-jet momenta) as

$$\begin{aligned}&\int\!\!\!\!\!\!-\,\mathrm{d}^4k_s S(k_s,\{n_i\}) = \\ &\quad\frac{1}{C_AC_F}\int\mathrm{d}^4k_s\big\langle 0\big|\overline{\mathrm{T}}\Big[Y_{n_2}^\dagger Y_{n_3}^\dagger T^A Y_{n_3}Y_{n_1}\Big]\delta^4(k_s^\mu-i\partial^\mu)\mathrm{T}\Big[Y_{n_1}^\dagger Y_{n_3}^\dagger T^A Y_{n_3}Y_{n_2}\Big]\big|0\big\rangle \\ &\quad=\int\mathrm{d}^4k_{\mathrm{out}}\,\mathrm{d}^4k_3\,S(k_{\mathrm{out}},k_3,\{n_i\})\,,\end{aligned} \tag{2.34}$$

where $\{n_i\}=\{n_q,n_{\bar{q}},n_g\}$ and T ($\overline{\mathrm{T}}$) denotes (anti-) time ordering. $S(k_{\mathrm{out}},k_3,\{n_i\})$ is then defined as

$$\begin{aligned}S(k_{\mathrm{out}},k_3,\{n_i\}) \equiv \frac{1}{C_AC_F}\big\langle 0\big|\overline{\mathrm{T}}\Big[Y_{n_2}^\dagger Y_{n_3}^\dagger T^A Y_{n_3}Y_{n_1}\Big]\delta^4(k_3-\hat{k}_3) \\ \times\,\delta^4(k_{\mathrm{out}}-\hat{k}_{\mathrm{out}})\mathrm{T}\Big[Y_{n_1}^\dagger Y_{n_3}^\dagger T^A Y_{n_3}Y_{n_2}\Big]\big|0\big\rangle\,,\end{aligned} \tag{2.35}$$

and it is understood that the replacement $k_s \to k_{\rm out} + k_3$ should be made wherever k_s appears. The operators $\hat{k}_{\rm out}$ and $\hat{k}_3$ are defined as

$$\begin{aligned}\hat{k}_3^\mu &\equiv \hat{\Theta}^R_{\rm soft,3} i\partial^\mu \\ \hat{k}_{\rm out}^\mu &\equiv \Big(1 - \hat{\Theta}^R_{\rm soft,3}\Big) i\partial^\mu \,. \end{aligned} \tag{2.36}$$

Finally, using that the spin- and color-averaged square of the Born matrix element M_B, $\overline{|M_B|^2}$, can be written in terms of M_i as

$$\begin{aligned}\overline{|M_B|^2} \equiv \frac{1}{4C_A^2}\sum_{\rm spin,color}|M_B|^2 &= -\frac{{\rm Tr}[T^A T^A]}{4C_A^2}\sum_{i,i'} M_i^{\alpha\beta\mu}\overline{M}_{i'}^{\bar\alpha\bar\beta\bar\mu}(p\!\!\!/_1)^{\alpha\bar\alpha}(p\!\!\!/_2)^{\bar\beta\beta} g^{\perp 3}_{\mu\bar\mu} \\ &= -\frac{C_F}{4C_A}\hat{s}\sum_{i,i'} M_i^{\alpha\beta\mu}\overline{M}_{i'}^{\bar\alpha\bar\beta\bar\mu}\Big(\frac{n\!\!\!/_1}{2}\Big)^{\alpha\bar\alpha}\Big(\frac{n\!\!\!/_2}{2}\Big)^{\bar\beta\beta} g^{\perp 3}_{\mu\bar\mu}\,, \end{aligned} \tag{2.37}$$

we see that the Dirac structure of the matrix elements in Equations (2.32) and (2.33) naturally gives rise to the Born cross section.

To simplify the notation, we define a hard function H which includes all perturbative corrections contained in the matching coefficients C_{ij} as

$$H(\{n_i,\omega_i\}) \equiv -\frac{\frac{C_F}{4C_A}\hat{s}\sum_{i,i',j,j'} C_{ij}(\{\tilde{p}_k\})C^*_{i'j'}(\{\tilde{p}_k\}) M_j^{\alpha\beta\mu}\overline{M}_{j'}^{\bar\beta\bar\alpha\bar\mu}\Big(\frac{n\!\!\!/_1}{2}\Big)^{\alpha\bar\alpha}\Big(\frac{n\!\!\!/_2}{2}\Big)^{\bar\beta\beta} g^{\perp 3}_{\mu\bar\mu}}{\overline{|M_B|^2}}\,, \tag{2.38}$$

where ω_i are the labels on the three collinear fields. H by definition is 1 to leading order in α_s. Putting this together, we arrive at the expression

$$\begin{aligned}\frac{{\rm d}\sigma}{{\rm d}^2 p_J^{\rm T}{\rm d}\tanh\eta_J {\rm d}\Phi_q} = \frac{E_J}{2E_{\rm cm}^2}\int\frac{{\rm d}x_1}{x_1}\frac{{\rm d}x_2}{x_2}\overline{|M_B|^2}\int\!\!\!\!\!\!\not{\rm d}^4 p_3\int{\rm d}^4 k_{\rm out}\int{\rm d}^4 k_3 \\ \times H(\{n_i,\omega_i\}) f_q(x_1) f_{\bar q}(x_2) J^g_\omega(p_3) S_{q\bar q\to g}(k_{\rm out},k_3,\{n_i\}) \\ \times (2\pi)^4\delta^4\Big(x_1 E_{\rm cm}\frac{n}{2} + x_2 E_{\rm cm}\frac{\bar n}{2} - q - k_{\rm out} - p_3 - k_3\Big)\,. \end{aligned} \tag{2.39}$$

The final step is to simplify the momentum-conserving delta function. We use Equations (2.8) and (2.11) to write it, up to power corrections in λ, as

$$\begin{aligned}&\delta^4\Big(x_1 E_{\rm cm}\frac{n}{2} + x_2 E_{\rm cm}\frac{\bar n}{2} - q - k_{\rm out} - p_3 - k_3\Big) \\ &\quad= \frac{2}{E_{\rm cm}^2\tau}\delta\Big(1 - z - \frac{1}{\hat{s}}\Big[2p_I\cdot k_{\rm out} + 2p_I^0(p_c^+ + k_3^+)\Big]\Big) \\ &\qquad\times \delta^2(\mathbf{p}_J^{\rm T} + \mathbf{q}_J^{\rm T})\,\delta\bigg(Y - \tanh^{-1}\Big(\frac{p_J^{\rm T}\sinh\eta_J + q_z}{p_J^{\rm T}\cosh\eta_J + q_0}\Big)\bigg)\,, \end{aligned} \tag{2.40}$$

where p_I is the total (partonic) initial-state momentum, $p_I^0 = (x_1 + x_2)E_{\rm cm}/2$ and $p_I^z = (x_1 - x_2)E_{\rm cm}/2$. Here, we used that

$$\delta\big[f(x,y)\big]\delta\big[g(x,y)\big] = \frac{\delta(x-x_0)\delta(y-y_0)}{\left|\frac{\partial(f,g)}{\partial(x,y)}\right|}\,, \tag{2.41}$$

where $f(x_0,y_0) = g(x_0,y_0) = 0$ and made the change of variables

$$\begin{aligned} x_1 &= \sqrt{\frac{\tau}{z}}e^{Y} \\ x_2 &= \sqrt{\frac{\tau}{z}}e^{-Y}\,. \end{aligned} \tag{2.42}$$

In switching from $x_{1,2}$ to z and the total rapidity Y, we will also need that

$$\int \frac{\mathrm{d}x_1}{x_1}\frac{\mathrm{d}x_2}{x_2} = \int_\tau^1 \frac{\mathrm{d}z}{z}\int_{-\frac{1}{2}\ln\frac{z}{\tau}}^{\frac{1}{2}\ln\frac{z}{\tau}} \mathrm{d}Y\,. \tag{2.43}$$

Now, since there is no dependence on the soft momenta other than on the components $p_I\cdot k_{\rm out}$ and k_3^+ and the only unconstrained component of p_3 is the plus-component p_3^+, we can integrate over the other variables to obtain our final expression

$$\begin{aligned} \frac{\mathrm{d}\sigma}{\mathrm{d}^2p_J^{\rm T}\mathrm{d}\tanh\eta_J\mathrm{d}\Phi_q} = \frac{\pi}{E_{\rm cm}^4\tau}\int_\tau^1\mathrm{d}z\int_{-\frac{1}{2}\ln\frac{z}{\tau}}^{\frac{1}{2}\ln\frac{z}{\tau}}\mathrm{d}Y\,\overline{|M_B|^2}H_{q\bar q\to gX}(\{n_i,\omega_i\})f_q(x_1)f_{\bar q}(x_2) \\ \times\int\mathrm{d}p_3^+\,J_\omega^g(p_3^+)\int\mathrm{d}k_{\rm out}^0\int\mathrm{d}k_3^+\,S_{q\bar q\to g}(k_{\rm out}^0,k_3^+)\delta^2(\mathbf{p}_J^{\rm T}+\mathbf{q}^{\rm T}) \\ \times\delta\bigg(Y-\tanh^{-1}\bigg(\frac{p_J^{\rm T}\sinh\eta_J+q_z}{p_J^{\rm T}\cosh\eta_J+q_0}\bigg)\bigg) \\ \times\delta\left[1-z-\frac{2}{\sqrt{\hat s}}\Big(\cosh Y\big(p_c^+ + k_{\rm in}^+\big)+k_{\rm out}^0\Big)\right]\,. \end{aligned} \tag{2.44}$$

The soft function in Equation (2.44) is defined as

$$\begin{aligned} S_{q\bar q\to g}(k_{\rm out}^0,k_3^+,\{n_i\}) &\equiv \frac{1}{C_AC_F}\big\langle 0\big|\overline{\rm T}\Big[Y_{n_2}^\dagger Y_{n_3}^\dagger T^A Y_{n_3}Y_{n_1}\Big]\delta(k_3^+-\hat k_3^+)\delta\Big(k_{\rm out}^0-\frac{p_I\cdot\hat k_{\rm out}}{|p_I|}\Big) \\ &\qquad\times{\rm T}\Big[Y_{n_1}^\dagger Y_{n_3}^\dagger T^A Y_{n_3}Y_{n_2}\Big]\big|0\big\rangle \\ &= \delta(k_{\rm out}^0)\delta(k_3^+)+\mathcal{O}(\alpha_s)\,. \end{aligned} \tag{2.45}$$

Note that, despite our notation, $k_{\rm out}^0 \equiv p_I\cdot k_{\rm out}/|p_I|$ is simply the projection of the soft momentum outside of all jets onto a timelike vector. This function is most easily computed in the partonic center-of-mass frame where p_I is in fact purely timelike.

However, in general p_I will have nonzero spatial components, in which case $k^0_{\rm out}$ is not simply the energy component of the $k_{\rm out}$ four-vector. The jet function in Equation (2.44) is defined as

$$J^g_\omega(p^+) g_\perp^{\mu\nu}\delta^{AB} \equiv -\frac{\omega}{2\pi}\int \mathrm{d}^4x\, e^{ip\cdot x}\langle 0|B^{\mu,A}_{\perp,\omega}(x)\hat{\Theta}^R_{\rm coll,3}B^{\nu,B}_{\perp,\omega}(0)|0\rangle = \delta(p^+)g_\perp^{\mu\nu}\delta^{AB} + \mathcal{O}(\alpha_s)\,, \tag{2.46}$$

where, again, the label ω is set to $\omega = 2E_J = 2p^J_{\rm T}\cosh\eta_J$.

The majority of the above discussion goes through in much the same way for the channel $qg \to q$. The main differences are that the matrix element of final state fields gives rise to a quark jet function, defined by

$$\int \not{d}^4p_3'\,\big\langle 0\big|\chi^{c'}_{\alpha'}(p_3')\,\hat{\Theta}^R_{\rm coll,3}\delta(\eta_J-\hat{\eta})\delta^2(\mathbf{p}_J^{\rm T}-\hat{\mathbf{p}}^{\rm T})\bar{\chi}^c_\alpha(p_3)\big|0\big\rangle = \delta^{c'c}\Big(\frac{\not{n}_3}{2}\Big)_{\alpha'\alpha}J^q_\omega(p_3)\,, \tag{2.47}$$

which, after integrating over all but the p^+ component, becomes

$$J^q_\omega(p^+)\delta^{ab} \equiv \frac{1}{2\pi}\int \mathrm{d}^4x\, e^{ip\cdot x}\langle 0|\frac{\bar{\not{n}}}{2}\chi^a_{n,\omega}(x)\hat{\Theta}^R_{\rm coll,3}\bar{\chi}^b_{n,\omega}(0)|0\rangle = \delta(p^+)\delta^{ab} + \mathcal{O}(\alpha_s)\,. \tag{2.48}$$

For the initial-state gluon, we obtain the gluon pdf via the relation

$$\int \not{d}^4p\,\not{d}^4p'\langle P|B^{\dagger A}_\nu(p')B^B_\mu(p)|P\rangle = \frac{g^\perp_{\mu\nu}}{D-2}\delta_{AB}\int_0^1\frac{\mathrm{d}x}{x}f_g(x)\,. \tag{2.49}$$

Finally, the soft function is defined as in Equation (2.34) but with the appropriate modification in the definition of the Wilson lines for incoming and outgoing fields given in Equation (2.31). The final result after these differences are taken into account is of the form Equation (2.44) but with the substitutions $f_{\bar{q}} \to f_g$, $J^g \to J^q$, and $S_{q\bar{q}\to g} \to S_{qg\to q}$.

2.5.2 Extension to N Jets

The above results clearly generalize. The only nontrivial complication is due to mixing in color space. To avoid cumbersome notation, we will explain what generalizes and state the result rather than write down the N-jet derivation. Explicitly, for every quark, antiquark and gluon in the final (initial) state, the all-orders jet function (pdf) has precisely the Dirac and color structure to contract with the non-QCD matrix element $M_i^{\alpha\beta\cdots\mu\cdots}$ to give the Born matrix element at tree level. The pdfs and jet functions have the same definitions as in the single jet case. However, due to the fact that operators with different color structures in general mix, the hard and soft functions in these formulas should be interpreted as matrices in color space.

Since the main difference in the generalization to N jets is in the soft function, we will discuss it in more detail. It takes the general form

$$S(k^0_{\rm out},\{n_i,k_i^+\}) \equiv \frac{1}{\mathcal{N}}\langle 0|O_S^\dagger\,\delta\Big(k^0_{\rm out}-\frac{p_I\cdot\hat{k}_{\rm out}}{|p_I|}\Big)\prod_i^N\delta(k_i^+-\hat{k}_i^+)\,O_S|0\rangle\,, \tag{2.50}$$

where $\mathcal{N}$ is a normalization factor such that the soft function is unity (times delta functions in its arguments) at tree level and the operator O_S is the product of Wilson lines that arise from the BPS field redefinitions Equation (2.30), appropriately traced. As for the one jet case, the arguments k_i in the soft function run over all final state jets and the n_i include all directions, both initial and final. The operators $\hat{k}_{\rm out}$ and $\hat{k}_i$ that appear in Equation (2.50) are defined as

$$\begin{aligned}\hat{k}_i^\mu &\equiv \hat{\Theta}^R_{{\rm soft},i}\,i\partial^\mu\\ \hat{k}^\mu_{\rm out} &\equiv \Big(1-\sum_i^N\hat{\Theta}^R_{{\rm soft},i}\Big)i\partial^\mu\,.\end{aligned} \tag{2.51}$$

The result of going through the same steps as for the single jet case leads to the N-jet factorization formula,

$$\begin{aligned}\frac{{\rm d}\sigma}{\prod_i^N{\rm d}^2p_{J_i}^{\rm T}{\rm d}\tanh\eta_{J_i}{\rm d}\Phi_q} &= \frac{1}{E_{\rm cm}^4\tau}\int_\tau^1{\rm d}z\int_{-\frac{1}{2}\ln\frac{z}{\tau}}^{\frac{1}{2}\ln\frac{z}{\tau}}{\rm d}Y\,\overline{|M_B|^2}H(\{n_i,\omega_i\})f_1(x_1)f_2(x_2)\\ &\quad\times\prod_i^N\int\frac{{\rm d}p_i^+}{2\cdot(2\pi)^3}J_i(p_i^+)\prod_i^N\int{\rm d}k_i^+\int{\rm d}k^0_{\rm out}S(k^0_{\rm out},\{n_i,k_i^+\})\\ &\quad\times(2\pi)^4\,\delta\left[1-z-\frac{2}{\sqrt{\hat{s}}}\Big(\cosh Y\sum_i^N\big(p_i^+ + k_i^+\big)+k^0_{\rm out}\Big)\right]\\ &\quad\times\delta\left(Y-\tanh^{-1}\left(\frac{\sum_i^N p_{J_i}^\perp\sinh\eta_{J_i}+q_z}{\sum_i^N p_{J_i}^\perp\cosh\eta_{J_i}+q_0}\right)\right)\\ &\quad\times\delta^2(\sum_i^N\mathbf{p}_{J_i}^{\rm T}+\mathbf{q}^{\rm T})\,.\end{aligned} \tag{2.52}$$

In Equation (2.52), both H and S are matrices in color space, while J and f are proportional to the identity in color space and there is an implicit trace. Loop corrections will in general mix color structures, which means that beyond tree level H and S will contain off diagonal elements. The details of resummation in the presence of color mixing is discussed in [42].

2.6 Anomalous dimensions

Now that we have shown that a generic N-jet cross section factorizes in the limit of $1-z \ll 1$, we are left to calculate each ingredient of the factorization theorem. In this section, we focus on the consistency of the factorization theorem to $\mathcal{O}(\alpha_s)$, and we therefore need the one-loop anomalous dimensions for the hard, jet and soft functions. Note that the results presented here are enough to resum threshold logarithms at NLL[4].

2.6.1 Hard, Jet, and Parton Distribution Functions

Both the Born-level matrix element and the hard function, which can be found by calculating the virtual corrections to the Born-level matrix element in the $\overline{\text{MS}}$ scheme, are process dependent, so they can not be calculated generically. However, the hard anomalous dimension, defined as

$$\frac{\mathrm{d}H(\{n_i,\omega_i\};\mu)}{\mathrm{d}\,\ln\mu} \equiv \gamma_H\left(\{n_i,\omega_i\};\mu\right) H\left(\{n_i,\omega_i\};\mu\right)\,, \tag{2.53}$$

only depends on the directions n_i, label momenta ω_i, and color charges $\mathbf{T}_i$ of the collinear particles and is given by ([55], [15], [32], [73], [33])

$$\gamma_H(\{n_i,\omega_i\};\mu) = \sum_{i\in\{\text{partons}\}}\left(-\Gamma_{\text{cusp}}\,\mathbf{T}_i^2\,\ln\frac{\mu^2}{\omega_i^2}-\gamma_i\right) - 2\,\Gamma_{\text{cusp}}\sum_{\langle i,j\rangle}\mathbf{T}_i\cdot\mathbf{T}_j\,\ln\frac{n_i\cdot n_j}{2}\,. \tag{2.54}$$

The cusp anomalous dimension at two loops is given by

$$\Gamma_{\text{cusp}} = \frac{\alpha_s}{\pi}+\frac{\alpha_s^2}{4\pi^2}\left[C_A\left(\frac{67}{9}-\frac{\pi^2}{3}\right)-\frac{20}{9}C_F T_F n_f\right]\,. \tag{2.55}$$

The γ_i to one-loop are given by

$$\gamma_q = \frac{3\alpha_s}{2\pi}C_F \qquad \text{and} \qquad \gamma_g = \frac{\alpha_s}{2\pi}\beta_0\,, \tag{2.56}$$

for quarks and gluons, respectively, where β_0 is defined as

$$\beta_0 = \frac{11C_A}{3}-\frac{2N_f}{3}\,. \tag{2.57}$$

The sum on $\langle i,j\rangle$ is a sum over all distinct pairs of partons i and j for $i\neq j$.

[4]There are several different ways to define precisely what is meant by NLL. In this thesis, we will use the convention of [35].

The quark and gluon jet functions have been calculated previously, e.g.[28, 43, 18], and were first calculated with a jet algorithm in [66]. Their anomalous dimensions, defined by

$$\frac{\mathrm{d}J_i(p_i^+;\mu)}{\mathrm{d}\,\ln\mu} = \int_0^{p_i^+} \mathrm{d}p'^+_i \gamma_{J_i}(p_i^+ - p'^+_i;\mu) J_i(p'^+_i;\mu)\,, \tag{2.58}$$

are given by

$$\gamma_{J_i}(p_i^+;\mu) = \left(2\,\Gamma_{\rm cusp}\,\mathbf{T}_i^2\,\ln\frac{\mu}{\omega_i} + \gamma_i\right)\delta(p_i^+) - 2\,\Gamma_{\rm cusp}\,\mathbf{T}_i^2\,\frac{1}{\mu}\left(\frac{\mu}{p_i^+}\right)_+ . \tag{2.59}$$

The expressions for $\Gamma_{\rm cusp}$ and γ_i are the same as for the hard function. Note that the algorithm in [66] used a polar angle for the measure and not Equation (2.16). However, since the anomalous dimension in that case did not depend on the algorithm parameter R, the result must be independent of which measure is chosen since the precise definition of the jet boundaries is not associated with any singularities. It does however affect the finite parts of the jet function, which become important starting at NNLL accuracy.

It is well-known that the parton distribution functions are not perturbatively calculable; in practice, they can be expressed as universal matrix elements, which are then extracted from experiment. However, the evolution of the pdfs with μ can be computed,

$$\frac{\mathrm{d}f_i(x_i;\mu)}{\mathrm{d}\,\ln\mu} = \frac{\alpha_s}{\pi}\int_{x_i}^1 \frac{\mathrm{d}z}{z} P_{ij}(z) f_j\left(\frac{x_i}{z};\mu\right)\,, \tag{2.60}$$

where the repeated index j is summed over and P_{ij} are the Altarelli-Parisi splitting functions. Near hadronic threshold, the splitting functions simplify and can be written as

$$\frac{\alpha_s}{\pi}P_{ij}(x) = \left[2\,\Gamma_{\rm cusp}\,\mathbf{T}_i^2\,\frac{1}{(1-x)_+} + \gamma_i\,\delta(1-x)\right]\delta_{ij}\,. \tag{2.61}$$

2.6.2 Soft Function

In general, the soft function depends on the null component of the soft momentum inside each jet as well as the timelike component $k^0_{\rm out}$ (defined in Section 2.5 as $k^0_{\rm out} \equiv p_I \cdot k_{\rm out}/|p_I|$). At order α_s, the soft function can be written as a sum of functions that depend only on one momentum variable, with trivial dependence on the others and is given by

$$S(k^0_{\rm out},\{n_i,k_i^+\}) = S_{\rm out}(k^0_{\rm out})\prod_{i\in\{\rm jets\}}\delta(k_i^+) + \delta(k^0_{\rm out})\sum_{i\in\{\rm jets\}} S_{\rm in}(k_i^+)\prod_{\substack{j\in\{\rm jets\}\\ j\neq i}}\delta(k_j^+)\,, \tag{2.62}$$

where the sum over $i \in \{\text{jets}\}$ is over all i corresponding to outgoing jets and does not include the incoming partons (and we remind the reader that the dependence here on k_i is only over final state jets but the n_i run over all initial and final partons). The timelike component of the soft function, S_{out}, receives contributions from soft gluons that are not inside any of the outgoing jets. We can find this by calculating the contribution of soft gluons going anywhere and then subtracting the contribution from gluons that enter one of the jets. This can be written in the hadronic center-of-mass frame as

$$S_{\text{out}}(k^0_{\text{out}}) = -\sum_{\langle i,j\rangle} \mathbf{T}_i\cdot\mathbf{T}_j\, 2g^2\mu^{2\epsilon} \int \frac{\mathrm{d}^d k}{(2\pi)^d} \frac{n_i\cdot n_j}{(n_i\cdot k)(n_j\cdot k)} \times 2\pi\delta(k^2)\delta\Big(\frac{p_I\cdot k}{|p_I|} - k^0_{\text{out}}\Big)\Bigg[1 - \sum_{k\in\{\text{jets}\}} \hat{\Theta}^R_{\text{soft},k}\Bigg], \tag{2.63}$$

where $\hat{\Theta}^R_k$ is the restriction that the gluon is in jet k, defined by a jet algorithm of size R as in Section 2.4. This is most easily calculated in the partonic center-of-mass frame. Denoting the directions and energies of the collinear partons in this frame as $\tilde{n}_i$ and $\tilde{\omega}_i$ respectively, we have that

$$S_{\text{out}}(k^0_{\text{out}}) = -\sum_{\langle i,j\rangle} \mathbf{T}_i\cdot\mathbf{T}_j\, 2g^2\mu^{2\epsilon} \int \frac{\mathrm{d}^d k}{(2\pi)^d} \frac{\tilde{n}_i\cdot\tilde{n}_j}{(\tilde{n}_i\cdot k)(\tilde{n}_j\cdot k)} \times 2\pi\delta(k^2)\delta(k^0 - k^0_{\text{out}})\Bigg[1 - \sum_{k\in\{\text{jets}\}} \hat{\Theta}^R_{\text{soft},k}\Bigg], \tag{2.64}$$

where we have used the fact that, for an $\eta-\phi$ algorithm, the jet algorithm restrictions are frame invariant.

The null components of the soft function, $S_{\text{in}}(k^+_i)$, are defined in the hadronic center-of-mass frame as

$$S_{\text{in}}(k^+_k) = -\sum_{\langle i,j\rangle} \mathbf{T}_i\cdot\mathbf{T}_j\, 2g^2\mu^{2\epsilon} \int \frac{\mathrm{d}^d k}{(2\pi)^d} \frac{n_i\cdot n_j}{(n_i\cdot k)(n_j\cdot k)} 2\pi\delta(k^2)\delta(n_k\cdot k - k^+_k)\hat{\Theta}^R_{\text{soft},k}\,. \tag{2.65}$$

In the partonic center-of-mass frame, this can be written as

$$S_{\text{in}}(k^+_k) = -\sum_{\langle i,j\rangle} \mathbf{T}_i\cdot\mathbf{T}_j\, 2g^2\mu^{2\epsilon} \int \frac{\mathrm{d}^d k}{(2\pi)^d} \frac{\tilde{n}_i\cdot\tilde{n}_j}{(\tilde{n}_i\cdot k)(\tilde{n}_j\cdot k)} 2\pi\delta(k^2)\frac{\omega_k}{\tilde{\omega}_k}\delta\left(k^+ - \frac{\omega_k}{\tilde{\omega}_k}k^+_k\right)\hat{\Theta}^R_{\text{soft},k}\,. \tag{2.66}$$

The calculation of S_{in} and S_{out} in the partonic center-of-mass frame can be related to the calculation of the soft function in [66]. While [66] uses a polar angle measure,

we will show that, even though $S_{\rm in}$ and $S_{\rm out}$ separately depend on the parameter R, the anomalous dimension is R independent. This implies that all algorithms with the same singularity structure as the polar angle algorithm used in [66] have the same anomalous dimension for this observable. Specifically, the anomalous dimension calculated in the partonic center-of-mass frame should be the same for both a polar angle measure and an $\eta - \phi$ measure. Since the $\eta - \phi$ measure is boost invariant, the R independence of the anomalous dimension must be true in all frames[5]. The relations of $S_{\rm in}$ and $S_{\rm out}$ to the soft function in [66] are given by

$$S_{\rm out}(k^0_{\rm out}) = 2\sum_{\langle i,j\rangle} \frac{\rm d}{{\rm d}\Lambda}\left[S^{\rm incl}_{ij} + \sum_{k\in\{\rm jets\}} S^k_{ij}\right]_{\Lambda=k^0_{\rm out}}, \tag{2.67}$$

and

$$S_{\rm in}(k^+_k) = 2\sum_{\langle i,j\rangle} \frac{1}{\tilde\omega_k} S^{\rm meas}_{ij}(\tau^k_0)\,, \tag{2.68}$$

where $S^{\rm incl}_{ij}$, S^k_{ij}, and $S^{\rm meas}_{ij}$ are defined and computed in [66]. In calculating $S^{\rm meas}_{ij}$, we use the definitions $\tau^k_0 = k^+_k/\tilde\omega_k$ and $\delta_R = \delta\left(\tau^k_0 - k^+/\omega_k\right)$, where τ_a and δ_R are originally defined in [66].

The anomalous dimension of this soft function is defined as

$$\begin{aligned}\frac{{\rm d}S(k^0_{\rm out},\{n_i,k^+_i\};\mu)}{{\rm d}\,\ln\mu} = \prod_{i\in\{\rm jets\}}\int_0^{k^+_i}{\rm d}k'^+_i\int_0^{k^0_{\rm out}}{\rm d}k'^0_{\rm out}\,\gamma_S(k^0_{\rm out}-k'^0_{\rm out},\{n_i,k^+_i-k'^+_i\};\mu)\\ \times S(k'^0_{\rm out},\{n_i,k'^+_i\};\mu)\,.\end{aligned} \tag{2.69}$$

Using the results of [66], together with Eqs. (2.67) and (2.68), the result for the anomalous dimension can be written as

$$\begin{aligned}\gamma_S(k^0_{\rm out},\{n_i,k^+_i\};\mu) = \sum_{i\in\{\rm jets\}}\gamma_{S_i}(k^+_i;\mu)\prod_{\substack{j\in\{\rm jets\}\\ j\neq i}}\delta(k^+_j)\,\delta(k^0_{\rm out})\\ +\gamma_{S_{\rm out}}(k^0_{\rm out};\mu)\prod_{i\in\{\rm jets\}}\delta(k^+_i)\,.\end{aligned} \tag{2.70}$$

with

$$\gamma_{S_i}(k^+_i;\mu) = 2\,\Gamma_{\rm cusp}\mathbf{T}^2_i\,\frac{\omega_i}{\mu\,\tilde\omega_i}\left(\frac{\mu\,\tilde\omega_i}{k^+_i\omega_i}\right)_+ \tag{2.71}$$

$$\gamma_{S_{\rm out}}(k^0_{\rm out};\mu) = \Gamma_{\rm cusp}\sum_{\langle i,j\rangle}\mathbf{T}_i\cdot\mathbf{T}_j\left(2\,\ln\frac{\tilde n_i\cdot\tilde n_j}{2}\right)\delta(k^0_{\rm out}) - 4\,\Gamma_{\rm cusp}\,(\mathbf{T}^2_1+\mathbf{T}^2_2)\frac{1}{\mu}\left(\frac{\mu}{2k^0_{\rm out}}\right)_+. \tag{2.72}$$

[5]We have verified this explicitly for small R by making the replacement $R\to R/\cosh\eta$, which relates the polar angle and $\eta-\phi$ measures in the small R limit.

2.7 Consistency of Factorization to $\mathcal{O}(\alpha_s)$

Consistency is a nontrivial check of our factorization theorem. The factorized cross section should be independent of the factorization scale μ in the threshold limit and thus renormalization group invariant. Starting from the generic N-jet cross section, Equation (2.52), ignoring multiplicative factors that do not affect the derivative, and using the shorthand notation

$$\frac{\mathrm{d}\sigma}{\mathrm{d}\,\ln\mu} \equiv \frac{\mathrm{d}}{\mathrm{d}\,\ln\mu}\frac{\mathrm{d}\sigma}{\prod_i \mathrm{d}^2 p_{J_i}^{\mathrm{T}}\mathrm{d}\eta_{J_i}\mathrm{d}\Phi_q}\,, \tag{2.73}$$

we have that

$$\begin{aligned}
\frac{\mathrm{d}\sigma}{\mathrm{d}\,\ln\mu} \propto \int_\tau^1 \mathrm{d}z \int_{-\frac{1}{2}\ln\frac{z}{\tau}}^{\frac{1}{2}\ln\frac{z}{\tau}} \mathrm{d}Y\, H(\{n_i,\omega_i\};\mu) f_1(x_1;\mu) f_2(x_2;\mu) \\
\times \prod_{i\in\{\text{jets}\}} \int \mathrm{d}p_i^+ J_i(p_i^+;\mu) \prod_{i\in\{\text{jets}\}} \int \mathrm{d}k_i^+ \int \mathrm{d}k_{\text{out}}^0 S(k_{\text{out}}^0,\{n_i,k_i^+\};\mu) \\
\times \left(\frac{\mathrm{d}\,\ln H(\{n_i,\omega_i\};\mu)}{\mathrm{d}\,\ln\mu} + \frac{\mathrm{d}\,\ln f_1(x_1;\mu)}{\mathrm{d}\,\ln\mu} + \frac{\mathrm{d}\,\ln f_2(x_2;\mu)}{\mathrm{d}\,\ln\mu} \right. \\
\left. + \sum_{i\in\{\text{jets}\}} \frac{\mathrm{d}\,\ln J_i(p_i^+;\mu)}{\mathrm{d}\,\ln\mu} + \frac{\mathrm{d}\,\ln S(k_{\text{out}}^0,\{n_i,k_i^+\};\mu)}{\mathrm{d}\,\ln\mu} \right) \\
\times \delta\left[1 - z - \frac{2}{\sqrt{\hat{s}}}\Big(\cosh Y \sum_{i\in\{\text{jets}\}} (p_i^+ + k_i^+) + k_{\text{out}}^0 \Big) \right] .
\end{aligned} \tag{2.74}$$

There are several simplifications we can make to check the independence of μ. First, μ only enters perturbative expressions, and whether or not the cross section depends on μ is independent of nonperturbative physics. This allows us to use the perturbative definition of the parton distribution functions. Second, given that the μ dependence of each of the factorization ingredients starts at order α_s, we can use the tree level expressions for the hard, jet and soft functions, as well as for the pdfs,

$$f_i(x;\mu) = \delta(1-x) \tag{2.75}$$

$$H(\{n_i,\omega_i\};\mu) = 1 \tag{2.76}$$

$$J_i(p_i^+;\mu) = \delta(p_i^+) \tag{2.77}$$

$$S(k_{\text{out}}^0,\{n_i,k_i^+\};\mu) = \delta(k_{\text{out}}^0) \prod_{i\in\{\text{jets}\}} \delta(k_i^+)\,. \tag{2.78}$$

Using this and working to lowest order in α_s, we can simplify Eq. (2.74) to get

$$\begin{aligned}\frac{\mathrm{d}\sigma}{\mathrm{d}\,\ln\mu} \propto \frac{\alpha_s}{\pi}P_{11}(\tau) + \frac{\alpha_s}{\pi}P_{22}(\tau) + \frac{\sqrt{\hat{s}}}{2\cosh Y}\sum_{i\in\{\text{jets}\}}\gamma_{J_i}\left(\frac{\sqrt{\hat{s}}}{2\cosh Y}(1-\tau);\mu\right) \\ + \frac{\sqrt{\hat{s}}}{2\cosh Y}\sum_{i\in\{\text{jets}\}}\gamma_{S_i}\left(\frac{\sqrt{\hat{s}}}{2\cosh Y}(1-\tau);\mu\right) + \gamma_H(\mu)\,\delta(1-\tau) \\ + \frac{\sqrt{\hat{s}}}{2}\gamma_{S_{\text{out}}}\left(\frac{\sqrt{\hat{s}}}{2}(1-\tau);\mu\right). \qquad (2.79)\end{aligned}$$

After plugging in Equations (2.54), (2.59), and (2.70), rescaling the plus functions using the identity

$$\left(\frac{1}{ax}\right)_+ = \frac{\ln a}{a}\delta(x) + \frac{1}{a}\left(\frac{1}{x}\right)_+, \qquad (2.80)$$

and combining the various terms, we find

$$\begin{aligned}\frac{\mathrm{d}\sigma}{\mathrm{d}\,\ln\mu} \propto \Gamma_{\text{cusp}}\Bigg[\sum_{\langle i,j\rangle}\mathbf{T}_i{\cdot}\mathbf{T}_j\left(2\,\ln\frac{\tilde{n}_i{\cdot}\tilde{n}_j}{n_i{\cdot}n_j}\right) + \mathbf{T}_1^2\,\ln\frac{\omega_1^2}{\hat{s}} \qquad (2.81)\\ + \mathbf{T}_2^2\,\ln\frac{\omega_2^2}{\hat{s}} + \sum_{i\in\{\text{jets}\}}\mathbf{T}_i^2\left(2\,\ln\frac{\omega_i}{\tilde{\omega}_i}\right)\Bigg]. \qquad (2.82)\end{aligned}$$

After making the simplification

$$\sum_{\langle i,j\rangle}\mathbf{T}_i{\cdot}\mathbf{T}_j\left(2\,\ln\frac{\tilde{n}_i{\cdot}\tilde{n}_j}{n_i{\cdot}n_j}\right) = \sum_{\substack{i,j\\ i\neq j}}\mathbf{T}_i{\cdot}\mathbf{T}_j\left(\ln\frac{\omega_i}{\tilde{\omega}_i} + \ln\frac{\omega_j}{\tilde{\omega}_j}\right) = \sum_{i\in\{\text{partons}\}}\mathbf{T}_i^2\left(-2\,\ln\frac{\omega_i}{\tilde{\omega}_i}\right), \qquad (2.83)$$

where we have used that $\tilde{p}_i{\cdot}\tilde{p}_j = p_i{\cdot}p_j$ and $\sum_i \mathbf{T}_i = 0$, Equation (2.81) gives

$$\frac{\mathrm{d}\sigma}{\mathrm{d}\,\ln\mu} = 0\,. \qquad (2.84)$$

This result confirms that our factorization theorem is consistent at hadronic threshold and justifies using the renormalization group to resum logarithms of $1-\tau$.

Chapter 3

A Measure of Effectiveness for Threshold Resummation

3.1 Introduction

In this section, we parameterize the enhancement of threshold effects away from hadronic endpoint that arise due to the steeply falling nature of parton distribution functions, within the context of soft-collinear effective theory. This is accomplished in a process-independent way by directly linking the characteristic scale of soft and collinear radiation, λ, to the shape of the pdfs. This allows us quantify the power corrections to partonic threshold resummation as a function of the invariant mass and rapidity of the final state. In the context of SCET, being able to compute λ in a process-independent manner allows us to determine the correct scale for threshold resummation after integration with the pdfs, without any additional procedure.

There has been much effort to increase the accuracy and precision of predictions for observables at hadron colliders. The standard technique to improve the accuracy of calculations is to add fixed orders in perturbation theory. Many observables have been calculated to next-to-leading order (NLO) in QCD, and for some next-to-next-to-leading order (NNLO) has been achieved [78, 10, 101, 8, 44, 9, 11, 12, 7, 75, 50]. Frequently, observables contain large ratios of scales, usually due to experimental cuts or the presence of several mass scales in the process. In such cases, one can increase the precision and accuracy of theoretical calculations by resumming the large logarithms of these ratios to all orders in perturbation theory. Standard techniques allow for the resummation of these logarithms at next-to-leading logarithmic order (NLL) and beyond [110, 48, 42], while recent advances in effective theory methods [23, 25, 31, 30] provide a systematically improvable alternative to resummation in hard-scattering processes [24].

It is well known that, beyond leading order, partonic cross sections contain terms

of the form

$$\alpha_s^n \left(\frac{\log^m(1-z)}{1-z} \right)_+ , \tag{3.1}$$

where $m \leq 2n-1$ and $z = \hat{s}_{\min}/\hat{s}$ is a measure of excess radiation in the process. These terms are due to collinear and soft singularities in the real emission diagrams of the perturbative series and can be resummed with the same techniques used for other large logarithms. Threshold resummation has been applied to several Standard Model processes, including (inclusive) Drell-Yan [110, 48, 82, 35], prompt photon [51, 37], Higgs production [97, 89, 83, 2, 3], and dijet and heavy-particle production [90, 40, 52, 86, 87, 85].

It is important to understand when threshold logarithms are phenomenologically relevant. The partonic endpoint (where logarithms of z become large) cannot be observed, since one integrates over the partonic variable z when the partonic cross section is convolved with parton distribution functions (pdfs). The exception is near the hadronic endpoint, where the partonic and hadronic endpoints are equivalent. As an example, consider Drell-Yan, where the rescaled leptonic center of mass energy is given by $\tau = m_{\ell\ell}^2/s$. The hadronic cross section is then

$$\frac{\mathrm{d}\sigma}{\mathrm{d}\tau} = \int_\tau^1 \mathrm{d}z \, \mathcal{L}(\tau/z)\hat{\sigma}(\tau, z) \, , \tag{3.2}$$

where

$$\mathcal{L}(z) = \int_{-\log\frac{z}{\tau}}^{\log\frac{z}{\tau}} \mathrm{d}Y \, \left[f_1\left(\sqrt{\frac{\tau}{z}}e^Y\right) f_2\left(\sqrt{\frac{\tau}{z}}e^{-Y}\right) + f_1\left(\sqrt{\frac{\tau}{z}}e^{-Y}\right) f_2\left(\sqrt{\frac{\tau}{z}}e^Y\right) \right] \tag{3.3}$$

is the parton luminosity. From this expression, one can immediately see that a measurement of Drell-Yan close to the hadronic endpoint ($\tau \to 1$) also forces the partonic center of mass energy z to its endpoint, such that these logarithms become important. However, away from the hadronic endpoint, the integration variable z is not forced to one, such that it is not clear that the threshold terms given in Eq. (3.1) should dominate over terms which are, for example, polynomial in z.

By comparing resummed cross sections with available fixed order calculations it has been noted that, in certain cases, the threshold terms at $\mathcal{O}(\alpha_s)$ give the dominant effect of the full NLO correction, even far away from the hadronic endpoint [13, 51, 35]. This observation has been used to suggest that threshold resummation is effective not only in the hadronic endpoint, where it is clearly necessary, but also for much lower values of τ. One possible explanation for this is the shape of parton luminosities [13, 51]. For steeply falling parton luminosities, the integration in Eq. (3.2) is dominated by the smallest values of τ/z, which is the region $z \to 1$. By assuming a simple, analytical form for the parton luminosity, one can make this argument more precise [35]. However, the corrections to threshold resummation applied away from hadronic endpoint have not yet been studied without assuming a model for parton luminosities.

The goal of this section is to provide a model-independent, quantitative measure of the corrections to partonic threshold resummation. Using only the shape of the pdfs, we define a parameter λ that can be used as the expansion parameter in SCET. This implies that corrections to the threshold resummation are power suppressed in λ. Since we will use the measured pdfs to calculate λ, our definition does not require the assumption of a particular form for the parton luminosities. Thus, λ can be viewed as a model-independent definition of the steepness of a parton luminosity. We will determine the numerical size of λ for various parton luminosities as a function of the hadronic threshold variables τ and Y. In addition to quantifying power corrections, λ allows us to determine the scales relevant to threshold resummation in SCET after convolving the partonic cross section with the pdfs. This avoids integrating over unphysical regions (a consequence of setting the scales before integration) or introducing a process-specific procedure to calculate the scales.

This section is organized as follows. In Section 3.2, we will define the relevant expansion parameter in threshold resummation and show that it has the expected behavior for a simple choice of the pdfs. In Section 3.4, we show the consistency of the factorization theorem assuming only small values of λ, but keepinig an arbitrary functional form for the pdfs, while in Section 3.3 we discuss the scaling in λ of integrals against the pdfs. In Section 3.5, we will determine the numerical values of this expansion parameter for the actual pdfs.

3.2 Definition of Steepness

The only assumptions one has to make to allow for the resummation of threshold logarithms is that $1 - z \ll 1$, where z is appropriately defined, along with the statement that pdfs factorize from the partonic cross section [60, 56]. We will use the definitions

$$z \equiv \frac{\hat{s}_{\min}}{\hat{s}}\,, \qquad\qquad \tau \equiv \frac{\hat{s}_{\min}}{s}\,, \tag{3.4}$$

with

$$\hat{s}_{\min} = \Big(q + \sum_i^N p_J^i\Big)^2 . \tag{3.5}$$

Here q denotes the sum of the momenta of all non-strongly interacting particles, and p_J^i is the momentum of the ith jet. This momentum is defined in terms of p_J^{T} and η_J of the jet as

$$p_J \equiv (p_J^{\mathrm{T}} \cosh\eta_J, \mathbf{p}_J^{\mathrm{T}}, p_J^{\mathrm{T}} \sinh\eta_J)\,. \tag{3.6}$$

Thus, the jet 4-momentum is reconstructed from the measured transverse momentum and rapidity, assuming zero mass.

A generic hadronic cross section can be written as

$$\mathrm{d}\sigma = \int_{-\frac{1}{2}\ln\frac{1}{\tau}}^{\frac{1}{2}\ln\frac{1}{\tau}} \mathrm{d}Y \int_{\tau e^{-2|Y|}}^{1} \mathrm{d}z\, f_1\left(\sqrt{\frac{\tau}{z}}e^{Y}\right) f_2\left(\sqrt{\frac{\tau}{z}}e^{-Y}\right) \mathrm{d}\hat{\sigma}(z,\tau,Y) + (1 \leftrightarrow 2)\,. \quad (3.7)$$

One can use soft-collinear effective theory to analyze the partonic cross section, with corrections being suppressed by powers of $1-z$

$$\mathrm{d}\hat{\sigma}(z,\tau,Y) = \mathrm{d}\hat{\sigma}(z,\tau,Y)_{\mathrm{SCET}} + \mathcal{O}(1-z)\,. \quad (3.8)$$

As was shown in Chapter 2, the SCET partonic cross section factorizes, and renormalization group equations can be used to resum threshold logarithms. No assumptions were made about the kinematics of the event other than $1-z \sim \lambda^2$, where λ is the usual SCET power counting parameter, which relates the hard, collinear and soft scales via $\mu_c/\mu_h \sim \mu_s/\mu_c \sim \lambda$.

From Eq. (3.7) it is clear that z is forced to one if the kinematics force us close to hadronic threshold, $\tau \to 1$. In this case, $1-z \ll 1$, which means that the power corrections in Eq. (3.8) are small. Away from hadronic threshold, however, the partonic cross section gets integrated over values of z for which $1-z \sim \mathcal{O}(1)$. For generic parton luminosities, threshold resummation will have $\mathcal{O}(1)$ power corrections when applied away from hadronic threshold, if the region $1-z \sim \mathcal{O}(1)$ is large.

If the parton luminosities are dominated by the region where $1-z \ll 1$, however, the SCET expression gives the dominant contribution to the hadronic cross section. We can quantify the corrections due to this by defining a parameter

$$\epsilon(\lambda,\tau,Y) = \frac{\int_{\tau e^{-2|Y|}}^{1-\lambda^2} \mathrm{d}z\, \left|f_1\left(\sqrt{\frac{\tau}{z}}e^{Y}\right)\right| \left|f_2\left(\sqrt{\frac{\tau}{z}}e^{-Y}\right)\right|}{\int_{1-\lambda^2}^{1} \mathrm{d}z\, \left|f_1\left(\sqrt{\frac{\tau}{z}}e^{Y}\right)\right| \left|f_2\left(\sqrt{\frac{\tau}{z}}e^{-Y}\right)\right|}\,. \quad (3.9)$$

In other words, the parameter ϵ measures how much of the parton luminosity is contained in the region $\tau e^{-2|Y|} < z < 1-\lambda^2$ compared to the region $1 > z > 1-\lambda^2$. This parameter obviously depends not only on our choice of λ, but also on the hadronic center of mass energy τ and the total rapidity of the event Y. Note that for fixed values of τ and Y, ϵ is as a monotonically decreasing function of λ.

Using this definition, we can write

$$\mathrm{d}\sigma = \int_{-\frac{1}{2}\ln\frac{1}{\tau}}^{\frac{1}{2}\ln\frac{1}{\tau}} \mathrm{d}Y \int_{1-\lambda^2}^{1} \mathrm{d}z\, f_1\left(\sqrt{\frac{\tau}{z}}e^{Y}\right) f_2\left(\sqrt{\frac{\tau}{z}}e^{-Y}\right) \mathrm{d}\hat{\sigma}(z,\tau,Y)_{\mathrm{SCET}} + \mathcal{O}(\epsilon,\lambda^2)\,, \quad (3.10)$$

where the $\mathcal{O}(\lambda^2)$ correction comes from the fact that $1-z$ in Eq. (3.10) is bounded by λ^2. The total correction to threshold resummation can therefore be estimated as $\max(\epsilon,\lambda^2)$. However, since ϵ decreases with increasing λ^2, the total correction is

minimized if we choose $\epsilon = \lambda^2$. The corrections are then $\mathcal{O}(\lambda^2)$. This also allows us to define λ^2 through the relation

$$\lambda^2 = \frac{\int_{\tau e^{-2|Y|}}^{1-\lambda^2} \mathrm{d}z \, \left| f_1\left(\sqrt{\frac{\tau}{z}} e^{Y}\right)\right| \left| f_2\left(\sqrt{\frac{\tau}{z}} e^{-Y}\right)\right|}{\int_{1-\lambda^2}^{1} \mathrm{d}z \, \left| f_1\left(\sqrt{\frac{\tau}{z}} e^{Y}\right)\right| \left| f_2\left(\sqrt{\frac{\tau}{z}} e^{-Y}\right)\right|}, \tag{3.11}$$

where $\lambda^2 \equiv \lambda^2(\tau, Y)$. We can also define λ^2 for a single pdf

$$\lambda^2 = \frac{\int_{x}^{1-\lambda^2} \mathrm{d}z \, \left| f\left(\frac{x}{z}\right)\right|}{\int_{1-\lambda^2}^{1} \mathrm{d}z \, \left| f\left(\frac{x}{z}\right)\right|}, \tag{3.12}$$

where here $\lambda^2 \equiv \lambda^2(x)$. This definition will be useful for determining if endpoint Altarelli-Parisi functions are valid when evolving the pdfs.

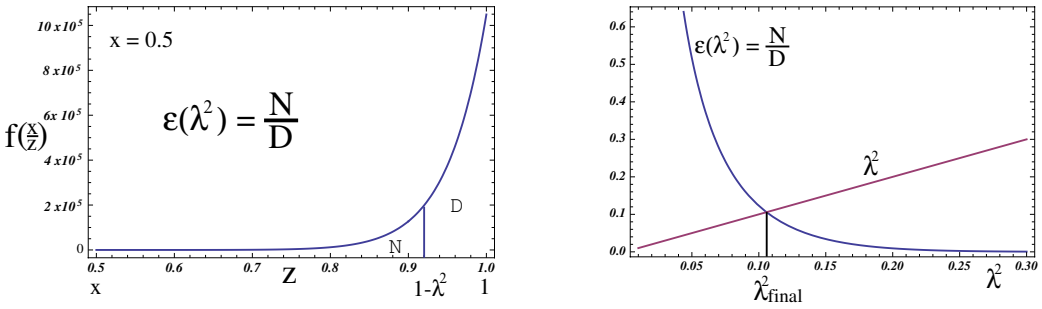

Figure 3.1: Left: The parameter ϵ, defined in Eq. (3.9), illustrated as the ratio of two areas. Right: For power corrections that go as $\max(\epsilon, \lambda^2)$, there is a choice of $\lambda^2 = \lambda^2_{\text{final}}$ such that the corrections are minimized. This choice, called λ^2 in the text, is defined in Eqs. (3.11) and (3.12).

We illustrate our definitions in Figure 3.1, with a simple example function $f(x)$. The graphic on the left shows ϵ as the ratio of two areas: the region D, where $1-z < \lambda^2$ and the region N, where $1 - z > \lambda^2$. For $N \ll D$ and $\lambda^2 \ll 1$, we see that the area under the curve is dominated by a region where $1 - z \ll 1$. The right graphic shows that Eq. (3.12) has a solution where power corrections are minimized, labelled λ^2_{final}.

Independent of the form of the pdfs, we can see that λ^2_{final} goes to 0 as τ (or x) goes to 1, as expected. First, note that $\tau \to 1$ forces $Y \to 0$, which sets the lower bound of the integral in the numerator of Eq. (3.9) to τ. Next, we can examine the limits on λ^2. As λ^2 goes to 0, ϵ goes to ∞ (here we've assumed that the pdf implicitly contains a Θ function that sets it to 0 if the argument is greater than 1 or less than 0). Similarly, as λ^2 goes to $1 - \tau$, ϵ goes to 0. Therefore, the crossover point, where $\epsilon = \lambda^2$, is between 0 and $1 - \tau$, which means $\lambda^2_{\text{final}} \to 0$ as $\tau \to 1$. For the remainder of this section, we will omit the subscript final on λ^2.

Note that these definitions do not assume anything about the form of the pdfs and are therefore completely model independent. Given that pdfs are not observable quantities, many pdf sets do not constrain them to be positive. For this reason, we have used absolute values of the pdfs in our definition. Of course, the value of λ^2 depends on the functional form of the pdfs, but this can be determined numerically using any of the available pdf sets. We will present the numerical results for the power counting parameter λ^2 in Section 3.5.

We end this section by showing the behavior of λ^2 for a particularly simple form of the pdfs. This will illustrate our proposal with an analytic example and should convince the reader that corrections to threshold resummation behave as expected. The assumed form of the pdfs does not represent their observed shape and is only chosen so that the analytic results can be easily studied. All numerical results presented in Section 3.5 will use the measured pdfs.

Consider the simple model

$$f_i(x) = x^{-a_i}\,, \tag{3.13}$$

where the pdf becomes steeper as a increases. Given this form, Eq. (3.11) becomes

$$\lambda^2 = \frac{(1-\lambda^2)^{1+(a_1+a_2)/2} - (\tau e^{-2|Y|})^{1+(a_1+a_2)/2}}{1-(1-\lambda^2)^{1+(a_1+a_2)/2}}\,. \tag{3.14}$$

To simplify this equation, we define

$$r \equiv A\lambda^2\,, \qquad \text{with} \qquad A \equiv 1 + \frac{a_1+a_2}{2}\,. \tag{3.15}$$

The equation can then be written as

$$\left(1+\frac{r}{A}\right)\left(1-\frac{r}{A}\right)^A = \frac{r}{A} + (\tau e^{-2|Y|})^A\,. \tag{3.16}$$

We can clearly see that $r \to 0$ in the hadronic endpoint $\tau \to 1$ (for which $Y \to 0$), independent of the value of the parameter A. However, for large values of A, and therefore steep pdfs, we can use the approximations $1+r/A \approx 1$ and $(1-r/A)^A \approx e^{-r}$ to find

$$r = W(A)\,, \tag{3.17}$$

where $W(A)$ denotes the product logarithm of A. Since the $W(A)$ only grows logarithmically with A, we find the desired result that $\lambda^2 \to 0$ as $A \to \infty$.

3.3 General Power Corrections

It is instructive to understand the power corrections and scaling of various test functions integrated against a steep distribution, $f(z)$, where steep is defined as

$$\frac{\int_{z_{\min}}^{1-\lambda^2} \mathrm{d}z\, f(z)}{\int_{1-\lambda^2}^{1} \mathrm{d}z\, f(z)} = \lambda^2 \ll 1\,. \tag{3.18}$$

We define all scaling relative to $\int_{1-\lambda^2}^{1} \mathrm{d}z\, f(z)$, which can be taken to be $\mathcal{O}(1)$ without loss of generality.

The simplest choice for a test function is a non-singular polynomial of z, $g(z)$. In general, we can express g as a Taylor series about $z = 1$,

$$g(z) = \sum_{n=0}^{\infty} \frac{g^{(n)}(1)}{n!}(z-1)^n\,, \tag{3.19}$$

where we assume all $g^{(n)}(1)$ are $\mathcal{O}(1)$. We can evaluate the integral of $f(z)g(z)$ by dividing the integration region into two parts,

$$\int_{z_{\min}}^{1} \mathrm{d}z\, f(z)g(z) = \int_{z_{\min}}^{1-\lambda^2} \mathrm{d}z\, f(z)g(z) + \int_{1-\lambda^2}^{1} \mathrm{d}z\, f(z)g(z)\,. \tag{3.20}$$

In the region $z_{\min} < z < 1-\lambda^2$, the integral is $\mathcal{O}(\lambda^2)$, since $f(z)$ and $f(z)g(z)$ are of the same order and the integral of $f(z)$ over this region is $\mathcal{O}(\lambda^2)$. For $1-\lambda^2 < z < 1$,

$$\begin{aligned}\int_{1-\lambda^2}^{1} \mathrm{d}z\, f(z)g(z) &= \sum_{n=0}^{\infty} \frac{g^{(n)}(1)}{n!} \int_{1-\lambda^2}^{1} \mathrm{d}z\, f(z)(z-1)^n \\ &\sim \sum_{n=0}^{\infty} \frac{g^{(n)}(1)}{n!} \int_{1-\lambda^2}^{1} \mathrm{d}z\, f(z) \times \left(\lambda^2\right)^n\,. \end{aligned} \tag{3.21}$$

In this region, the integral is dominated by the zeroth order term in the power expansion. Therefore, we can write the integral of $g(z)$ against the distribution $f(z)$ as

$$\int_{z_{\min}}^{1} \mathrm{d}z\, f(z)g(z) = g(1) \int_{1-\lambda^2}^{1} \mathrm{d}z\, f(z) + \mathcal{O}(\lambda^2)\,. \tag{3.22}$$

A second possible test function is a δ-function at $z = 1$. The integral is trivially $f(1)$, but we would like to know the scaling of this result. Assuming f is monotonically increasing from $z_{\min}$ to 1,

$$\int_{1-\lambda^2}^{1} \mathrm{d}z\, f(z) \leq f(1) \times \lambda^2\,. \tag{3.23}$$

Since this integral is $\mathcal{O}(1)$, we can say that $f(1)$ is $\mathcal{O}(\lambda^{-2})$.

The last class of test functions we will consider is $\log^n(1-z)/(1-z)$ plus functions,

multiplied by a non-singular function $g(z)$. When integrated against $f(z)$, this gives

$$\begin{aligned}
&\int_{z_{\min}}^1 \mathrm{d}z\, f(z)g(z) \left(\frac{\log^n(1-z)}{1-z}\right)_+ \\
&\quad = \int_{z_{\min}}^1 \mathrm{d}z\, \log^n(1-z) \frac{f(z)g(z)-f(1)g(1)}{1-z} - f(1)g(1) \int_0^{z_{\min}} \mathrm{d}z\, \frac{\log^n(1-z)}{1-z} \\
&\quad = \int_{1-\lambda^2}^1 \mathrm{d}z\, \log^n(1-z) \frac{f(z)g(z)-f(1)g(1)}{1-z} \\
&\qquad + \int_{z_{\min}}^{1-\lambda^2} \mathrm{d}z\, \log^n(1-z) \frac{f(z)g(z)}{1-z} + f(1)g(1) \frac{\log^{n+1}\lambda^2}{n+1}\,. \qquad (3.24)
\end{aligned}$$

Since $f(z)$ is at most $\mathcal{O}(\lambda^2)$ over the interval $z_{\min} < z < 1-\lambda^2$, the second term is clearly power suppressed relative to the final term. Focusing on the first term, if we express g as a Taylor series about $z = 1$, we see that the zeroth order term is again dominant. This gives

$$\int_{z_{\min}}^1 \mathrm{d}z\, f(z)g(z) \left(\frac{\log^n(1-z)}{1-z}\right)_+ = g(1) \int_{1-\lambda^2}^1 \mathrm{d}z\, f(z) \left(\frac{\log^n(1-z)}{1-z}\right)_+ + \mathcal{O}(\lambda^2)\,. \qquad (3.25)$$

Note that Eq. (3.24) shows that the scaling of this integral is $\mathcal{O}(\lambda^{-2}\log^{n+1}\lambda^2)$ and therefore, for small λ^2, threshold effects are important.

The Altarelli-Parisi (AP) kernels, $P_{ij}(z)$, are polynomial functions of z for $i \neq j$ and a combination of δ-functions and plus functions for $i = j$. This means that for steep pdfs (assuming all λ_i^2 are small), the P_{ij} for $i \neq j$ are suppressed in λ^2 compared to P_{ii}. Moreover, any polynomial functions of z in $P_{ii}(z)$ can be evaluated at $z = 1$, up to power corrections in λ^2. The result is endpoint AP kernels, given at NLL accuracy by

$$\frac{\alpha_s}{\pi} P_{ij}(z) = \left[2\,\Gamma_{\mathrm{cusp}}\,\mathbf{T}_i^2 \left(\frac{1}{1-z}\right)_+ + \gamma_i\,\delta(1-z)\right]\delta_{ij}\,. \qquad (3.26)$$

3.4 Consistency of Threshold Resummation

As discussed in Chapter 2 threshold resummation can be derived using effective field theory methods. Using SCET, and assuming $1 - z \sim \lambda^2 \ll 1$ as well as $\mathrm{d}\sigma = f \otimes f \otimes \mathrm{d}\hat{\sigma}$, one can derive a factorization theorem for a generic differential cross section. One check of this factorization theorem is consistency, which is the μ independence of the factorized result. In Chapter 2 we showed the consistency of our factorization theorem using the partonic definition of the pdfs $f_i(x;\mu) = \delta(1-x)$. Since we have just shown that away from the true hadronic endpoint it is the functional form of the pdfs that defines the expansion parameter λ, we wish to repeat this proof using the full functional form, subject only to the constraint of large steepness (or small λ).

We start from the derivative with respect to $\ln\mu$ of the factorized differential cross section derived in Chapter 2, together with the anomalous dimensions for the hard, jet, and soft functions, given in the same reference. Using the result of Section 3.3 for the Altarelli-Parisi splitting kernel, and performing trivial integrations and cancellation, we find

$$\begin{aligned}
\frac{\mathrm{d}\sigma}{\mathrm{d}\,\ln\mu} \propto \int \mathrm{d}Y f_1(\sqrt{\tau}e^{Y}) f_2(\sqrt{\tau}e^{-Y}) \\
\Bigg[\mathbf{T}_1^2\,\ln\frac{\omega_1}{\sqrt{\hat{s}}} + \mathbf{T}_2^2\,\ln\frac{\omega_2}{\sqrt{\hat{s}}} \\
+ \sum_{\langle i,j\rangle} \mathbf{T}_i\cdot\mathbf{T}_j\,\ln\frac{\tilde{n}_i\cdot\tilde{n}_j}{n_i\cdot n_j} + \sum_{i\in\{\text{jets}\}} \mathbf{T}_i^2\,\ln\frac{\omega_i}{\tilde{\omega}_i} \\
+ \mathbf{T}_1^2\Bigg(\int_{\sqrt{\tau}e^{Y}}^1 \mathrm{d}w_1 \frac{f_1\left(\frac{\sqrt{\tau}e^{Y}}{w_1}\right)}{f_1(\sqrt{\tau}e^{Y})}\frac{1}{(1-w_1)_+} \\
- \int_{\tau e^{|2Y|}}^1 \mathrm{d}z\,\frac{f_1\left(\sqrt{\frac{\tau}{z}}e^{Y}\right) f_2\left(\sqrt{\frac{\tau}{z}}e^{-Y}\right)}{f_1\left(\sqrt{\tau}e^{Y}\right) f_2\left(\sqrt{\tau}e^{-Y}\right)}\frac{1}{(1-z)_+}\Bigg) \\
+ \mathbf{T}_2^2\Bigg(\int_{\sqrt{\tau}e^{-Y}}^1 \mathrm{d}w_2 \frac{f_2\left(\frac{\sqrt{\tau}e^{-Y}}{w_2}\right)}{f_2(\sqrt{\tau}e^{-Y})}\frac{1}{(1-w_2)_+} \\
- \int_{\tau e^{|2Y|}}^1 \mathrm{d}z\,\frac{f_1\left(\sqrt{\frac{\tau}{z}}e^{Y}\right) f_2\left(\sqrt{\frac{\tau}{z}}e^{-Y}\right)}{f_1\left(\sqrt{\tau}e^{Y}\right) f_2\left(\sqrt{\tau}e^{-Y}\right)}\frac{1}{(1-z)_+}\Bigg)\Bigg]\,. \qquad (3.27)
\end{aligned}$$

The first line in Eq. (3.27) can be shown to vanish using the identity

$$\sum_{\langle i,j\rangle} \mathbf{T}_i\cdot\mathbf{T}_j\,\ln\frac{\tilde{n}_i\cdot\tilde{n}_j}{n_i\cdot n_j} = \sum_{i\in\{\text{partons}\}} \mathbf{T}_i^2\,\ln\frac{\tilde{\omega}_i}{\omega_i}\,. \qquad (3.28)$$

The first term in the second line can be made identical to the second term through the substitution $Y' = Y - \frac{1}{2}\log w_1$, followed by the relabeling $Y' \to Y$. Thus these two terms cancel, and using a similar substitution $Y' = Y + \frac{1}{2}\log w_2$, with the same relabeling, the third line vanishes as well. Thus, we find

$$\frac{\mathrm{d}\sigma}{\mathrm{d}\,\ln\mu} = 0 + \mathcal{O}(\lambda^2)\,, \qquad (3.29)$$

and therefore consistency of the factorization formula. Note that in both cases $Y' = Y + \mathcal{O}(\lambda^2)$, which means we can be differential in Y, up to power corrections in λ^2, and still have consistency.

3.5 Numerical Results for λ^2

Now that we have defined a measure of steepness, it is a simple matter to determine numerically what λ^2 is for the physical pdfs and parton luminosities. In this section, we will give our results and discuss their implications for the relevance of threshold resummation. As discussed above, the expansion parameter for threshold resummation is given by λ^2, and we make the assumption that this expansion becomes reliable for $\lambda^2 < 0.25$. Note that while this value is chosen somewhat ad-hoc, it serves to assess the importance of threshold resummation.

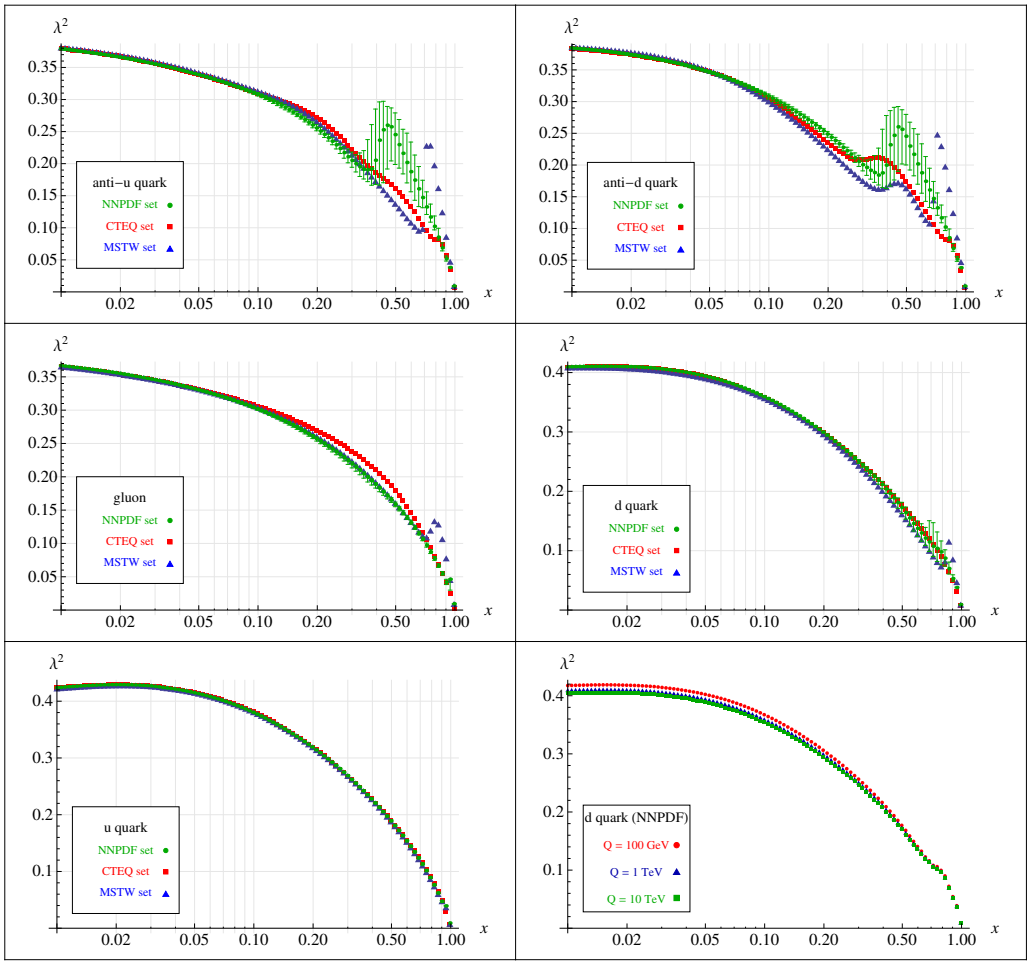

Figure 3.2: The value of λ^2 for single pdfs as a function of x, as defined in Eq. (3.12).

There are two different types of objects for which steepness is a necessary ingredient of our factorization theorem. The first is individual pdfs, where $\lambda^2 \ll 1$ allows us to use endpoint AP kernels in determining the consistency of our factorization theorem. The second is parton luminosities, in the form of two pdfs which

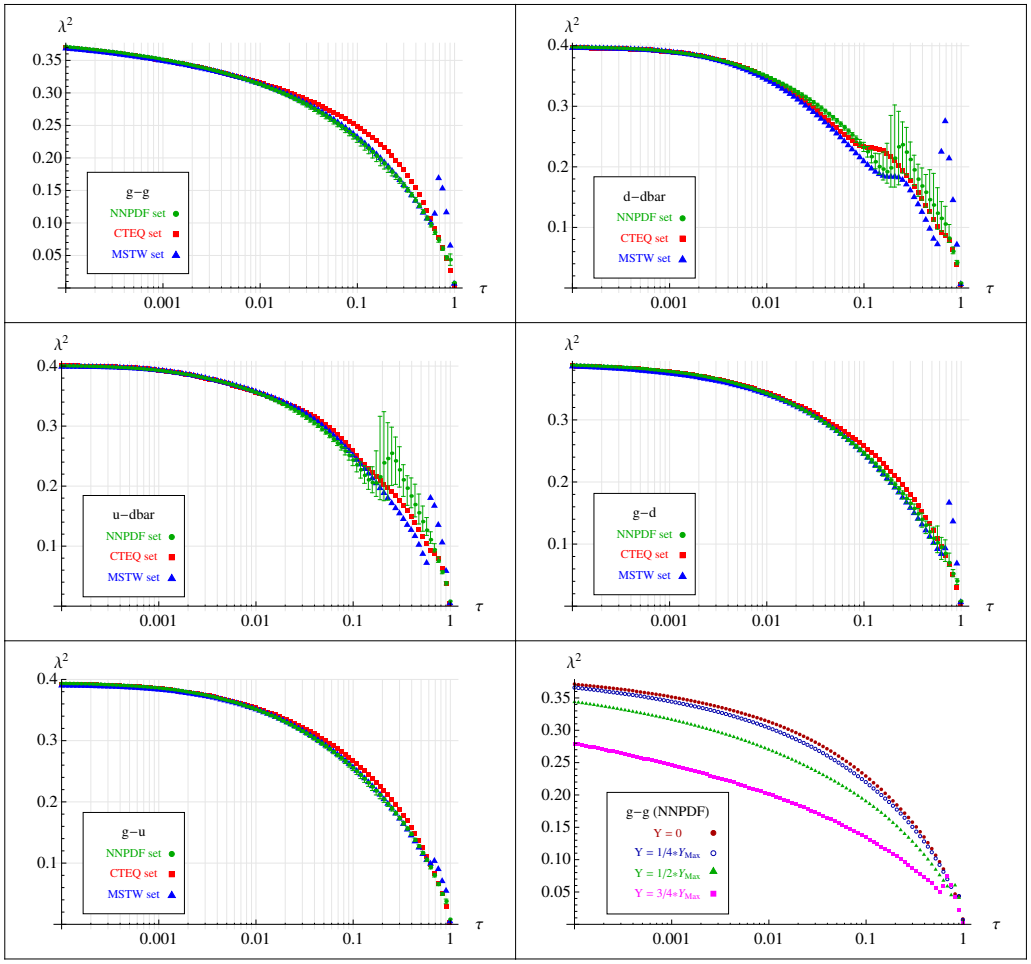

Figure 3.3: The value of λ^2 for a selection of parton luminosities as a function of τ, as defined in Eq. (3.11).

are convolved in Y and z. Since it is possible to be differential in Y up to power corrections in λ^2 (see Section 3.4), we will focus on the case where Y is fixed and z is the only convolution variable. We will present plots using the CTEQ6.6 [100], MSTW2008NLO [96] and NNPDF2.0 [16] pdf sets, with a default renormalization scale of 1 TeV. To study the uncertainties in our predictions for λ, we use the 100 replica set provided by NNPDF2.0. The central value is given by the median of the results, while the error bars show the range where 68% of the points lie, with equal number of points on either side of the median.

In Figure 3.2 we present the value of λ^2 for a single pdfs as a function of x, as defined in Eq. (3.12), which characterizes how important the non-singular terms in the AP evolution kernels are. In each plot we show the result for CTEQ, MSTW and NNPDF sets, with errors presented for the NNPDF set. One clearly sees that the value of λ^2 is decreasing as $x \to 1$, as expected, and that λ^2 is small not only in the region where $1 - x \ll 1$ but for smaller values of x as well. Irrespective of the type of parton, the value of λ becomes smaller than 0.25 for $x > 0.3$, implying that in that region the singular AP evolution kernel becomes a reasonable approximation to QCD, even though $1 - x = \mathcal{O}(1)$. The feature in the sea-quark distributions for $x \sim 0.5$ is due to the steepness falling off in the measured pdfs, giving a rising value of λ^2, which then gets forced to zero due to x approaching 1. In the lower right plot of Figure 3.2, we illustrate the dependence of steepness on the renormalization scale of the pdfs. Between 100 GeV and 10 TeV, there is at most an $\mathcal{O}(5\%)$ variation, while for most values of x the variation is $\mathcal{O}(1\%)$. In this plot, we only present the results for the down quark, however, the effect is similar ($\mathcal{O}(1 - 5\%)$) for all other pdfs.

Next, we study the value of λ^2 as obtained from the convolution of two pdfs, as defined in Eq. (3.11). The results are shown in Figure 3.3 for $Y = 0$. While the distributions in general do not peak exactly at $Y = 0$, the peak is sufficiently close to this value for these plots to illustrate the observed behavior. Again we show the result for CTEQ, MSTW and NNPDF sets, with errors presented for the NNPDF set. The value of λ^2 becomes less that 0.25 for $\tau > 0.05 - 0.1$. This implies that threshold resummation is not limited to the region where $1 - \tau \ll 1$, however, for most values of phenomenological interest, the power corrections are potentially large. In the lower right hand side of Figure 3.3 we show the variation of steepness with Y, presented as a function of $Y_{\max} = -(1/2) \ln \tau$. While this variation is considerable, one should keep in mind that the majority of the phase space is close to $Y = 0$. The variation of λ^2 with renormalization scale is not shown for the parton luminosities, but is similar to the result for the single pdfs.

Chapter 4

A Subtraction Method for Soft Function Calculations

4.1 Introduction

In this section, we present a method to calculate the soft function in soft-collinear effective theory to NLO for N-jet events, defined with respect to arbitrarily complicated observables and algorithms, using a subtraction-based method. We show that at one loop the singularity structure of most observable/algorithm combinations can be classified as one of two types. Type I jets include jets defined with inclusive algorithms for which a jet shape is measured. Type II jets include jets found with exclusive algorithms, as well as jets for which only the direction and energy are measured. Cross sections that are inclusive over a certain region of phase space, such as the forward region at a hadron collider, are examples of Type II jets. We show that for a large class of measurements the required subtractions are already known analytically, including traditional jet shape measurements at hadron colliders.

The first step in resummation in SCET is to factorize an N-jet cross section into hard, jet, and soft functions

$$\mathrm{d}\sigma_N \quad \sim \quad B_N \, H_N \times [J\,]^n \otimes S_N \,. \tag{4.1}$$

Here B_N denotes the Born-level cross section in full QCD, H_n reproduces the virtual corrections of full QCD, while the J's and S_n together encode real emission diagrams in the collinear and soft limits. There is one jet function for each jet in the final state, and both the jet and soft functions depend on the algorithm used to define the jets, as well as the observables measured. Note that Equation (4.1) must be modified in the case of hadron collisions, since there will also be PDFs and, for some measurements, beam functions [113]. At tree level, the hard, jet, and soft functions are trivial, but each has to be calculated order by order in perturbation theory.

The simplest jet definition involves exactly two jets, each consisting of all particles in one of the two hemispheres defined by a plane perpendicular to the thrust axis, and

is typically only used in e^+e^- collisions. In this case resummation has been achieved at NNNLL [36].

For more complicated jet definitions, however, the required calculations are more involved, and in many cases we do not know the NLO results for the jet and soft functions. One counter example is cone or inclusive k_T-type algorithms in e^+e^- collisions, where the distance measure is the angle θ of each particle with respect to the jet axis, and the total energy outside of the jets is less than Λ. For this example, the jet and soft functions are known to $\mathcal{O}(\alpha_s)$ [66].

Unlike for e^+e^-, jet definitions at hadron colliders are usually required to be boost invariant. As a result, distance is usually measured in η-ϕ space, where η and ϕ are defined with respect to the beam axis, and there is a restriction on the total $|\mathbf{p}_\mathrm{T}|$ outside of jets, rather than energy. The absence of results for more complicated phase space configurations has been one of the biggest hurdles in deriving more precise predictions for jet cross sections at hadron colliders. The solution to this problem is the topic of the current section.

4.2 Notation and Definitions

4.2.1 The Soft Function in SCET

A soft function in SCET takes the general form

$$S(\mathcal{A};\mathcal{M};\sigma_1,\dots\sigma_n) = \left\langle 0 \left| \mathcal{Y}_s\, \mathcal{O}_s(\mathcal{A};\mathcal{M};\sigma_1,\dots\sigma_n)\, \mathcal{Y}_s^\dagger \right| 0 \right\rangle . \tag{4.2}$$

Here $\mathcal{Y}_s$ denotes a set of soft Wilson lines, which arise in SCET from the BPS field redefinition [30] that decouples the interactions of collinear and soft degrees of freedom. The function $\mathcal{O}_s$ denotes an operator insertion, which determines how a given soft particle contributes to the observables σ_i. This operator depends on the details of the jet algorithm $\mathcal{A}$, which assigns soft particles to a given jet, and on the definition of the measurement $\mathcal{M}$. Note that the soft function at tree level is completely trivial,

$$\mathcal{S}^{(0)}(\mathcal{A};\mathcal{M};\sigma_1,\dots\sigma_n) = \delta(\sigma_1)\dots\delta(\sigma_n)\,, \tag{4.3}$$

such that it is independent of the algorithm and the details of the measurement. At higher orders, the jet algorithm introduces highly non-trivial dependence on the final state momentum, even at one loop.

Soft functions in SCET are most conveniently calculated in pure dimensional regularization. Since no additional scales are introduced into the problem, all expressions that do not contain external scales vanish identically. This implies that all purely virtual diagrams at higher loop order vanish exactly, and only diagrams that include real emissions need to be considered. The momentum of the real emission is called q in the following.

We will restrict ourselves to shape-type observables, where σ_i is a smooth function of the particles' momenta assigned to jet i. We will only be concerned with observables that are defined to be positive semi-definite and such that $\sigma_i \to 0$ in both the soft and collinear limits. We also ignore power correction that vanish as $\sigma_i \to 0$. At one-loop, this allows us to write

$$\mathcal{O}_s(q; \mathcal{A}; \mathcal{M}; \sigma_1, \ldots \sigma_n) = \sum_{k=0}^{N} \Theta_{\mathcal{A}}^k(q)\, \Delta_{\text{meas}}^k(q; \sigma_1, \ldots \sigma_n)\,. \tag{4.4}$$

Here $\Theta_{\mathcal{A}}^i(q)$ restricts the momenta q to be part of jet i and $\Theta_{\mathcal{A}}^0(q)$ restricts q to be outside of all jets (while also including any out-of-jet veto such as an energy or p_T cutoff). The function $\Delta_{\text{meas}}^k(q; \sigma_1, \ldots \sigma_n)$ measures an observable in jet k, while setting the observables in the other jets to zero

$$\Delta_{\text{meas}}^k(q; \sigma_1, \ldots \sigma_n) = \delta\left(\sigma_k - \sigma_k(q)\right) \prod_{l \neq k} \delta\left(\sigma_l\right)\,. \tag{4.5}$$

Note that for a jet where no jet shape is measured, $\Delta_{\text{meas}}^k = \prod_l \delta(\sigma_l)$.

Putting this information together, the soft function at one-loop can therefore be written as

$$\mathcal{S}^{(1)}(\mathcal{A}; \mathcal{M}; \sigma_1, \ldots \sigma_n) = \sum_k \sum_{\langle i,j \rangle} \int \frac{\mathrm{d}^{d-1}q}{(2\pi)^{d-1} 2E_q} N_{ij}(q) \Theta_{\mathcal{A}}^k(q) \Delta_{\text{meas}}^k(q; \sigma_1, \ldots \sigma_n)\,, \tag{4.6}$$

where N_{ij} is defined as

$$N_{ij}(q) = -g^2 \mu^{2\epsilon}\, \mathbf{T}_i \cdot \mathbf{T}_j\, \frac{n_i \cdot n_j}{n_i \cdot q\; n_j \cdot q}\,, \tag{4.7}$$

where $n_i = (1, \mathbf{n}_i)$ are the jet directions and $\mathbf{T}_i$ are the color charges of the jets (in the notation of Ref. [47]). In Equation (4.6), for each jet we sum over all pairs of soft emission sources i and j, which includes the jets and, in the case of hadron collisions, the beams.

We can define moments of the soft function with respect to the σ_k as

$$\langle \sigma_k^n \rangle \equiv \prod_l \int_0^{\sigma_k^{\max}} \mathrm{d}\sigma_l \left(\frac{\sigma_k}{\sigma_k^{\max}}\right)^n \mathcal{S}\left(\mathcal{A}; \mathcal{M}; \{\sigma_m\}\right)\,, \tag{4.8}$$

where $\sigma_k^{\max}$ is the maximum allowed value for the observable σ_k. Note that we are suppressing the dependence of the moments on the algorithm and measurement. At one loop, the moments of the soft function are given by

$$\langle \sigma_k^n \rangle = \sum_{\langle i,j \rangle} \int \frac{\mathrm{d}^{d-1}q}{(2\pi)^{d-1} 2E_q} N_{ij}(q)\, \mathcal{I}_k^n(\mathcal{A}; \mathcal{M}; q)\,, \tag{4.9}$$

where $\mathcal{I}_k^n$ is defined as

$$\mathcal{I}^0(\mathcal{A};\mathcal{M};q) = \Theta^0_{\mathcal{A}}(q) + \sum_{k\in\{\text{meas}\}} \Theta^k_{\mathcal{A}}(q)\,\theta(\sigma_k(q) < \sigma_k^{\max}) + \sum_{k\notin\{\text{meas}\}} \Theta^k_{\mathcal{A}}(q)\,, \tag{4.10}$$

for the zeroth moment and

$$\begin{aligned}\mathcal{I}^{n>0}_{k\in\{\text{meas}\}}(\mathcal{A};\mathcal{M};q) &= \Theta^k_{\mathcal{A}}(q)(\sigma_k(q)/\sigma_k^{\max})^n\,\theta(\sigma_k(q) < \sigma_k^{\max})\,,\\ \mathcal{I}^{n>0}_{k\notin\{\text{meas}\}}(\mathcal{A};\mathcal{M};q) &= 0\,,\end{aligned} \tag{4.11}$$

for the higher moments. Here we have omitted the subscript on the zeroth moment, since there is only one for all k. The label "$k \in \{\text{meas}\}$" refers to the set of jets where a shape has been measured and "$k \notin \{\text{meas}\}$" refers to the set of unmeasured jets.

The soft function defined in Equation (4.6) is a distribution in the various σ_k, which can be written in terms a delta function $\delta(\sigma_k)$ and the distributions $\mathcal{L}_m(\sigma_k/\sigma_k^{\max})$, where

$$\mathcal{L}_m(x) \equiv \left[\frac{\theta(x)\log^m(x)}{x}\right]_+\,, \tag{4.12}$$

where the '+' function is defined as distribution that, when integrated against smooth test functions $f(x)$, gives

$$\int_a^b \left[\frac{\theta(x)\log^m(x)}{x}\right]_+ f(x) = \int_a^b \frac{\theta(x)\log^m(x)}{x}[f(x) - \theta(a\le 0)f(0)]\,. \tag{4.13}$$

It is straightforward to show that at one loop the soft function can be written in terms of its moments as

$$\begin{aligned}\mathcal{S}^{(1)}\left(\mathcal{A};\mathcal{M};\sigma_1,\ldots\sigma_n\right) =& \langle\sigma^0\rangle \prod_k \delta\left(\sigma_k\right) \\ &+ \sum_k \left[4\langle\sigma_k^2\rangle - \langle\sigma_k^1\rangle\right]\frac{\theta(\sigma_k < \sigma_k^{\max})}{\sigma_k^{\max}}\mathcal{L}_0\left(\frac{\sigma_k}{\sigma_k^{\max}}\right)\prod_{l\neq k}\delta\left(\sigma_l\right) \\ &+ \sum_k \left[4\langle\sigma_k^2\rangle - 2\langle\sigma_k^1\rangle\right]\frac{\theta(\sigma_k < \sigma_k^{\max})}{\sigma_k^{\max}}\mathcal{L}_1\left(\frac{\sigma_k}{\sigma_k^{\max}}\right)\prod_{l\neq k}\delta\left(\sigma_l\right)\,.\end{aligned} \tag{4.14}$$

As mentioned above, we are assuming the is soft and collinear limits give $\sigma_k \to 0$ and we are dropping power corrections that vanish in this limit.

We finish this section with an example of jet algorithm and jet measurement. For a cone algorithm of size R at an e^+e^- collider, where the out-of-jet energy is restricted to be less than Λ, we have

$$\Theta^k_{\text{cone}}(q) = \theta\left(\frac{n_k\cdot q}{\bar{n}_k\cdot q} < \tan^2\frac{R}{2}\right)\,, \qquad \Theta^0_{\text{cone}}(q) = \left(1 - \sum_{k=1}^n \Theta^k_{\text{cone}}(q)\right)\theta(E_q < \Lambda)\,. \tag{4.15}$$

SCET is applicable only for *exclusive* N-jet cross-sections. This means that there must be a veto on out-of-jet soft radiation, which can be for example an energy or a p_T cut. All such vetoes can be formulated as a direction-dependent restriction on the out-of-jet energy. That is,

$$\Theta^0_{\mathcal{A}}(q) = \left(1 - \sum_{k=1}^{n} \Theta^k_{\mathcal{A}}(q)\right) \theta(E_q < E^{\rm cut}(\Omega_q)) \,. \tag{4.16}$$

One set of jet measurements which satisfies the criteria mentioned above are the angularities [39], which are parametrized by a continuous, real parameter a. When restricted to jets, multiple conventions can be used for the definition (cf. Refs. [5], [66]). We take the convention of Ref. [66], which gives that the contribution from a single emission of momentum q is

$$\tau^k_a(q) = \frac{1}{\omega_k} (n_k \cdot q)^{1-a/2} (\bar{n}_k \cdot q)^{a/2} \,, \tag{4.17}$$

where ω_k is an arbitrary normalization (with units of energy). We restrict $a < 2$ for infrared safety. We will find that angularities form a basis for a very wide class of phenomenologically relevant observables.

4.2.2 The Classification of Jets: Type I vs. Type II

We can think of a jet algorithm $\mathcal{A}$ as defining a region $\mathcal{R}_k(\mathcal{A}; E_q)$ in θ-ϕ space, such that a particle with energy E_q and $\Omega_q \in \mathcal{R}_k(\mathcal{A}, E_q)$ belongs to jet k. Similarly, a measurement $\mathcal{M}$ defines a region $\mathcal{R}_k(\mathcal{M}, \sigma; E_q)$ in θ-ϕ space, for which a particle with energy E_q and $\Omega_q \in \mathcal{R}_k(\mathcal{M}, \sigma; E_q)$ gives a value of the observable σ_k satisfying $\sigma_k < \sigma$.

As an example, for a cone algorithm of size R

$$\mathcal{R}_k(\text{cone}; E_q) = \{\theta_{q,k} < R\} \,, \tag{4.18}$$

where $\theta_{q,k}$ is the angle of q with respect to the direction of jet k and the quantity in braces on the right-hand side refers to the set of all points points in θ-ϕ space that lie within an angle R of the axis of jet k. For the jet thrust observable (thrust T is related to the $a = 0$ angularity discussed above via $\tau_0 = 1 - T$), we have

$$\mathcal{R}_k(\text{thrust}, \sigma; E_q) = \left\{\theta_{q,k} < \arccos\left(1 - \frac{\omega_k \, \sigma}{E_q}\right)\right\} \,. \tag{4.19}$$

In this work, we will consider two broad classes of jets, which we label as Type I and Type II. They are defined as:

$$\underline{\text{Type I}}: \quad \lim_{E_q \to \infty} \mathcal{R}_k(\mathcal{M}, \sigma; E_q) \subset \lim_{E_q \to \infty} \mathcal{R}_k(\mathcal{A}; E_q) \quad \forall \, \sigma \,, \tag{4.20a}$$

$$\underline{\text{Type II}}: \quad \lim_{E_q \to \infty} \mathcal{R}_k(\mathcal{A}; E_q) \subset \lim_{E_q \to \infty} \mathcal{R}_k(\mathcal{M}, \sigma; E_q) \quad \forall \, \sigma \,. \tag{4.20b}$$

Jets where no observable is measured are clearly included in Type II.

In terms of the notation introduced in Section 4.2.1, for Type I jets we have, by definition,

$$\lim_{E_q\to\infty} \Theta^k_{\mathcal{A}}(q)\,\theta(\sigma_k(q) < \sigma_k^{\max}) = \lim_{E_q\to\infty} \theta(\sigma_k(q) < \sigma_k^{\max})\ , \tag{4.21}$$

while for Type II jets

$$\lim_{E_q\to\infty} \Theta^k_{\mathcal{A}}(q)\,\theta(\sigma_k(q) < \sigma_k^{\max}) = \lim_{E_q\to\infty} \Theta^k_{\mathcal{A}}(q)\,. \tag{4.22}$$

It is important to note that this definition implies that for Type I jets the divergent part of the one loop contribution, and therefore the anomalous dimension, is independent of the jet algorithm. Conversely, for Type II jets, the anomalous dimension is independent of the observable. For these jets, the divergent part of the one loop contribution is proportional to $\delta(\sigma_k)$, which means the higher moments are finite.

While it may seem that these two classes are restrictive, in reality they include many if not most of the phenomenologically relevant observable/algorithm combinations.

4.2.3 Soft Functions via Subtractions

The goal of this section is to express an unknown (target) soft function in terms of a known (subtraction) soft function and a numerically calculable difference. As discussed earlier, a general soft function is most easily expressed in terms of its moments. If two soft functions agree on which jets are measured and on $\sigma_k^{\max}$ for each jet, we can write

$$\begin{aligned}
&\mathcal{S}^{(1)}\left(\mathcal{A},\mathcal{M};\sigma_1,\ldots\sigma_n\right) = \widetilde{\mathcal{S}}^{(1)}\left(\widetilde{\mathcal{A}},\widetilde{\mathcal{M}};\sigma_1,\ldots\sigma_n\right) \\
&+ \mathcal{D}^0\prod_k \delta\left(\sigma_k\right) + \sum_{k=1}^{n}\left[4\mathcal{D}_k^2 - \mathcal{D}_k^1\right]\frac{1}{\sigma_k^{\max}}\mathcal{L}_0\left(\frac{\sigma_k}{\sigma_k^{\max}}\right)\prod_{l\neq k}\delta\left(\sigma_l\right) \\
&+ \sum_{k=1}^{n}\left[4\mathcal{D}_k^2 - 2\mathcal{D}_k^1\right]\frac{1}{\sigma_k^{\max}}\mathcal{L}_1\left(\frac{\sigma_k}{\sigma_k^{\max}}\right)\prod_{l\neq k}\delta\left(\sigma_l\right)\ .
\end{aligned} \tag{4.23}$$

Here $\mathcal{D}_k^n$ is defined as the difference of two moments

$$\mathcal{D}_k^n \equiv \langle\sigma_k^n\rangle - \widetilde{\langle\sigma_k^n\rangle} = \sum_{\langle i,j\rangle}\int\frac{\mathrm{d}^3q}{(2\pi)^3 2E_q}N_{ij}(q)\left[\mathcal{I}_k^n(\mathcal{A};\mathcal{M};q) - \mathcal{I}_k^n(\widetilde{\mathcal{A}};\widetilde{\mathcal{M}};q)\right]\ , \tag{4.24}$$

where the limit $d = 4$ has been taken.

The result in Equation (4.23) describes an ideal subtraction. However, it may be possible to take a known result and convert to a suitable form. The first possible issue

is that the subtraction and the target disagree as to which jets are measured. Since we need the subtraction to have the same number of observables as the target, the subtraction must be modified. For jets that are measured in the target and not the subtraction, we can simply multiply by a delta function, such that the subtraction is now a function of these variables. For jets that are measured in the subtraction and not the target, we need to somehow remove the extra variables from the subtraction. The simplest way to do this is to integrate the offending variables from 0 to $\widetilde{\sigma}^{\max}$.

The second possible issue is that, for one or more jets, the target and subtraction both measure the jet, but disagree as to $\sigma^{\max}$. In this case, the two soft functions have different regions of support and we cannot write the target in terms of the subtraction and maintain the form in Equation (4.14). In order to solve this problem, we can remove the dependence of the subtraction on $\sigma^{\max}$ by removing the $(1/\sigma)_+$ and $(\log\sigma/\sigma)_+$ terms. To accomplish this goal, we can integrate over σ in the subtraction from 0 to $\widetilde{\sigma}^{\max}$, then multiply by $\delta(\sigma)$. While the two functions will still have different regions of support, the form of Equation (4.14) is achieved due to the fact that the subtraction is now simply proportional to $\delta(\sigma)$.

We can make this procedure somewhat more formal by defining $\{\text{meas}\}$ to be the set of measured jets for the target and $\{\widetilde{\text{meas}}\}$ for the subtraction. The modified subtraction, $\widetilde{\mathcal{S}}^{(1)}_{\text{new}}(\widetilde{\mathcal{A}};\widetilde{\mathcal{M}};\sigma_i\dots\sigma_n)$, is then given by

$$\widetilde{\mathcal{S}}^{(1)}_{\text{new}}(\widetilde{\mathcal{A}};\widetilde{\mathcal{M}};\sigma_1\dots\sigma_n) = \prod_{i\in\{\text{meas}\}\setminus\{\widetilde{\text{meas}}\}}\delta(\sigma_i)\prod_{j\in\{\widetilde{\text{meas}}\}\setminus\{\text{meas}\}}\int_0^{\widetilde{\sigma}_j^{\max}}\mathrm{d}\sigma_j\prod_{k|\sigma_k^{\max}\neq\widetilde{\sigma}_k^{\max}}\delta(\sigma_k) \times\int_0^{\widetilde{\sigma}_k^{\max}}\mathrm{d}\sigma_k\,\widetilde{\mathcal{S}}^{(1)}(\widetilde{\mathcal{A}};\widetilde{\mathcal{M}};\sigma_l\dots\sigma_m)\,. \tag{4.25}$$

Here, $\{\text{meas}\}\setminus\{\widetilde{\text{meas}}\}$ is the relative complement of $\{\widetilde{\text{meas}}\}$ in $\{\text{meas}\}$, *i.e.* all jets measured in the target that are not measured in the subtraction. The sum over k is over all jets were $\sigma_k^{\max}\neq\widetilde{\sigma}_k^{\max}$. The target is now found using Equation (4.23), with $\widetilde{\mathcal{S}}^{(1)}_{\text{new}}$ in place of $\widetilde{\mathcal{S}}^{(1)}$.

4.3 The Divergent Structure of Soft Functions

The moments defined in Equation (4.9) have three types of divergences, arising from singularities in the one-loop integrand $N_{ij}(q)$ defined in Equation (4.7)

1. Collinear divergence: $n_i\cdot n_q\to 0$ or $n_j\cdot n_q\to 0$ (where $n_q^\mu = q^\mu/E_q = (1,\mathbf{n}_q)$ is the direction of q)
2. Soft divergence: $E_q\to 0$
3. UV divergence: $E_q\to\infty$

In order for the difference of two soft functions to be calculable numerically, we need to show that the difference between two moments in Equation (4.24) are finite in $d = 4$. This is most easily done by showing that the different $\mathcal{I}_k^n(\mathcal{A};\mathcal{M};q) - \mathcal{I}_k^n(\widetilde{\mathcal{A}};\widetilde{\mathcal{M}};q)$ multiplying $N_{ij}(q)$ vanishes in all three of the divergent limits.

In the soft limit, where $E_q \to 0$, infrared safety dictates that $\sigma_i(q) \to 0$. This implies that all higher moments (and therefore their differences) vanish

$$\lim_{E_q\to 0} \mathcal{I}_k^{n>0}(\mathcal{A};\mathcal{M};q) = 0\,. \tag{4.26}$$

For the zeroth moment, we can use that for both algorithms the restriction from the observables, as well as out-of-jet restriction becomes trivial

$$\begin{aligned}\lim_{E_q\to 0} \theta(\sigma_k(q) < 1) &= 1\\ \lim_{E_q\to 0} \theta(E_q < E^{\text{cut}}(\Omega_q)) &= 1\,.\end{aligned} \tag{4.27}$$

Using Equation (4.16), this allows to write

$$\begin{aligned}&\lim_{E_q\to 0} \mathcal{I}^0(\mathcal{A};\mathcal{M};q) - \mathcal{I}^0(\widetilde{\mathcal{A}};\widetilde{\mathcal{M}};k)\\ &\quad= \lim_{E_q\to 0}\left\{\left[\Theta^0_{\mathcal{A}}(q) - \Theta^0_{\widetilde{\mathcal{A}}}(q)\right] + \sum_k \left[\Theta^k_{\mathcal{A}}(q) - \Theta^k_{\widetilde{\mathcal{A}}}(q)\right]\right\}\\ &\quad= \lim_{E_q\to 0}\left\{\left[1 - \sum_k \Theta^k_{\mathcal{A}}(q)\right] - \left[1 - \sum_k \Theta^k_{\widetilde{\mathcal{A}}}(q)\right] + \sum_k \left[\Theta^k_{\mathcal{A}}(q) - \Theta^k_{\widetilde{\mathcal{A}}}(q)\right]\right\}\\ &\quad= 0\,.\end{aligned}$$

In the collinear limit, when $n_i \cdot n_q \to 0$, IR safety once again tells us that $\sigma_i(q) \to 0$, which immediately implies

$$\lim_{n_i\cdot n_q\to 0} \mathcal{I}_k^{n>0}(\mathcal{A};\mathcal{M};q) = 0\,. \tag{4.28}$$

In addition, for fixed E_q, any IR-safe algorithm will assign the emission to jet i in this limit, such that $\Theta^k_{\mathcal{A}} \to \delta_{ik}$. Thus, in this limit the difference between zeroth moments becomes

$$\lim_{n_i\cdot n_q\to 0} \mathcal{I}^0(\mathcal{A};\mathcal{M};k) - \mathcal{I}^0(\widetilde{\mathcal{A}};\widetilde{\mathcal{M}};k) = \lim_{n_i\cdot n_q\to 0} \sum_k \left[\delta_{ik} - \delta_{ik}\right] = 0 \tag{4.29}$$

The UV limit, in which $E_q \to \infty$, requires a more careful analysis. As the energy of the gluon goes to infinity, any out-of-jet cut will veto the emission, which means we only need to consider radiation in the jets. In this work, we will only consider Type I and Type II jets. Since these two jet types have a different behavior as $E_q \to \infty$, it

should clear that the difference between two soft functions can never be UV finite if there is disagreement over which jets are Type I versus Type II. Therefore, we assume that both agree on which jets are Type I and Type II.

Using Equations (4.21) and (4.22), we can write for the zeroth moment

$$\lim_{E_q\to\infty} \mathcal{I}^0(\mathcal{A};\mathcal{M};q) - \mathcal{I}^0(\widetilde{\mathcal{A}};\widetilde{\mathcal{M}};q) = \lim_{E_q\to\infty} \Bigg\{ \sum_{k\in \mathrm{I}} \Big[\theta(\sigma_k(q)<1) - \theta(\widetilde{\sigma}_k(q)<1)\Big] + \sum_{k\in \mathrm{II}} \Big[\Theta^k_{\mathcal{A}}(q) - \Theta^k_{\widetilde{\mathcal{A}}}(q)\Big] \Bigg\}, \tag{4.30}$$

while for higher moments we find

$$\lim_{E_q\to\infty} \mathcal{I}^{n>0}_{k\in \mathrm{I}}(\mathcal{A};\mathcal{M};q) = \lim_{E_q\to\infty} \left[\sigma^n_k(q)\,\theta(\sigma_k(q)<1) - \widetilde{\sigma}^n_k(q)\,\theta(\widetilde{\sigma}_k(q)<1)\right], \tag{4.31}$$

for Type I jets and

$$\lim_{E_q\to\infty} \mathcal{I}^{n>0}_{k\in \mathrm{II}}(\mathcal{A};\mathcal{M};q) = \lim_{E_q\to\infty} \left[\sigma^n_k(q)\Theta^k_{\mathcal{A}}(q) - \widetilde{\sigma}^n_k(q)\Theta^k_{\widetilde{\mathcal{A}}}(q)\right], \tag{4.32}$$

for Type II jets.

In order to have finite expressions in the UV, we need the limits in Equations (4.30), (4.31) and (4.32) to be vanishing. This implies that Type I jets must satisfy

$$\lim_{E_q\to\infty} \mathcal{R}(\mathcal{M},\sigma;E_q) = \lim_{E_q\to\infty} \mathcal{R}(\widetilde{\mathcal{M}},\sigma;E_q) \quad \forall\,\sigma\,. \tag{4.33}$$

Note that this must be true for all σ so that Equation (4.31) goes to 0, as well as for our formalism to be independent of normalization. For Type II, the requirement for the second half of Equation (4.30) to cancel is

$$\lim_{E_q\to\infty} \mathcal{R}(\mathcal{A};E_q) = \lim_{E_q\to\infty} \mathcal{R}(\widetilde{\mathcal{A}};E_q)\,. \tag{4.34}$$

Since the anomalous dimension for Type II jets is independent of the observable, at one loop the divergent pieces must be proportional to $\delta(\sigma_i)$. Therefore, Equation (4.32) is finite.

In summary, the differences between moments of the soft function contain no soft or collinear divergences as long as both the jet algorithm and the jet measurement are infrared safe. This fact can be seen as a consequence of the fact that, for IR safe algorithms and measurements, the (scaleless) virtual diagrams should convert the IR divergences in the real emission diagrams to UV divergences, and since the virtual diagrams are universal, any divergence in the difference between two soft functions must be of UV origin. However, we have also seen that the UV divergences are the same for all soft functions that have the same classes of jets, since the measurement regions become equal for Type I jets and the algorithm regions become equal for Type II in the limit $E_q \to \infty$.

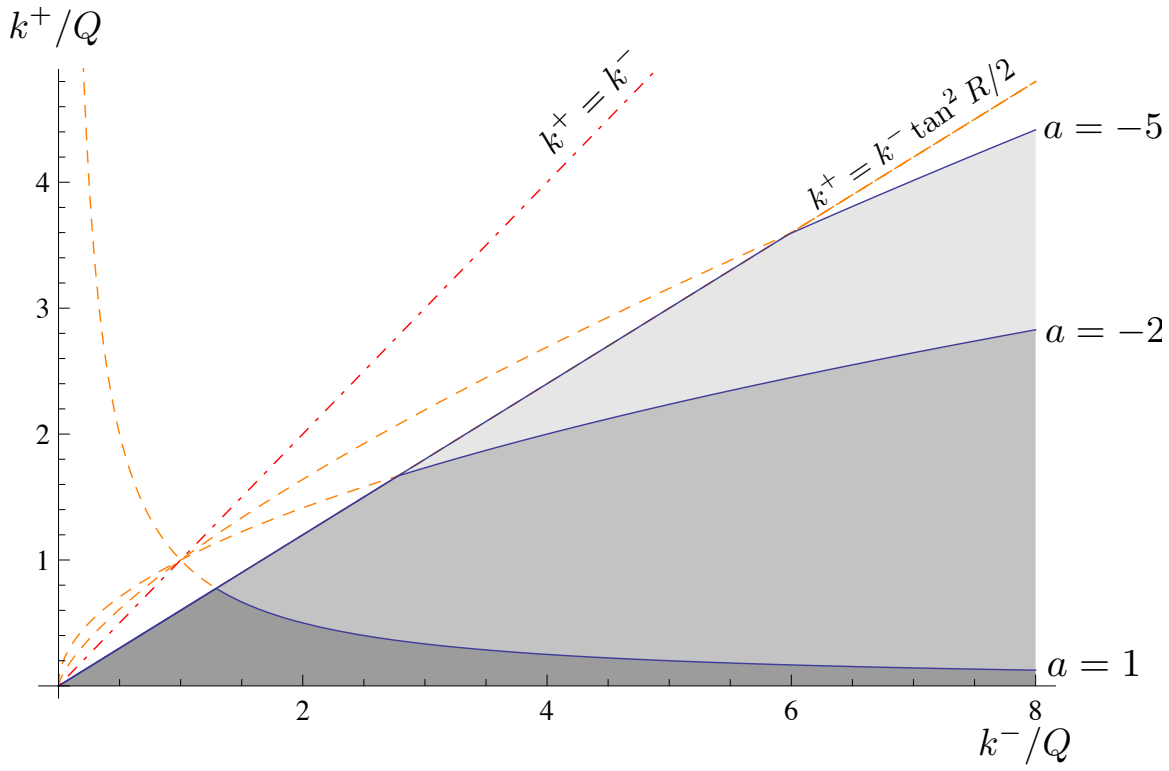

Figure 4.1: The regions of integration over q when q is restricted both to be within an inclusive-type jet (cone or inclusive k_T, anti-k_T, or CA) of size R (or R') and to have a measurement $\sigma_k < 1$ when $\sigma_k = \tau_k^a$ (angularity) as a function of a in both the (a) $q^+ - q^-$ and (b) $E_q - \theta$ planes. Regardless of the choice of R, the measurement restriction is dominant in the UV (that is, in the limit (a) $q^\pm \to \infty$ or (b) $E_q \to \infty$, $\theta_q \to 0$). Also, all measurements that correspond to a smooth, monotonic curve in these planes will asymptote to an angularity curve for some a (and some choice of ω_k) in the UV. For measurements that depend on this azimuthal angle ϕ about the jet axis, the above is true for each value of ϕ.

4.4 Subtractions for Inclusive Algorithms and Azimuthally-symmetric Shapes

While the discussion so far has been rather general, there is an important special case we will discuss now, which will serve to illustrate our method. For inclusive algorithms (*e.g.* anti-k_T) and measurements whose minimum is when all particles in the jet are collinear (*e.g.* jet thrust), the calculations in [66] can be used to construct a subtraction. In [66] the soft function was calculated for an arbitrary number of soft Wilson lines under the following conditions:

- The jet algorithm is a cone or inclusive k_T-type algorithm, where the distance measure is the angle θ-ϕ space
- The total energy outside of all jets is less than Λ
- For each jet one measures either the angularity of all particles in the jet, or the jet remains unmeasured

In other words, the jet algorithm in the soft sector satisfies

$$\Theta^k_{\text{cone}}(q) = \theta\left(\frac{n_k\cdot q}{\bar{n}_k\cdot q} < \tan^2\frac{R}{2}\right), \qquad \Theta^0_{\text{cone}}(q) = \left(1 - \sum_{k=1}^{n}\Theta^k_{\text{cone}}(q)\right)\theta(E_q < \Lambda)\,, \tag{4.35}$$

while the jet can either be unmeasured or the measurement is

$$\sigma_k \equiv \tau_k^a = \frac{1}{\omega_k}(n_k\cdot q)^{1-a/2}(\bar{n}_k\cdot q)^{a/2} = \frac{E_q}{\omega_k}\tau_k^a(\Omega_q)\,. \tag{4.36}$$

One important simplification of a cone or inclusive k_T-type jet algorithms is that at one loop, in the soft region, these algorithms only depend on the angle between the soft gluon and the jet axis, and not on the energy of this gluon

$$\Theta^k_{\vec{\mathcal{A}}}(q) = \Theta^k_{\vec{\mathcal{A}}}(\Omega_q)\,. \tag{4.37}$$

Assuming the same is true for the target algorithm, we can perform the integral over the gluon energy analytically. Note that Equation (4.37) implies that the region $\mathcal{R}(\mathcal{A};E)$ does not change in the $E\to\infty$ limit. Therefore Type II jets only consist of unmeasured jets, since $\mathcal{R}(\mathcal{M},\sigma;E)$ goes to 0 in this limit. Furthermore, for the difference between the target and the subtraction to be finite, $\mathcal{R}(\mathcal{A};E) = \mathcal{R}(\widetilde{\mathcal{A}};E)$ in the limit $E\to\infty$ for Type II jets (see Section 4.3). Since we are assuming $\mathcal{R}(\mathcal{A};E)$ does not change in this limit, we know that for all Type II jets, the algorithm must

be identical. This allows us to write

$$\mathcal{D}^0 = \frac{1}{2}\sum_{\langle i,j\rangle}\int\frac{\mathrm{d}\Omega_q}{(2\pi)^3}N_{ij}(\Omega_q)\int\frac{\mathrm{d}E_q}{E_q}\Bigg\{\Big[\Theta^0_{\mathcal{A}}(q)-\Theta^0_{\mathrm{cone}}(q)\Big] + \sum_{k\in\mathrm{I}}\left[\Theta^k_{\mathcal{A}}(\Omega_q)\theta\left(E_q<\frac{\omega_k}{\sigma_k(\Omega_q)}\right)-\Theta^k_{\mathrm{cone}}(\Omega_q)\theta\left(E_q<\frac{\omega_k}{\tau^a_k(\Omega_q)}\right)\right]\Bigg\}$$

$$\mathcal{D}^{n>0}_{k\in\mathrm{I}} = \frac{1}{2}\sum_{\langle i,j\rangle}\int\frac{\mathrm{d}\Omega_q}{(2\pi)^3}N_{ij}(\Omega_q)\int\frac{\mathrm{d}E_q}{E_q}\frac{E_q^n}{\omega_k^n}\Bigg[\sigma^n_k(\Omega_q)\Theta^k_{\mathcal{A}}(\Omega_q)\theta\left(E_q<\frac{\omega_k}{\sigma_k(\Omega_q)}\right) - \left[\tau^a_k(\Omega_q)\right]^n\Theta^k_{\mathrm{cone}}(\Omega_q)\theta\left(E_q<\frac{\omega_k}{\tau^a_k(\Omega_q)}\right)\Bigg]$$

$$\mathcal{D}^{n>0}_{k\in\mathrm{II}} = 0\,. \tag{4.38}$$

where the form of the target observables, $\sigma_k(q)=\frac{E_q}{\omega_k}\sigma_k(\Omega_q)$, is dictated by IR safety, with ω_k as an external normalization scale that makes σ_k dimensionless. Here we have assumed that all σ_k are unbounded, which is typical for Type I jets, such that $\sigma_k^{\max}=1$ and the functions $\theta(\sigma_k<\sigma_k^{\max})$ are dropped. Since the normalization for angularities is arbitrary, we have set it to be the same as the normalization for the target observables.

After performing the integral over the gluon energy, we can show

$$\mathcal{D}^0 = \frac{1}{2}\sum_{\langle i,j\rangle}\int\frac{\mathrm{d}\Omega_q}{(2\pi)^3}N_{ij}(\Omega_q)\Bigg\{\left[1-\sum_k\Theta^k_{\mathcal{A}}(\Omega_q)\right]\log\frac{E_{\mathrm{cut}}(\Omega_q)}{\Lambda} + \sum_{k\in\mathrm{I}}\left[\Theta^k_{\mathcal{A}}(\Omega_q)\log\frac{\omega_k}{\Lambda\sigma_k(\Omega_q)}-\Theta^k_{\mathrm{cone}}(\Omega_q)\log\frac{\omega_k}{\Lambda\tau^a_k(\Omega_q)}\right]\Bigg\}$$

$$\mathcal{D}^{n>0}_{k\in\mathrm{I}} = \frac{1}{2}\sum_{\langle i,j\rangle}\int\frac{\mathrm{d}\Omega_q}{(2\pi)^3}N_{ij}(\Omega_q)\frac{1}{n}\left[\Theta^k_{\mathcal{A}}(\Omega_q)-\Theta^k_{\mathrm{cone}}(\Omega_q)\right]$$

$$\mathcal{D}^{n>0}_{k\in\mathrm{II}} = 0\,. \tag{4.39}$$

Note that for jet algorithms that do not have an out-of-jet region, the cut on the out-of-jet energy is of course not defined. However, in this case we have

$$\left[1-\sum_k\Theta^k_{\mathcal{A}}(\Omega_q)\right]=0 \tag{4.40}$$

such that the above equation is in fact independent of this out-of-jet energy cut.

Using Equation (4.39), we can write Equation (4.23) as

$$\mathcal{S}^{(1)}\left(\mathcal{A},\mathcal{M};\sigma_1,\ldots\sigma_n\right)=\widetilde{\mathcal{S}}^{(1)}\left(\text{cone},\text{ang};\sigma_1,\ldots\sigma_n\right)+\mathcal{D}^0\prod_k\delta\left(\sigma_k\right)+\sum_{k\in\{\text{meas}\}}\mathcal{D}_k^1\mathcal{L}_0\left(\sigma_k\right)\prod_{l\neq k}\delta\left(\sigma_l\right)\,, \tag{4.41}$$

where $\mathcal{D}^0$ and $\mathcal{D}_k^1$ are given by Equation (4.39) and $\widetilde{\mathcal{S}}^{(1)}\left(\text{cone},\text{ang};\sigma_1,\ldots\sigma_n\right)$ can be found in [66]. This subtraction can be applied to inclusive algorithms, where $\Theta_{\mathcal{A}}^k(q)=\Theta_{\mathcal{A}}^k(\Omega_q)$, and observables that are azimuthally symmetric about the jet and have the property

$$\lim_{E_q\to\infty}\mathcal{R}(\mathcal{M},\sigma;E_q)=\{\theta_q<\left(\sigma\frac{\omega_k}{E_q}\right)^\alpha\} \tag{4.42}$$

where $0<\alpha<1$. Unmeasured Type II jets that are cone or k_T-type can also be easily included.

We should briefly discuss the numerical implementation of Equation (4.41). While the required integrals are two dimensional, they are well-bounded integrals over the full solid angle. In addition, these integrals contain no singularities, and can generally be binned uniformly in $\cos\theta_q$ and ϕ_q. We have found good performance and excellent convergence using these methods.

4.5 Two Simple Examples

4.5.1 Type I

As an example of the subtraction in Section 4.4, we will consider an example where result and the moments $\mathcal{D}^0$ and $\mathcal{D}_k^1$ are known analytically. Specifically, we will reproduce the hemisphere soft function, using the soft function of [66] as a subtraction. This will give us a chance to demonstrate our method without resorting to numerical comparisons.

The hemisphere soft function has two collinear directions, given by $n_i=n$ and $n_j=\bar{n}$. In this section, for simplicity, we will use $\tau^0=1-\text{T}$ as the target observable,

$$\begin{aligned}\sigma_n(q)&=\frac{n\cdot q}{\omega_n}\\ \sigma_{\bar{n}}(q)&=\frac{\bar{n}\cdot q}{\omega_{\bar{n}}}\,,\end{aligned} \tag{4.43}$$

where the ω_i are normalization scales, typically some multiple of the jet energy. The

hemisphere algorithm has the form

$$\begin{aligned}\Theta^{n}_{\text{hemi}} &= \theta(n\cdot q < \bar{n}\cdot q) \\ \Theta^{\bar{n}}_{\text{hemi}} &= \theta(\bar{n}\cdot q < n\cdot q) \\ \Theta^{0}_{\text{hemi}} &= 0\,.\end{aligned} \tag{4.44}$$

Following Section 4.4, we construct our subtraction using the soft function in [66]. For two collinear directions, $\mathbf{T}_n\cdot\mathbf{T}_{\bar{n}} = -\mathbf{T}_n^2 = -\mathbf{T}_{\bar{n}}^2 = -C_F$ and, since $n_i = n = \bar{n}_j$, $1/t_{ij}^2 = 0$. This leads to

$$\begin{aligned}&\widetilde{\mathcal{S}}^{(1)}(\text{cone},\text{thrust};\sigma_n,\sigma_{\bar{n}}) = \\ &-\frac{\alpha_s}{\pi}C_F\Bigg[\delta(\sigma_n)\delta(\sigma_{\bar{n}})\Bigg(\frac{1}{\epsilon^2}+\frac{1}{2\epsilon}\log\frac{\mu^4}{\omega_n^2\omega_{\bar{n}}^2}+\frac{\pi^2}{12}-\frac{1}{2}\log^2\frac{\mu^2}{4\Lambda^2}+\frac{1}{2}\log^2\frac{\mu^2}{4\Lambda^2\tan^2\frac{R}{2}} \\ &+\frac{1}{4}\log^2\frac{\mu^2\tan^2\frac{R}{2}}{\omega_n^2}+\frac{1}{4}\log^2\frac{\mu^2\tan^2\frac{R}{2}}{\omega_{\bar{n}}^2}+2\text{Li}_2\left[-\tan^2\frac{R}{2}\right]\Bigg) \\ &+\delta(\sigma_n)\left(\frac{1}{\sigma_{\bar{n}}}\right)_+\left(-\frac{1}{\epsilon}-\log\frac{\mu^2\tan^2\frac{R}{2}}{\omega_{\bar{n}}^2}\right)+2\,\delta(\sigma_n)\left(\frac{\log\sigma_{\bar{n}}}{\sigma_{\bar{n}}}\right)_+ \\ &+\delta(\sigma_{\bar{n}})\left(\frac{1}{\sigma_n}\right)_+\left(-\frac{1}{\epsilon}-\log\frac{\mu^2\tan^2\frac{R}{2}}{\omega_n^2}\right)+2\,\delta(\sigma_{\bar{n}})\left(\frac{\log\sigma_n}{\sigma_n}\right)_+\Bigg]\,.\end{aligned} \tag{4.45}$$

We now need to calculate $\mathcal{D}^0$, $\mathcal{D}^1_n$, and $\mathcal{D}^1_{\bar{n}}$ in order to construct $\mathcal{S}(\text{hemi},\text{thurst})$. Using Equation (4.39), we find

$$\begin{aligned}\mathcal{D}^0 = \frac{\alpha_s}{\pi}C_F\int_{-1}^{1}\text{d}\cos\theta\,\frac{1}{1-\cos^2\theta}\Bigg[&\Big(\Theta(\cos\theta>0)-\Theta(\cos\theta>\cos R)\Big)\log\frac{\omega_n}{\Lambda(1-\cos\theta)} \\ &+\Big(\Theta(\cos\theta<0)-\Theta(\cos\theta<-\cos R)\Big)\log\frac{\omega_{\bar{n}}}{\Lambda(1+\cos\theta)}\Bigg]\end{aligned} \tag{4.46}$$

$$\mathcal{D}^1_n = \frac{\alpha_s}{\pi}C_F\int_{-1}^{1}\text{d}\cos\theta\,\frac{1}{1-\cos^2\theta}\Big(\Theta(\cos\theta>0)-\Theta(\cos\theta>\cos R)\Big) \tag{4.47}$$

$$\mathcal{D}^1_{\bar{n}} = \frac{\alpha_s}{\pi}C_F\int_{-1}^{1}\text{d}\cos\theta\,\frac{1}{1-\cos^2\theta}\Big(\Theta(\cos\theta<0)-\Theta(\cos\theta<-\cos R)\Big)\,, \tag{4.48}$$

where θ is defined with respect to the $\mathbf{n}$ direction and we have done the trivial ϕ

integration. After integrating over θ, we get

$$\mathcal{D}^0 = \frac{\alpha_s}{\pi} C_F \left(\frac{\pi^2}{6} + \frac{1}{2} \log \frac{4\Lambda^2}{\omega_n^2} \log \tan^2 \frac{R}{2} + \frac{1}{2} \log \frac{4\Lambda^2}{\omega_{\bar{n}}^2} \log \tan^2 \frac{R}{2} + \log^2 \tan^2 \frac{R}{2} + 2\mathrm{Li}_2 \left[-\tan^2 \frac{R}{2} \right] \right) \tag{4.49}$$

$$\mathcal{D}_n^1 = \mathcal{D}_{\bar{n}}^1 = -\frac{\alpha_s}{\pi} C_F \log \tan^2 \frac{R}{2} \,. \tag{4.50}$$

Combining this with Equations (4.41) and (4.45), we arrive at the hemisphere soft function

$$\begin{aligned} &\mathcal{S}^{(1)}(\mathrm{hemi}, \mathrm{thrust}; \sigma_n, \sigma_{\bar{n}}) = \\ &- \frac{\alpha_s}{\pi} C_F \left[\delta(\sigma_n)\delta(\sigma_{\bar{n}}) \left(\frac{1}{\epsilon^2} + \frac{1}{2\epsilon} \log \frac{\mu^4}{\omega_n^2 \omega_{\bar{n}}^2} - \frac{\pi^2}{12} + \frac{1}{4} \log^2 \frac{\mu^2}{\omega_n^2} + \frac{1}{4} \log^2 \frac{\mu^2}{\omega_{\bar{n}}^2} \right) \right. \\ &+ \delta(\sigma_n) \left(\frac{1}{\sigma_{\bar{n}}} \right)_+ \left(-\frac{1}{\epsilon} - \log \frac{\mu^2}{\omega_{\bar{n}}^2} \right) + 2\,\delta(\sigma_n) \left(\frac{\log \sigma_{\bar{n}}}{\sigma_{\bar{n}}} \right)_+ \\ &\left. + \delta(\sigma_{\bar{n}}) \left(\frac{1}{\sigma_n} \right)_+ \left(-\frac{1}{\epsilon} - \log \frac{\mu^2}{\omega_n^2} \right) + 2\,\delta(\sigma_{\bar{n}}) \left(\frac{\log \sigma_n}{\sigma_n} \right)_+ \right] . \end{aligned} \tag{4.51}$$

This matches the known result in the literature [71], as well as Equation (4.45) in the limit $\tan^2 \frac{R}{2} \to 1$, where each cone occupies an entire hemisphere.

4.5.2 Type II

While the discussion of Section 4.4 and Section 4.5.1 has focused on Type I jets, we would like to give an example of subtractions involving Type II jets. We can define an algorithm in which particles are merged if the pairwise measure d_{ij} is less than a fixed cut y_{cut}, where d_{ij} is defined as

$$d_{ij} = \frac{1}{Q} \min\{E_i, E_j\}(1 - \cos\theta_{ij}) \,. \tag{4.52}$$

Here Q is a high scale energy used as normalization, typically the center of mass energy. We require $Q y_{\mathrm{cut}} < E_i^{\mathrm{jet}}$ for all i, such that two distinct jets are not merged. This is similar to the original "exclusive k_T" algorithm [46], except that the energies in Equation (4.52) are raised to a single power instead of squared. This is done because factorization of exclusive k_T is problematic in $\mathrm{SCET_I}$ and therefore outside the scope of this paper. For the rest of this work, we will refer to the algorithm in Equation (4.52) using the label excl, as an example of a generic exclusive algorithm.

As in Section 4.5.1, we will look at the case of two back-to-back jets, with $n_i = \bar{n}_j = n$. For out-of-jet radiation, we will employ an energy cut Λ on gluons not assigned to a jet. If there is no observable, the soft function is given by

$$\begin{aligned} S^{(1)}(\text{excl}, \text{unmeasured}) =& 2 \int \frac{\mathrm{d}^d q}{(2\pi)^d} N_{n\bar{n}}(q) 2\pi\delta(q^2) \Big[\theta(n\cdot q < Q y_{\text{cut}}) \theta(n\cdot q < \bar{n}\cdot q) \\ &+ \theta(\bar{n}\cdot q < Q y_{\text{cut}}) \theta(\bar{n}\cdot q < n\cdot q) \\ &+ \theta(E_q < \Lambda) \theta(n\cdot q > Q y_{\text{cut}}) \theta(\bar{n}\cdot q > Q y_{\text{cut}}) \Big] , \end{aligned} \tag{4.53}$$

where we have expanded Equation (4.52) in the soft limit to get the restriction $\theta(n\cdot q < Q y_{\text{cut}})$. This integral can be done analytically, with the result

$$\begin{aligned} S^{(1)}(\text{excl}, \text{unmeasured}) =& -\frac{\alpha_s}{\pi} C_F \left[\frac{1}{\epsilon^2} + \frac{1}{\epsilon} \log \frac{\mu^2}{Q^2 y_{\text{cut}}^2} - \frac{\pi^2}{12} + \frac{1}{2} \log^2 \frac{\mu^2}{Q^2 y_{\text{cut}}^2} \right. \\ &\left. + \Theta(\Lambda > Q y_{\text{cut}}) \Big(\frac{\pi^2}{6} - \log^2 \frac{Q y_{\text{cut}}}{2\Lambda} - 2\text{Li}_2 \frac{Q y_{\text{cut}}}{2\Lambda} \Big) \right] . \end{aligned} \tag{4.54}$$

For angularities with $a < 0$, the algorithm in Equation (4.52) leads to Type II jets. In this case, the soft function is given by

$$\begin{aligned} S^{(1)}(\text{excl}, \text{ang}; \sigma_n, \sigma_{\bar{n}}) =& 2 \int \frac{\mathrm{d}^d q}{(2\pi)^d} N_{n\bar{n}}(q) 2\pi\delta(q^2) \\ &\times \Big[\theta(n\cdot q < Q y_{\text{cut}}) \theta(n\cdot q < \bar{n}\cdot q) \delta(\sigma_n - \tau_n^{a_n}(q)) \delta(\sigma_{\bar{n}}) \\ &+ \theta(\bar{n}\cdot q < Q y_{\text{cut}}) \theta(\bar{n}\cdot q < n\cdot q) \delta(\sigma_{\bar{n}} - \tau_{\bar{n}}^{a_{\bar{n}}}(q)) \delta(\sigma_n) \\ &+ \theta(E_q < \Lambda) \theta(n\cdot q > Q y_{\text{cut}}) \theta(\bar{n}\cdot q > Q y_{\text{cut}}) \delta(\sigma_n) \delta(\sigma_{\bar{n}}) \Big] . \end{aligned} \tag{4.55}$$

In order to use Equation (4.54) as a subtraction for Equation (4.55), we need to multiply Equation (4.54) by $\delta(\sigma_n)\delta(\sigma_{\bar{n}})$, such that both are functions of σ_n and $\sigma_{\bar{n}}$. This is an example of the procedure discussed in Section 4.2.3. After this is done, we can see that the zeroth moments of $S^{(1)}_{\text{new}}(\text{excl}, \text{unmeasured}; \sigma_n, \sigma_{\bar{n}})$ and $S^{(1)}(\text{excl}, \text{ang}; \sigma_n, \sigma_{\bar{n}})$ are equal, and is $\mathcal{D}^0 = 0$. Given this exact cancellation, the higher moments, $\mathcal{D}_k^{n>0}$, are independent of $S^{(1)}_{\text{new}}(\text{excl}, \text{unmeasured}; \sigma_n, \sigma_{\bar{n}})$, such that they trivially reproduce the higher moments of $S^{(1)}(\text{excl}, \text{ang}; \sigma_n, \sigma_{\bar{n}})$. One might worry that these higher moments are divergent and could not be calculated numerically; however, since these are Type II jets, all higher moments are finite. The analytical calculation, which is possible for Equation (4.55), agrees with numerical calculations of the higher moments.

Chapter 5

Notes on Azimuthally Asymmetric Observables

5.1 Introduction

Jet shape observables that are sensitive to the azimuthal angle about the jet axis are becoming increasingly common in substructure analysis. However, no such observable has been resummed to date. The dimensional regularization techniques currently available for calculating IR safe observables that depend only on the energies and polar angles of particles in a jet are straightforward generalizations of those used originally for case of electroweak decays by Peccei et al. However, to further extend this technique to observables with azimuthal dependence requires care and leads to complicated and counter-intuitive relations between the physical angles and the variables of integration. We demonstrate that an extension based instead on the pioneering work of 't Hooft and Veltman leads to a much more transparent relation between physical and integration variables and can be carried out straightforwardly. We apply this latter scheme to jet angularities τ_a in the case that there is an out-of-jet energy veto Λ, extended to the case that both the parameter a and the normalization factor ω in the definition of τ_a depend on the azimuthal angle, a generalization that represents a very generic azimuthally dependent jet shape.

Recently, there has been considerable progress in using jet substructure to discriminate QCD initiated background jets from jets arising from the decay of new physics in collider events (see for example Ref. [104] and references therein). This success hinges on the ability to predict intrajet properties and most commonly these predictions are based on Monte Carlo event generators. As the approximations used in event generators are not systematically improvable and our ability to estimate the errors associated with these approximations is often not well understood, an alternative that does not share these features is crucial.

The class of substructure analyses that we focus on in this paper is that of jet

shapes. Jet shapes are broadly defined as smooth functions of the 4-momenta of a jet's constituents that characterize the profile of energy flow within the jet, and as such lend themselves straightforwardly to perturbative, first-principles predictions, in particular to both fixed-order and resummed calculations. In addition to new physics discrimination, jet shapes have historically been used as precision tests of QCD and for event generator tuning [1, 108]. Examples include event shapes (such as the classic thrust and jet broadening) restricted to the constituents of a jet as well as the original energy profile $\Psi(r/R)$ dubbed "the jet shape" [67, 68, 1].

Generally, jet shape distributions, represented in this paper by τ, contain logarithms at fixed order of the form

$$\frac{\mathrm{d}\sigma}{\mathrm{d}\tau} \sim \sum_{i=1}^{\infty} \sum_{j=0}^{2i-1} \alpha_s^i \frac{\log^j \tau}{\tau}\,, \tag{5.1}$$

which become large for narrow jets, which we've taken to correspond to $\tau \sim 0$ (there are additional terms in the cross section which are finite or power suppressed at $\tau \to 0$). In order for perturbation theory to be well behaved for all values of τ, these logarithms have to be resummed. This can be accomplished with either soft-collinear effective theory [23, 25, 31, 30] or with more traditional QCD-based methods [58, 111]. Relative to event generation, this approach to describing substructure can be used to make predictions more accurately and with uncertainties. It can also be used in conjunction with event generators, which have the often indisposable advantage of providing fully exclusive, hadronized final states, to illuminate when the predictions of event generators are not to be trusted, and, when the two approaches are in agreement, to allow meaningful assignment of errors to an event generator [112].

To date, all jet shapes that have been resummed share an azimuthal symmetry about the jet axis. However, polarization, spin, and color connection effects can all correlate radiation in and around a jet with the plane defined by the jet axis and another axis in the event, e.g., the beam axis, and these correlations will in general be different for pure QCD jets and new physics decays. Thus, the azimuthal distribution of radiation about a jet itself can be used to delineate signal events from otherwise irreducible background events, and some observables have been proposed that attempt to exploit precisely this fact (in particular, planar flow [5], pull [72], and dipolarity [79]). On the other hand, the ability of event generators to correctly describe these properties is much less well understood than their ability to describe more classic (and azimuthally symmetric) observables. In fact, many commonly used event generators are known to not correctly contain the physics responsible for the above correlations (and for the case of color correlations can not even in principle incorporate the appropriate physics since this effect disallows the Markovian interpretation inherit in parton showers for finite N_C). It is the purpose of this section to develop techniques that allow one to include azimuthal dependence in resummed jet shape calculations. From the point of view of SCET where dimensional regular-

ization is the most convenient. As we will see, this will require recasting the basic formulation of dimensionally regularized radiative corrections.

This paper is organized as follows. In Section 5.1.1, we begin by describing the dimensional regularization technique that has been traditionally used for azimuthally symmetric observables in the literature to date, referred to as the "partial-democratic" method. We then illustrate how one can utilize an alternative formulation, referred to as the "undemocratic" method, which, using the physical angles (the polar and the azimuthal angle present in $d = 4$ dimensions) as integration variables directly, allows straightforward extension to the general case. By comparing the two methods, we are able to identify the nontrivial correspondence between angles in the traditional case and the physical angles, further demonstrating that using the traditional method in such cases is considerably more difficult and counter-intuitive. In Section 5.1.2, we use this technology to define a class of azimuthally symmetric observables which, for each fixed azimuthal angle ϕ, reduces to that of angularities [39][1], but which is generalized to allow ϕ-dependent normalization ω and angularity parameter a. We refer to this class of observables as ϕ-angularities. In Section 5.2, we present the details of the calculation of the soft function for ϕ-angularities.

5.1.1 A New Take on Dimensional Regularization

In order to calculate the distribution of a jet shape in SCET, we begin by assuming a factorization theorem, which typically takes the form [24]

$$\frac{\mathrm{d}\sigma}{\mathrm{d}\tau_1 \dots \mathrm{d}\tau_n} = H \times \int \mathrm{d}\tau_1' \dots \mathrm{d}\tau_n' \, J_1(\tau_1') \times \cdots \times J(\tau_n') \times S(\tau_1 - \tau_1', \dots, \tau_n - \tau_n') \,, \quad (5.2)$$

has been established for the observable at hand. Factorization theorems of this type generally hold only up to power corrections of $\mathcal{O}(\tau_i)$. While the hard function, H, is independent of the observable (and of any other restrictions on the final state) and the jet function only depends on one direction (with limited dependence on final state phase space restrictions), the soft function, S, depends on all observables and the full details of any phase space restrictions. Therefore the calculation of S is typically the most difficult part of these calculations and this is what we will focus on.

When calculating the contribution of the soft function to an azimuthally asymmetric observable, we have to calculate the higher order virtual and real emission diagrams. To do this, we will use pure dimensional regularization to regulate divergences encountered in these calculations. Dimensional regularization is particularly useful in effective theories such as SCET, since virtual diagrams are generally scaleless and can be set to zero. Therefore, in this paper we will concentrate only on the real

[1] To be precise, with our conventions it reduces to the version of angularities later defined in [66] which differs from that in [39] with a polar angle dependent normalization such that radiation at the boundaries of jets is defined not to contribute in [39].

emission contributions. While we focus primarily on the one-loop soft function, the techniques clearly extend both to the jet function and to higher order diagrams.

In previous real emission calculations in dimensional regularization [77], the $d-1$ spatial dimensions have been treated "democratically," in that once a time-like direction is factored out, the phase space is taken to be a Euclidean space with no "special" subspace identified. In these calculations, the full phase space (including the on-shell delta function) can be written as

$$\mathrm{d}^d k\, \delta(k^2) = \frac{1}{2|\mathbf{k}|}\mathrm{d}^{d-1}k = \frac{1}{2}|\mathbf{k}|^{d-3}\mathrm{d}|\mathbf{k}|\mathrm{d}\Omega_{d-2}\,. \tag{5.3}$$

Here, $\mathrm{d}\Omega_n$ is the n-dimensional spherical volume element, defined as

$$\mathrm{d}\Omega_n = \sin^{n-2}\theta_1 \sin^{n-3}\theta_2 \cdots \sin\theta_{n-2}\,\mathrm{dcos}\,\theta_1 \cdots \mathrm{dcos}\,\theta_{n-1}\,\mathrm{d}\phi\,, \tag{5.4}$$

where $\cos\theta_i$ runs from -1 to 1 and ϕ from 0 to 2π. $\mathrm{d}\Omega_n$ satisfies the recursion relation

$$\mathrm{d}\Omega_n = \sin^{n-1}\theta\,\mathrm{d}\theta\,\mathrm{d}\Omega_{n-1} \tag{5.5}$$

and integrates to

$$\int \mathrm{d}\Omega_n = \frac{2\pi^{\frac{n+1}{2}}}{\Gamma\left(\frac{n+1}{2}\right)}\,. \tag{5.6}$$

Before proceeding, we note that cartesian components of a vector $\mathbf{k}$ living on this n-dimensional sphere can be written in terms of the $n-1$ polar angles θ_i and the azimuthal angle ϕ as

$$\begin{aligned}
\mathbf{k}_1 &= |\mathbf{k}|\cos\theta_1 \\
\mathbf{k}_2 &= |\mathbf{k}|\sin\theta_1\cos\theta_2 \\
\mathbf{k}_3 &= |\mathbf{k}|\sin\theta_1\sin\theta_2\cos\theta_3 \\
&\vdots \\
\mathbf{k}_n &= |\mathbf{k}|\sin\theta_1\sin\theta_2\ldots\sin\theta_{n-1}\cos\phi \\
\mathbf{k}_{n+1} &= |\mathbf{k}|\sin\theta_1\sin\theta_2\ldots\sin\theta_{n-1}\sin\phi\,.
\end{aligned} \tag{5.7}$$

In [81, 80], instead of factoring out only the time-like direction, the authors removed a light cone subspace and treated the resulting $d-2$ spatial dimensions democratically, i.e.,

$$\mathrm{d}^d k\, \delta(k^2) = \frac{1}{2}\mathrm{d}k^+\mathrm{d}k^-\mathrm{d}^{d-2}\mathbf{k}_\perp \delta(k^+k^- - |\mathbf{k}_\perp|^2) = \frac{1}{4}(k^+k^-)^{\frac{d-4}{2}}\mathrm{d}k^+\mathrm{d}k^-\mathrm{d}\Omega_{d-3}\,. \tag{5.8}$$

We refer to this as the "partial-democratic" method. Note that the physical polar angle is encoded in $k^\pm$ and has thus been factored out of the $(d-2)$-dimensional $\mathbf{k}_\perp$

democratic subspace. When integrands involve dot products with 2 distinct external directions, its easiest to align one of these directions along the z-direction such that the angle of the loop momentum $\mathbf{k}$ with respect this direction can be written in terms of $k^{\pm}$. One can then choose to align the 2nd external direction along the "1" direction within the $\mathbf{k}_{\perp}$ subspace (cf. Equation (5.7)) since then dot products only involve a single additional angle θ_1, which can be made an explicit integration variable using Equation (5.5). In general, when there are 3 or more linearly-indepedent directions, one needs to choose a plane for the external vectors within the $\mathbf{k}_{\perp}$ subspace. This is most easily done by choosing the "1-2" plane since dot products will then only involve the two angles $\theta_{1,2}$, which can be made explicit in $\mathrm{d}\Omega_{d-3}$ using Equation (5.5) twice. However, when an observable explicitly depends on the azimuthal angle ϕ about a jet, its not immediately clear how to express ϕ in terms of $\theta_{1,2}$ since, for one, these are polar angles (i.e., they run from 0 to π). Note also that making the azimuthal angle of Equation (5.4) explicit by aligning physical vectors in the "n-$(n+1)$" plane is in general prohibitively complicated since dot products involving this angle also involve all $n-1$ polar angles θ_i.

As an alternative, we propose an "undemocratic" method, based on the original dimensional regularization proposal of 't Hooft and Veltman [114][2], in which a 4 dimensional Minkowski space is factored out, and the remaining $d-4$ dimensional subspace is integrated over, i.e.,

$$\mathrm{d}^d k\, \delta(k^2) = \mathrm{d}^4\bar{k}\, \mathrm{d}^{d-4}\mathbf{K}\, \delta(\bar{k}^2 - |\mathbf{K}|^2) = \frac{1}{2}\mathrm{d}^4\bar{k}\, (\bar{k}^2)^{\frac{d-6}{2}} \mathrm{d}\Omega_{d-5}\,. \tag{5.9}$$

An important feature of this method is that physical 4-vectors (v) have no components in the $d-4$ dimensional subspace, i.e.

$$k\cdot v = \bar{k}\cdot v\,. \tag{5.10}$$

This applies to collinear directions and boson polarizations, as well as 4-momenta. The advantage of the undemocratic method is that the resulting Minkowski space contains an angle whose range is $0 < \phi < 2\pi$ and can be identified as the azimuthal angle about the jet direction.

We will now show that the partial-democratic and undemocratic schemes are equivalent, which confirms the natural assumption that the result is scheme independent (as long as the scheme consistently regulates all divergences) and allows us to illustrate how azimuthal dependence can be included in the partial-democratic

[2]Recently, it was noticed in [84] that the appropriate divergences in beam functions were correctly reproduced when a procedure to evaluate loop momenta that used aspects of our proposed method was used, but neither a general method for extending this procedure to other applications nor the relation to other schemes, formally necessary when combining the beam functions with other factorized ingredients calculated in a different scheme, were discussed. In addition, polarizations were treated in a way that, while not affecting any of the results in their paper, if generalized directly would not lead to a consistent scheme.

scheme. Similar comparisons can be made between the democratic/partial-democratic and democratic/undemocratic schemes, however, since the partial-democratic scheme is now the most widely used in SCET calculations, we will take it as the standard.

At one loop, any soft function, including phase space restrictions, can be written as

$$\mathcal{S} = \int \mathrm{d}^d k \, f(n_1\cdot k, \bar{n}_1\cdot k, n_2\cdot k, n_3\cdot k)\,, \tag{5.11}$$

where the n_i are light-like 4-vectors and $\mathbf{n}_1$, $\mathbf{n}_2$, and $\mathbf{n_3}$ are linearly independent. All dependence on other directions can be written in this basis, since these four vectors form a complete basis in 4 dimensions, where f is defined. In the partial-democratic (pd) scheme, we proceed by factoring out a light cone direction, which is most easily identified as n_1. After integrating over $|\mathbf{k}_\perp|$, as in Equation (5.8), we have

$$\mathcal{S}_{\mathrm{pd}} = \frac{1}{4}\int (k^+k^-)^{\frac{d-4}{2}} \mathrm{d}k^+\mathrm{d}k^-\mathrm{d}\Omega_{d-3} f(k^+,k^-,n_2\cdot k, n_3\cdot k)\,. \tag{5.12}$$

In order to write $n_2\cdot k$ and $n_3\cdot k$ in terms of the remaining integration variables, we employ Equation (5.5) and identify θ_1 as the angle between $\mathbf{k}_\perp$ and $\mathbf{n}_2^\perp$ in the $d-2$ dimensional space. The angle between $\mathbf{k}_\perp$ and $\mathbf{n}_3^\perp$ when projected onto the $d-3$ dimensional hyperplane perpendicular to $\mathbf{n}_2^\perp$ is given by θ_2, while ψ_{23} is the angle between $\mathbf{n}_2^\perp$ and $\mathbf{n}_3^\perp$. In terms of these variables, we have

$$\begin{aligned}\mathcal{S}_{\mathrm{pd}} = \frac{1}{4}\int \mathrm{d}k^+\mathrm{d}k^- &\sin^{d-4}\theta_1\,\mathrm{d}\theta_1 \sin^{d-5}\theta_2\,\mathrm{d}\theta_2\,\mathrm{d}\Omega_{d-5}(k^+k^-)^{\frac{d-4}{2}} \\ &\times f\Bigg(k^+,k^-,\frac{n_2^+k^- + n_2^-k^+}{2} - \sqrt{n_2^+n_2^-k^+k^-}\cos\theta_1, \\ &\qquad \frac{n_3^+k^- + n_3^-k^+}{2} - \sqrt{n_3^+n_3^-k^+k^-}(\cos\theta_1\cos\psi_{23} + \sin\theta_1\cos\theta_2\sin\psi_{23})\Bigg)\,.\end{aligned} \tag{5.13}$$

In the undemocratic (ud) scheme, after performing the integrations in Equation (5.9) and relabeling $\bar{k}$ as k, we have

$$\mathcal{S}_{\mathrm{ud}} = \frac{1}{2}\int \mathrm{d}^4k\,(k^2)^{\frac{d-6}{2}}\mathrm{d}\Omega_{d-5} f(n_1\cdot k, \bar{n}_1\cdot k, n_2\cdot k, n_3\cdot k)\,. \tag{5.14}$$

This illustrates an important feature of the undemocratic scheme, namely that $n\cdot k = n\cdot\bar{k}$ for any physical vector n, such that f is completely independent of the $d-4$ dimensional subspace. After making the transformation into light cone coordinates,

we have

$$\mathcal{S}_{\rm ud} = \frac{1}{4}\int \mathrm{d}k^+\mathrm{d}k^-\mathrm{d}k_x\,\mathrm{d}k_y\mathrm{d}\Omega_{d-5}(k^+k^- - k_x^2 - k_y^2)^{\frac{d-6}{2}} \times f\Bigg(k^+, k^-, \frac{n_2^+k^- + n_2^-k^+}{2} - \sqrt{n_2^+n_2^-}k_x, \frac{n_3^+k^- + n_3^-k^+}{2} - \sqrt{n_3^+n_3^-}(k_x\cos\psi_{23} + k_y\sin\psi_{23})\Bigg)\,. \tag{5.15}$$

If we now make the substitutions $k_x = \sqrt{k^+k^-}\cos\theta_1$ and $k_y = \sqrt{k^+k^-}\sin\theta_1\cos\theta_2$ and include the proper Jacobian, we see that the partial-democratic and undemocratic schemes are equivalent.

Given that we know the proper variable transformations to go between the two schemes, it is easy to see how one could include azimuthal dependence in the partial-democratic scheme. Using the fact that $\tan\phi = k_y/k_x$ we have

$$\tan\phi = \tan\theta_1\cos\theta_2\,. \tag{5.16}$$

In Equation (5.16), both θ_1 and θ_2 range from 0 to π, while ϕ goes from 0 to 2π. The fact that $\cos\theta_2$ goes from -1 to 1 allows us to recover the full range of $\tan\phi$ (which runs from $-\infty$ to ∞ twice). One might worry about over counting, since $\cos\theta_2$ takes a continuous range of values. However, the Jacobian between the partial-democratic and undemocratic schemes removes this problem by properly reweighting each combination of θ_1 and θ_2. Care must be taken when defining ϕ as an inverse tangent, as this does not generally cover the desired range. While we could use the partial-democratic scheme and include azimuthal dependence using Equation (5.16), it is clearly easier to use the undemocratic scheme, with spherical coordinates instead of light cone coordinates. We will see an example of this in the next section.

5.1.2 Azimuthally Asymmetric Jet Shapes in e^+e^-

In order to demonstrate the benefit of our regularization scheme, we will calculate an extension of angularities we will call ϕ-angularities, defined as

$$\tau_{a(\phi)} = \frac{1}{\omega(\phi)}\sum_{i\in\rm jet}(k_i^+)^{1-\frac{a(\phi)}{2}}(k_i^-)^{\frac{a(\phi)}{2}}\,. \tag{5.17}$$

Here, $k^\pm$ are given by

$$k^+ = n_{\rm jet}\cdot k \tag{5.18}$$

$$k^- = \bar{n}_{\rm jet}\cdot k\,, \tag{5.19}$$

where $n_{\rm jet} = (1, \mathbf{n}_{\rm jet})$ is a null vector along the light cone direction of the jet. The sum in Equation (5.17) is taken over all particles in the jet, where the jet is defined by a jet algorithm. In analogy with the calculation for traditional angularities, we restrict ourselves to jet algorithms that, at one loop, reduce to cones of size R in θ about the jet direction. This includes cone and k_T-type algorithms in e^+e^- collisions. We will also include a jet veto, Λ, for radiation outside of all jets.

If we look at e^+e^- initial states and take $\omega(\phi) \sim Q$, where $Q = \sqrt{s}$, then ϕ-angularities will factorize in the limit $\tau_{a(\phi)} \ll 1$. We will assume the factorization follows directly along the lines of traditional angularities in e^+e^- collisions. This factorization, including a jet algorithm and jet veto, is discussed in [66]. Along the lines of that calculation, we will divide our soft function into three pieces:

- $S_{ij}^{\rm incl}$: describes the interference term between the $i^{\rm th}$ and j^{th} Wilson lines, where the emitted gluon is allowed to go anywhere, with an energy less than Λ
- S_{ij}^{k}: describes the interference between the $i^{\rm th}$ and j^{th} Wilson lines, where the emitted gluon is found in the $k^{\rm th}$ jet, with energy greater than Λ. Using that the contribution of a gluon in a jet with any energy is zero (since it involves a scaleless integral), it can be shown that the sum of $S_{ij}^{\rm incl}$ and S_{ij}^{k} summed over k is the contribution of a gluon outside of all jets with energy less than Λ
- $S_{ij}(\tau_{a(\phi)}^{k})$: describes the contribution to $\tau_{a(\phi)}^{k}$ from the interference between the $i^{\rm th}$ and j^{th} Wilson lines.

The soft function is then given by

$$S(\tau_{a(\phi)}^{1}, \ldots, \tau_{a(\phi)}^{n}) = \sum_{i \neq j} \left[S_{ij}^{\rm incl} + \sum_{k=1}^{n} \left(S_{ij}^{k} + S_{ij}(\tau_{a(\phi)}^{k}) \right) \right] \tag{5.20}$$

Here we have assumed that a separate measurement of the ϕ-angularity has been made on each jet. However, as discussed in [66], factorization is also valid even if there is no measurement on a jet provided the jet size is small, $R \ll 1$, for that jet. In this case, $S_{ij}(\tau_{a(\phi)}^{k})$ is omitted. The full result for each piece is given in the appendix. From this point forward, we will drop the explicit ϕ dependence of a and ω; they will both be assumed to be in general arbitrary functions of ϕ.

To emphasize the difference between our regularization scheme and those previously used in the literature, we can compare one of the integrals from above with the corresponding integral in a different scheme. For example, if we take ω to be a

constant and $a(\phi) = \cos\phi - 1$, we have

$$\begin{aligned}\left(S_{ij}(\tau_a^i)\right)_{\rm ud} =& \frac{\alpha_{\rm s}}{2\pi^2}\left(\frac{4\pi\mu^2}{\omega^2}\right)^{\epsilon}\frac{\epsilon(\tau_a^i)^{-1-2\epsilon}}{\Gamma(1-\epsilon)}\mathbf{T}_i\cdot\mathbf{T}_j \\ & \int \mathrm{d}x\,\mathrm{d}\cos\theta\mathrm{d}\phi\frac{n_i\cdot n_j}{(x-\cos\theta)(x-\cos\theta\cos\theta_{ij}-\cos\phi\sin\theta\sin\theta_{ij})} \\ & \times (x^2-1)^{-1-\epsilon}(x-\cos\theta)^{(3-\cos\phi)\epsilon}(x+\cos\theta)^{(\cos\phi-1)\epsilon}\Theta(\theta<R), \end{aligned} \tag{5.21}$$

$$\begin{aligned}&\left(S_{ij}(\tau_a^i)\right)_{\rm pd} = \frac{\alpha_s}{2\pi^2}\left(\frac{4\pi\mu^2}{\omega^2}\right)^{\epsilon}(n_i\cdot n_j)(\mathbf{T}_i\cdot\mathbf{T}_j)\frac{\epsilon}{\Gamma(1-\epsilon)}\frac{\omega}{(\tau_a^i)^{2\epsilon}} \\ &\int \mathrm{d}k^-\mathrm{d}\theta_1\mathrm{d}\theta_2\sin^{-2\epsilon}\theta_1\sin^{-1-2\epsilon}\theta_2(k^-)^{-2}\left(\frac{\omega\tau_a^i}{k^-}\right)^{-1} \\ &\times\left[\left(\frac{\omega\tau_a^i}{k^-}\right)^{\frac{2\sqrt{1+\tan^2\theta_1\cos^2\theta_2}}{3\sqrt{1+\tan^2\theta_1\cos^2\theta_2-1}}}\cos^2\frac{\psi_{ij}}{2}+\sin^2\frac{\psi_{ij}}{2}\right. \\ &\left.-\left(\frac{\omega\tau_a^i}{k^-}\right)^{\frac{\sqrt{1+\tan^2\theta_1\cos^2\theta_2}}{3\sqrt{1+\tan^2\theta_1\cos^2\theta_2-1}}}\sin\psi_{ij}\cos\theta_1\right]^{-1} \\ &\times\Theta\left(\left(\frac{\omega\tau_a^i}{k^-}\right)^{\frac{2\sqrt{1+\tan^2\theta_1\cos^2\theta_2}}{3\sqrt{1+\tan^2\theta_1\cos^2\theta_2-1}}}<\tan^2\frac{R}{2}\right)\left(\frac{\omega\tau_a^i}{k^-}\right)^{2\epsilon\frac{2\sqrt{1+\tan^2\theta_1\cos^2\theta_2}-1}{3\sqrt{1+\tan^2\theta_1\cos^2\theta_2-1}}}. \end{aligned} \tag{5.22}$$

In Equation (5.22), $\cos\psi_{ij} \equiv 1 - n_i n_j$. As we can see, while Equation (5.21) is certainly not trivial, Equation (5.22) is prohibitively difficult. While the undemocratic scheme can be reduced to finite one dimensional numerical integrals for arbitrary a and ω, the analogous case in the partial-democratic scheme will generally involve a double numerical integral, which may contain $1/\epsilon$ poles.

5.2 Computation of the ϕ-Angularity Soft Function $S(\tau_a^k, \phi)$

We first define $S_{ij}(\tau_a^k, \phi)$ and $S_{ij}^k(\phi)$ via the relations

$$\begin{aligned} S_{ij}(\tau_a^k) &\equiv \int\frac{\mathrm{d}\phi}{2\pi}\,S_{ij}(\tau_a^i,\phi) \\ S_{ij}^k &\equiv \int\frac{\mathrm{d}\phi}{2\pi}\,S_{ij}^i(\phi)\,. \end{aligned} \tag{5.23}$$

In both cases, in the "undemocratic" method, the integration is decomposed as in Equation (5.9). Using that

$$\mathrm{d}^{d-4}K = \frac{-\epsilon\,\pi^{-\epsilon}}{\Gamma(1-\epsilon)}(K^2)^{\frac{d-6}{2}}\mathrm{d}K^2\,, \tag{5.24}$$

we find that

$$\int\frac{\mathrm{d}^4k\,\mathrm{d}^{d-4}K}{(2\pi)^d}\delta(k^2-K^2)\theta(k^0) = \frac{-\epsilon\,\pi^{-\epsilon}}{\Gamma(1-\epsilon)}\int_0^{2\pi}\frac{\mathrm{d}\phi}{2\pi}\int_{-1}^{1}\mathrm{d}\cos\theta\int_0^{\infty}\mathrm{d}|\mathbf{k}| \int_{|\mathbf{k}|}^{\infty}\mathrm{d}k^0((k^0)^2-(|\mathbf{k}|)^2)^{-1-\epsilon}\,. \tag{5.25}$$

There is a freedom in how the algorithm and the observable are defined away from $d=4$. For example, the definitions $\Theta_R=\theta(\theta<R)$ and $\Theta_R=\theta(k^+/k^-<\tan^2 R/2)$ coincide for $d=4$ but deviate for $k^0>|\mathbf{k}|$. We find that the precise definition affects both S_{ij}^k and $S_{ij}(\tau_a^k)$ separately for $R\sim\mathcal{O}(1)$, but that both S_{ij}^k for $R\ll 1$ and the sum $S_{ij}^k+S_{ij}(\tau_a^k)$ are independent of this. This can be attributed to the fact that for measured jets, it is always the sum that is needed and for unmeasured jets, one must take $R\ll 1$ in which case this dependence in S_{ij}^k becomes a power correction.

We take the convention that the algorithm restriction is

$$\Theta_R=\theta(\theta<R)\,. \tag{5.26}$$

For the angularity measurement generalized to allow both the normalization ω and the parameter a to be ϕ-dependent, we take

$$\delta_{\tau_a}=\delta\left(\tau_a-\frac{1}{\omega}(k^0-|\mathbf{k}|\cos\theta)^{1-a/2})(k^0+|\mathbf{k}|\cos\theta)^{a/2}\right)\,, \tag{5.27}$$

with $\omega=\omega(\phi)$ and $a=a(\phi)$.

Due to the difference in the singularity structure, we consider the cases $k=i$ or j and $k\neq i,j$ separately. For the former case, we define ϕ to be the azimuthal angle of the emitted gluon from the ij-plane about i. In the latter case, we define ϕ to be the angle of the emitted gluon about the ik-plane about k, and β_{ijk} to be the angle of the jk-plane with respect to the ik-plane about k. This means that ϕ should be shifted for each i,j,k to a common frame of reference.

We define for brevity

$$\begin{aligned} r &\equiv \tan R/2 \\ T_{ij} &\equiv \frac{r}{\tan\psi_{ij}/2}\,, \end{aligned} \tag{5.28}$$

where ψ_{ij} is the angle between $\mathbf{n}_i$ and $\mathbf{n}_j$, i.e., $\mathbf{n}_i \cdot \mathbf{n}_j = \cos\psi_{ij}$. For the case $k \neq i, j$, we also use

$$T_i \equiv T_{ik} = \frac{r}{\tan\psi_{ik}/2}$$
$$T_j \equiv T_{jk} = \frac{r}{\tan\psi_{jk}/2}\,. \tag{5.29}$$

Requiring non-overlapping jets is equivalent to $T < 1$ for every T.[3] We adopt the $\overline{\text{MS}}$ scheme in what follows.

5.2.1 S_{ij}^{incl}

Ref. [66] calculated S_{ij}^{incl} using the "partial-democratic" scheme with the definition of Θ_R given in Equation (5.26). Provided we stick with that definition throughout our calculation of the soft function, the result of Ref. [66] directly applies here. We quote the result for completeness.

$$S_{ij}^{\text{incl}} = -\frac{\alpha_s}{2\pi}\left(\frac{e^{\gamma_E}\mu^2}{4\Lambda^2}\right)^{\epsilon} \frac{\mathbf{T}_i\cdot\mathbf{T}_j}{\Gamma(1-\epsilon)}\left[\frac{1}{\epsilon^2} - \frac{1}{\epsilon}\ln\left(\frac{n_i\cdot n_j}{2}\right) - \frac{\pi^2}{6} - \text{Li}_2\left(1 - \frac{2}{n_i\cdot n_j}\right)\right] \tag{5.30}$$

5.2.2 $S_{ij}(\tau_a^i, \phi)$

Using that $S_{ji}(\tau_a^i, \phi) = S_{ij}(\tau_a^i, \phi)$ (up to redefining $\beta \to 2\pi - \beta$ and shifting $\phi \to \phi - \beta$), we need only focus on $S_{ij}(\tau_a^i, \phi)$. We obtain (in $\overline{\text{MS}}$)

$$S_{ij}(\tau_a^i, \phi) = \frac{\alpha_s}{\pi}\mathbf{T}_i\cdot\mathbf{T}_j\frac{(e^{\gamma_E}\mu^2)^{\epsilon}}{\Gamma(1-\epsilon)}\epsilon n_i\cdot n_j \int_{\cos R}^{1} \mathrm{d}\cos\theta \int_0^{\infty} \mathrm{d}|\mathbf{k}| \int_{|\mathbf{k}|}^{\infty} \mathrm{d}k^0 (k^2)^{-1-\epsilon} \frac{1}{k^0 - \mathbf{n}_i\cdot\mathbf{k}}\frac{1}{k^0 - \mathbf{n}_j\cdot\mathbf{k}}\delta_\tau\,. \tag{5.31}$$

Using the coordinate system where $\hat{\mathbf{n}}_i = \hat{z}$ and $\hat{\mathbf{n}}_j$ is in the xz-plane (where $\phi = 0$), using the delta function δ_τ to do the $|\mathbf{k}|$ integral, and changing variables to $x = k^0/|\mathbf{k}|$ and z $= \tan^2(\theta/2)/r^2$, we find

$$S_{ij}(\tau_a^i, \phi) = -\frac{\alpha_s}{2\pi}\mathbf{T}_i\cdot\mathbf{T}_j\frac{1}{\Gamma(1-\epsilon)}\left(\frac{e^{\gamma_E}\mu^2 r^{2(1-a)}}{\omega^2}\right)^{\epsilon}\frac{1}{\epsilon}(\tau_a^i)^{-1-2\epsilon}F_{ij}^i(\phi)\,, \tag{5.32}$$

where

$$F_{ij}^i(\phi) = -\frac{4n_i\cdot n_j\epsilon^2}{r^{-2+2(1-a)\epsilon}}\int_0^1 \mathrm{d}z \int_1^{\infty} \mathrm{d}x (x^2-1)^{-1-\epsilon}(x - 1 + r^2 z(x+1))^{-1+\epsilon(2-a)} \times F(x, z, \phi)\,, \tag{5.33}$$

[3] The results of [66] are in terms of the parameter t_{ij}, which corresponds to $t_{ij} \equiv 1/T_{ij}$.

where the nonsingular part of the expression has been grouped into $F(x,z,\phi)$ and is given by

$$F(x,z,\phi) \equiv \frac{(x+1+r^2z(x-1))^{\epsilon a}(1+r^2z)^{-2\epsilon}}{(x-1)(1+r^2z)+n_i\cdot n_j/P(z,\phi,T_{ij})}\,, \tag{5.34}$$

with

$$P(z,\phi,T) \equiv \frac{1}{1+T^2z-2T\sqrt{z}\cos\phi}\,. \tag{5.35}$$

To isolate the most singular contributions, we then split F^i_{ij} as

$$F^i_{ij}(\phi) = F^{i\,(1)}_{ij}(\phi) + F^{i\,(2)}_{ij}(\phi) \tag{5.36}$$

where

$$F^{i\,(1)}_{ij}(\phi) = -4n_i\cdot n_j r^2\epsilon^2\int_0^1 \mathrm{d}z\int_1^\infty \mathrm{d}x \frac{[F(x,z,\phi)-F(1,z,\phi)]|_{\epsilon=0}}{(x^2-1)(x-1+r^2z(x+1))}\,, \tag{5.37}$$

where we set $\epsilon=0$ in $F^{i\,(1)}_{ij}$ since, by construction, the divergences at $x=1$ and $z=0$ are regulated in this expression, and

$$\begin{aligned}
F^{i\,(2)}_{ij}(\phi) &= -\frac{4n_i\cdot n_j\epsilon^2}{r^{-2+2(1-a)\epsilon}}\int_0^1\mathrm{d}z\int_1^\infty \mathrm{d}x(x^2-1)^{-1-\epsilon}\\
&\quad\times(x-1+r^2z(x+1))^{-1+\epsilon(2-a)}F(1,z,\phi)\\
&= \frac{\Gamma(1-\epsilon)\Gamma(1-\epsilon(1-a))}{\Gamma(1-\epsilon(2-a)))}\\
&\quad\times\left(\frac{1}{1-a}+\epsilon f_1(T_{ij},\phi)+\epsilon^2\Big((1-a)f_2(T_{ij},\phi)-f_3(T_{ij},\phi,r)\Big)\right),
\end{aligned} \tag{5.38}$$

where we defined

$$\begin{aligned}
f_1(\phi,T) &\equiv \int_0^1\frac{\mathrm{d}z}{z}\big(P(z,\phi,T)-1\big) = 2\frac{\cos\phi}{|\sin\phi|}\left(\tan^{-1}\frac{\cos\phi}{|\sin\phi|}-\tan^{-1}\frac{\cos\phi-T}{|\sin\phi|}\right)\\
&\quad-\ln(1+T^2-2T\cos\phi)\\
f_2(\phi,T) &\equiv \int_0^1\frac{\mathrm{d}z}{z}\ln z\,\big(P(z,\phi,T)-1\big) = 2\,\Re((-1+i\cot\phi)\mathrm{Li}_2(e^{i\phi}T))\\
f_3(\phi,T,r) &\equiv \int_0^1\frac{\mathrm{d}z}{z}\ln(1+r^2z)P(z,\phi,T) = 2\Re[f_3(z,\phi,T,r)]\big|_{z=0}^{z=1},
\end{aligned} \tag{5.39}$$

with

$$f_3(z,\phi,T,r) = \ln r\Bigg[\ln(P(z,\phi,T)) + \cot\phi\Bigg(\tan^{-1}\frac{\sin\phi}{\cos\phi - Tz} - \tan^{-1}\frac{(1+Tz)\tan\frac{\phi}{2}}{Tz-1}\Bigg)\Bigg] - 2\mathrm{Li}_2(irz) + \frac{e^{i\phi}}{\sin\phi}\Bigg[\ln\left(\frac{i}{r}+z\right)\ln\left(1-\frac{T(1-irz)}{T-ire^{-i\phi}}\right) + \ln\left(-\frac{i}{r}+z\right)\ln\left(1-\frac{T(1+irz)}{T+ire^{-i\phi}}\right) + \mathrm{Li}_2\left(\frac{T(1-irz)}{T-ire^{-i\phi}}\right) + \mathrm{Li}_2\left(\frac{T(1+irz)}{T+ire^{-i\phi}}\right)\Bigg]. \tag{5.40}$$

5.2.3 $S^i_{ij}(\phi)$

Using the same variable transformations as for $S_{ij}(\tau^i_a)$, we find

$$S^i_{ij}(\phi) = \frac{\alpha_s}{4\pi}\mathbf{T}_i\cdot\mathbf{T}_j\frac{1}{\Gamma(1-\epsilon)}\left(\frac{e^{\gamma_E}\mu^2}{4\Lambda^2 r^2}\right)^{\epsilon}\frac{1}{\epsilon^2}G^i_{ij}(\phi)\,, \tag{5.41}$$

where

$$G^i_{ij}(\phi) = 4n_i\cdot n_j\epsilon^2 4^{\epsilon} r^{2(1+\epsilon)}\int_0^1 \mathrm{d}z\int_1^{\infty}\mathrm{d}x\frac{(x-1)^{-1-\epsilon}}{x-1+r^2z(x+1)}G(x,z,\phi)\,, \tag{5.42}$$

with

$$G(x,z,\phi) \equiv \frac{x^{2\epsilon}}{(x+1)^{1+\epsilon}}\frac{1}{(x-1)(1+r^2z)+n_i\cdot n_j/P(z,\phi,T)}\,. \tag{5.43}$$

We then split G^i_{ij} as

$$G^i_{ij}(\phi) = G^{i\,(1)}_{ij}(\phi) + G^{i\,(2)}_{ij}(\phi) \tag{5.44}$$

where

$$G^{i\,(1)}_{ij}(\phi) = -F^{i\,(1)}_{ij}(\phi) + \mathcal{O}(\epsilon^3)\,, \tag{5.45}$$

and

$$\begin{aligned} G^{i\,(2)}_{ij}(\phi) &= 4n_i\cdot n_j\epsilon^2 4^{\epsilon} r^{2+2\epsilon}\int_0^1\mathrm{d}z\int_1^{\infty}\mathrm{d}x\frac{(x-1)^{-1-\epsilon}}{x-1+r^2z(x+1)}G(1,z,\phi) \\ &= \Gamma(1+\epsilon)\Gamma(1-\epsilon)\Big(1-\epsilon f_1(\phi,T_{ij}) + \epsilon^2\Big(f_2(\phi,T_{ij}) - f_3(\phi,T_{ij},r)\Big)\Big) \\ &\quad + \mathcal{O}(\epsilon^3)\,. \end{aligned} \tag{5.46}$$

5.2.4 $S_{ij}(\tau_a^i,\phi)+S_{ij}^i(\phi)$

Adding the results of the two previous subsections, we obtain

$$\begin{aligned} S_{ij}(\tau_a^i,\phi)+S_{ij}^i(\phi) = \frac{\alpha_s}{4\pi}\mathbf{T}_i\cdot\mathbf{T}_j\Bigg\{ &-\frac{2}{\Gamma(1-\epsilon)}\left(\frac{e^{\gamma_E}\mu^2 r^{2(1-a)}}{\omega^2}\right)^{\epsilon}\frac{1}{\epsilon}\frac{1}{1-a}(\tau_a^i)^{-1-2\epsilon} \\ &+\frac{1}{\Gamma(1-\epsilon)}\left(\frac{e^{\gamma_E}\mu^2}{4r^2\Lambda^2}\right)^{\epsilon}\frac{1}{\epsilon^2}\delta(\tau_a^i)-f_1(\phi,T_{ij})\Bigg[\left(\frac{1}{\tau_a^i}\right)_+ \\ &+\ln\frac{\omega^2}{4\Lambda^2 r^{2(2-a)}}\delta(\tau_a^i)\Bigg]+\delta(\tau_a^i)\Big(2(2-a)f_2(\phi,T_{ij})-2f_3(\phi,T_{ij},r^2)\Big)\Bigg\}. \end{aligned} \tag{5.47}$$

Using the fact that

$$\begin{aligned} \int_0^{2\pi}\frac{\mathrm{d}\phi}{2\pi}f_1(\phi,T) &= -\ln(1-T^2) \\ \int_0^{2\pi}\frac{\mathrm{d}\phi}{2\pi}f_2(\phi,T) &= \frac{1}{4}\ln^2(1-T)+\frac{1}{2}\mathrm{Li}_2\left(\frac{-T^2}{1-T^2}\right) \\ \int_0^{2\pi}\frac{\mathrm{d}\phi}{2\pi}f_3(\phi,T,A) &= \mathrm{Li}_2\left(\frac{-T^2}{1-T^2}\right)-\mathrm{Li}_2\left(-\frac{T^2+A}{1-T^2}\right) \end{aligned} \tag{5.48}$$

we obtain agreement with the result of $S_{ij}(\tau_a^i)+S_{ij}^i$ in [66] when $\omega(\phi)$ and $a(\phi)$ are constant in ϕ.

5.2.5 $S_{ij}(\tau_a^k,\phi)$

We find

$$S_{ij}(\tau_a^k,\phi) = -\frac{\alpha_s}{2\pi}\mathbf{T}_i\cdot\mathbf{T}_j\frac{1}{\Gamma(1-\epsilon)}\left(\frac{e^{\gamma_E}\mu^2 r^{2(1-a)}}{\omega^2}\right)^{\epsilon}(\tau_a^i)^{-1-2\epsilon}I_{ij}^k(\phi)\,, \tag{5.49}$$

where

$$I_{ij}^k(\phi) = -\frac{n_i\cdot n_j\epsilon}{r^{-2+2(1-a)\epsilon}}\int_0^1\mathrm{d}z\int_1^\infty\mathrm{d}x(x^2-1)^{-1-\epsilon}I(x,z,\phi)\,, \tag{5.50}$$

with

$$\begin{aligned} I(x,z,\phi) \equiv (1+r^2z)^{-2\epsilon}&\frac{(x-1+r^2z(x+1))^{\epsilon(2-a)}}{(x-1)(1+r^2z)+n_i\cdot n_k/P(z,\phi,T_i)} \\ &\times\frac{(x+1+r^2z(x-1))^{\epsilon a}}{(x-1)(1+r^2z)+n_j\cdot n_k/P(z,\beta-\phi,T_j)}\,. \end{aligned} \tag{5.51}$$

As before, we split up $I^k_{ij}(\phi)$ as

$$I^k_{ij}(\phi) = I^{k\,(1)}_{ij}(\phi) + I^{k\,(2)}_{ij}(\phi) \tag{5.52}$$

where

$$I^{k\,(1)}_{ij}(\phi) = -n_i{\cdot}n_j\epsilon \int_0^1 \mathrm{d}z \int_1^\infty \mathrm{d}x \frac{[I(x,z,\phi) - I(1,z,\phi)]|_{\epsilon=0}}{(x^2-1)} + \mathcal{O}(\epsilon^2)\,, \tag{5.53}$$

and

$$\begin{aligned} I^{k\,(2)}_{ij}(\phi) &= 2r^{2(1+\epsilon)} \frac{n_i{\cdot}n_j}{n_i{\cdot}n_k n_j{\cdot}n_k} \int_0^1 \mathrm{d}z \int_1^\infty \mathrm{d}x \frac{(x^2-1)^{-1-\epsilon}}{x-1+r^2 z(x+1)} I(1,z,\phi) \\ &= (1+2\epsilon\ln r) g_1(\phi, T_i, T_j, \beta_{ijk}) + \epsilon((2-a) g_2(\phi, T_i, T_j, \beta_{ijk}, 0) \\ &\quad - 2g_2(\phi, T_i, T_j, \beta_{ijk}, r^{-1})) + \mathcal{O}(\epsilon^2)\,, \end{aligned} \tag{5.54}$$

where

$$\begin{aligned} g_1(\phi, T_1, T_2, \beta) &\equiv 2r^2 \frac{n_i{\cdot}n_j}{n_i{\cdot}n_k n_j{\cdot}n_k} \int_0^1 \mathrm{d}z P(z,\phi,T_1) P(z,\beta-\phi,T_2) \\ &= \frac{h_1(\phi,T_1,T_2,\beta) + h_1(\beta-\phi,T_2,T_1,\beta)}{T_i^2 + T_j^2 - 2T_iT_j\cos(\beta-2\phi)} \\ g_2(\phi, T_1, T_2, \beta, A) &\equiv 2r^2 \frac{n_i{\cdot}n_j}{n_i{\cdot}n_k n_j{\cdot}n_k} \int_0^1 \mathrm{d}z \ln(A^2+z)\, P(z,\phi,T_1) P(z,\beta-\phi,T_2) \\ &= 2\Re\left[\frac{h_2(z,\phi,T_1,T_2,\beta,A) - h_2(z,\beta-\phi,T_2,T_1,\beta,A)}{T_1 e^{-i(\beta/2-\phi)} - T_2 e^{i(\beta/2-\phi)}}\right]\Bigg|_{z=0}^{z=1}, \end{aligned} \tag{5.55}$$

where

$$\begin{aligned} h_1(\phi, T_1, T_2, \beta) &\equiv 2\csc\phi((T_1^2+T_2^2)\cos\phi - 2T_1T_2\cos(\beta-\phi)) \\ &\quad (\tan^{-1}\cot\phi - \tan^{-1}(\cot - T_1\csc\phi)) + (T_1^2 - T_2^2)\ln[1+T_1^2 - 2T_1\cos\phi] \end{aligned} \tag{5.56}$$

and

$$\begin{aligned} h_2(z,\phi,T_1,T_2,\beta,A) &= \frac{i\csc\phi}{T_1 e^{i\beta/2} - T_2 e^{-i\beta/2}} \Bigg[\ln(z+iA)\ln\left(1 - \frac{T_1(A-iz)}{AT_1 - ie^{-i\phi}}\right) \\ &+ \mathrm{Li}_2\left(\frac{T_1(A-iz)}{AT_1 - ie^{-i\phi}}\right) + \ln(z-iA)\ln\left(1 - \frac{T_1(A+iz)}{AT_1 + ie^{-i\phi}}\right) + \mathrm{Li}_2\left(\frac{T_1(A+iz)}{AT_1 + ie^{-i\phi}}\right)\Bigg] \end{aligned} \tag{5.57}$$

and we used

$$2r^2 \frac{n_i{\cdot}n_j}{n_i{\cdot}n_k n_j{\cdot}n_k} = T_i^2 + T_j^2 - 2T_iT_j\cos\beta\,. \tag{5.58}$$

5.2.6 $S_{ij}^k(\phi)$

We find for $S_{ij}^k(\phi)$

$$S_{ij}^k(\phi) = \frac{\alpha_s}{4\pi}\mathbf{T}_i\cdot\mathbf{T}_j\frac{1}{\Gamma(1-\epsilon)}\left(\frac{e^{\gamma_E}\mu^2}{4\Lambda^2 r^2}\right)^{\epsilon}\frac{1}{\epsilon}J_{ij}^k(\phi)\,, \tag{5.59}$$

where

$$J_{ij}^k(\phi) = 4n_i\cdot n_j\epsilon 4^{\epsilon}r^{2(1+\epsilon)}\int_0^1 \mathrm{d}z\int_1^{\infty}\mathrm{d}x(x^2-1)^{-1-\epsilon}J(x,z,\phi)\,, \tag{5.60}$$

with

$$\begin{aligned} J(x,z,\phi) \equiv x^{2\epsilon}&\frac{1}{(x-1)(1+r^2z)+n_i\cdot n_k/P(z,\phi,T_i)} \\ &\frac{1}{(x-1)(1+r^2z)+n_j\cdot n_k/P(z,\phi-\beta,T_j)}\,. \end{aligned} \tag{5.61}$$

We then split J_{ij}^k as

$$J_{ij}^k(\phi) = J_{ij}^{k\,(1)}(\phi) + J_{ij}^{k\,(2)}(\phi) \tag{5.62}$$

where

$$J_{ij}^{k\,(1)}(\phi) = -G_{ij}^{k\,(1)}(\phi)\,, \tag{5.63}$$

and

$$\begin{aligned} G_{ij}^{k\,(2)}(\phi) &= 4n_i\cdot n_j\epsilon^2 4^{\epsilon}r^{2+2\epsilon}\int_0^1\mathrm{d}z\int_1^{\infty}\mathrm{d}x\frac{(x-1)^{-1-\epsilon}}{x-1+r^2z(x+1)}J(1,z,\phi) \\ &= -2r^{2(1+\epsilon)}\frac{n_i\cdot n_j}{n_i\cdot n_k n_j\cdot n_k}g_1(\phi,T_1,T_2,\beta)\,. \end{aligned} \tag{5.64}$$

5.2.7 $S_{ij}(\tau_a^k,\phi) + S_{ij}^k(\phi)$

Adding the above results, we obtain

$$\begin{aligned} S_{ij}(\tau_a^k,\phi) + S_{ij}^k(\phi) =& \frac{\alpha_s}{4\pi}\mathbf{T}_i\cdot\mathbf{T}_j\Bigg\{g_1(\phi,T_1,T_2,\beta)\Bigg[-\left(\frac{2}{\tau_a^i}\right)_+ + \ln\frac{\omega^2}{4\Lambda^2 r^{2a}}\delta(\tau_a^i)\Bigg] \\ &+ \delta(\tau_a^i)\Big((2-a)g_2(\phi,T_1,T_2,\beta,0) - 2g_2(\phi,T_1,T_2,\beta,r^{-2})\Big)\Bigg\}\,. \end{aligned} \tag{5.65}$$

This agrees with the result of $S_{ij}(\tau_a^k) + S_{ij}^k$ in [66] for constant $\omega(\phi)$ and $a(\phi)$, as can be seen via the identities[4]

$$\begin{aligned}
\int_0^{2\pi} \frac{\mathrm{d}\phi}{2\pi} g_1(\phi, T_1, T_2, \beta) &= \ln\left(\frac{1 + T_1^2 T_2^2 - 2T_1 T_2 \cos\beta}{(T_1^2 - 1)(T_2^2 - 1)}\right) \\
\int_0^{2\pi} \frac{\mathrm{d}\phi}{2\pi} g_2(\phi, T_1, T_2, \beta, A) &= -\Bigg\{ g(T_1^{-1}, A) + g(T_2^{-1}, A) - 2\ln(A+1)\ln(T_1 T_2) \\
&\quad + 2\Re\left[\mathrm{Li}_2\left(\frac{1 - T_1 T_2 e^{i\beta}}{1 + A T_1 T_2 e^{i\beta}}\right) - \mathrm{Li}_2\left(\frac{1}{1 + A T_1 T_2 e^{i\beta}}\right)\right. \\
&\quad \left.\left. + \ln(1 - T_1 T_2 e^{i\beta}) \ln\frac{T_1 T_2 e^{i\beta}}{1 + A T_1 T_2 e^{i\beta}}\right]\right\},
\end{aligned} \tag{5.66}$$

where

$$\begin{aligned}
g(t, A) \equiv \mathrm{Li}_2\left(\frac{t^2}{t^2 + A}\right) - \mathrm{Li}_2\left(\frac{t^2 - 1}{t^2 + A}\right) + \ln(t^2 - 1)\ln(r + t^2) \\
- \ln(t^2)\ln((A+1)(A + t^2))\,.
\end{aligned} \tag{5.67}$$

[4]The functions on the right-hand side of Equation (5.66) correspond with the functions $f_{1,2}$ of [66].

Chapter 6

Conclusion

The LHC era is an incredibly exciting time for particle physics. Already we've seen strong hints suggesting that the Higgs boson will be found in the near future and hopefully there will be many more discoveries in the years to come. However, almost any new physics will be found in conjunction with (or buried beneath a background of) Standard Model jets. In order to make the most of the data from the LHC, it is imperative that we do as much as possible to understand jet physics.

In this thesis, we have presented several new techniques that will hopefully increase our understand of jets, especially in the context of collider physics. In Chapter 2, we derived a factorization theorem for the production of N jets, together with any number of non-strongly interacting particles, such as electroweak gauge bosons. This factorization theorem allows us to write the physical cross section in terms of a convolution of parton distribution functions, a hard function, and jet functions for each observed jet and a soft function describing among other things the color recombination between the initial and final state partons. Both the jet and the soft functions depend on the precise form of the jet algorithm chosen.

The main new ingredient in this factorization theorem is a soft function that depends on a timelike component of the soft momentum outside of the observed jets, and the lightlike component of the soft momentum in a given jet. This function is directly related to the soft function first proposed and calculated for the case of jet production in e^+e^- collisions in [66, 65]. This soft function allows us to interpolate between the soft function arising for final states without observed jets (which depends only on a timelike component of the soft momentum) and the soft function for completely inclusive jet production (which depends only on the lightlike component of the soft momentum).

We have derived the UV divergent parts of all ingredients of the factorization theorem to $\mathcal{O}(\alpha_s)$. These were then used to show that the combination of all ingredients of the factorization theorem is independent of the arbitrary factorization scale μ, and therefore the derived results satisfy the nontrivial requirement of consistency. While consistency was shown in this work only in the true hadronic endpoint, we have kept

the kinematics general enough (in particular allowing for a nonzero overall boost) to allow for a generalization of our results to the case where the steepness of the parton luminosities force events to be close to the partonic threshold. This result, which is by far more interesting phenomenologically, is discussed in Chapter 3.

Our results can be used to explicitly resum threshold logarithms to NLL accuracy (in the log-counting convention of [35]) for any process in hadron collisions with any number of jets and non-strongly interacting particles in the final state. The technology of going from the anomalous dimensions we present here to explicit resummed distributions is well-known. Beyond one jet, in addition to the standard resummation methods, we need the matrices $\mathbf{T}_i \cdot \mathbf{T}_j$, but these have been computed for many processes (see, e.g., [55, 86, 85, 64, 106, 107]), including all $2 \to 2$ and $2 \to 3$ partonic channels. The only other ingredient needed to obtain a NLL distribution is the Born matrix element.

In addition, if our results are extended to include two-loop results of the anomalous dimensions together with the full algorithm-dependent one-loop finite parts, NNLL results can be obtained for all processes for which the virtual NLO corrections are known. Together with recent advances in calculations of NLO cross sections (e.g., W^+W^-j [45, 63] and $Wjjj$ [38]), this would have a significant impact on the precision frontier of predictions at the LHC.

In Chapter 3, we presented a model-independent, quantitative measure of the power corrections to partonic threshold resummation. Previously, any quantitative study of the power corrections associated with applying hadronic threshold resummation away from the true endpoint necessitated simplified assumptions about the functional form of the pdfs. The expansion parameter of threshold resummation is given by a parameter λ^2, which can be defined unambiguously through integrals over pdfs. In SCET, the parameter λ^2 is related to the scale of soft and collinear radiation, such that the scales μ_c and μ_s can be chosen after convolving the partonic cross section with the pdfs. This allows us to avoid integrating through regions where the perturbative expansion is ill-defined, without having to define an arbitrary procedure for determining scales after integration. We have shown analytically that the value of λ approaches zero either in the true hadronic endpoint or in the limit of infinitely steep pdfs. Our numerical results indicate that while threshold resummation can be justified away from the region where $1 - \tau \ll 1$, we expect the corrections to become sizable for $\tau < 0.05 - 0.1$.

Most QCD resummation requires the calculation of a soft function, which describes the emission of low energy radiation from high energy partons. In Chapter 4, we demonstrated a new method that would allow for the calculation of soft functions with highly complex phase space constraints, using currently available calculations as a subtraction. At one loop, subtractions can be constructed that allow for new soft functions to be calculated numerically, using previously derived analytical results. Using only calculations that exist in the literature, the soft function can be calculated for a number of phenomenologically relevant observables and algorithms, including

jet shapes found using η-ϕ algorithms and N-jettiness, for arbitrary N. In order to calculate the soft function for most current measurements at hadron colliders, both Type I and Type II jets are required. We should also note that a similar argument can be used to calculate jet functions in the presence of algorithms; however, this is generally less relevant as algorithm corrections tend to be power suppressed.

Finally, in Chapter 5 we introduced a new regularization scheme (undemocratic regularization) for on-shell, d-dimensional integrals. Based on the work of 't Hooft and Veltman, this scheme provides an intuitive way of relating physical angles to angles of integration in the d-dimensional space of loop momenta. Similar relations in previous schemes are derived by studying the mapping onto the new scheme.

While we show that the undemocratic scheme is equivalent to previous schemes, we demonstrate that it is particularly well suited to calculate jet observables that depend on the azimuthal angle with respect to the jet direction. We demonstrate this by defining a new variable, ϕ-angularity, and comparing parts of the calculation for a specific ϕ-angularity. We then calculate the soft function for an arbitrary ϕ-angularity in terms of finite, one-dimenisonal numerical integrals.

Bibliography

[1] F. Abe et al. A Measurement of jet shapes in $p\bar{p}$ collisions at $\sqrt{s} = 1.8$ TeV. *Phys. Rev. Lett.*, 70:713–717, 1993.

[2] Valentin Ahrens, Thomas Becher, Matthias Neubert, and Li Lin Yang. Origin of the Large Perturbative Corrections to Higgs Production at Hadron Colliders. *Phys. Rev.*, D79:033013, 2009.

[3] Valentin Ahrens, Thomas Becher, Matthias Neubert, and Li Lin Yang. Renormalization-Group Improved Prediction for Higgs Production at Hadron Colliders. *Eur. Phys. J.*, C62:333–353, 2009.

[4] R. Akhoury and I.Z. Rothstein. The Extraction of V(ub) from inclusive B decays and the resummation of end point logs. *Phys.Rev.*, D54:2349–2362, 1996.

[5] Leandro G. Almeida et al. Substructure of high-p_T Jets at the LHC. *Phys. Rev.*, D79:074017, 2009.

[6] Guido Altarelli, N. Cabibbo, G. Corbo, L. Maiani, and G. Martinelli. Leptonic Decay of Heavy Flavors: A Theoretical Update. *Nucl. Phys.*, B208:365–380, 1982.

[7] Charalampos Anastasiou, Gunther Dissertori, and Fabian Stockli. NNLO QCD predictions for the H -¿ WW -¿ l l nu nu signal at the LHC. *JHEP*, 09:018, 2007.

[8] Charalampos Anastasiou, Lance J. Dixon, Kirill Melnikov, and Frank Petriello. Dilepton rapidity distribution in the Drell-Yan process at NNLO in QCD. *Phys. Rev. Lett.*, 91:182002, 2003.

[9] Charalampos Anastasiou, Lance J. Dixon, Kirill Melnikov, and Frank Petriello. High precision QCD at hadron colliders: Electroweak gauge boson rapidity distributions at NNLO. *Phys. Rev.*, D69:094008, 2004.

[10] Charalampos Anastasiou and Kirill Melnikov. Higgs boson production at hadron colliders in NNLO QCD. *Nucl. Phys.*, B646:220–256, 2002.

[11] Charalampos Anastasiou, Kirill Melnikov, and Frank Petriello. Higgs boson production at hadron colliders: Differential cross sections through next-to-next-to-leading order. *Phys. Rev. Lett.*, 93:262002, 2004.

[12] Charalampos Anastasiou, Kirill Melnikov, and Frank Petriello. Fully differential Higgs boson production and the di- photon signal through next-to-next-to-leading order. *Nucl. Phys.*, B724:197–246, 2005.

[13] David Appell, George Sterman, and Paul B. Mackenzie. SOFT GLUONS AND THE NORMALIZATION OF THE DRELL-YAN CROSS- SECTION. *Nucl. Phys.*, B309:259, 1988.

[14] Christian M. Arnesen, Joydip Kundu, and Iain W. Stewart. Constraint equations for heavy-to-light currents in SCET. *Phys. Rev.*, D72:114002, 2005.

[15] S. Mert Aybat, Lance J. Dixon, and George Sterman. The two-loop soft anomalous dimension matrix and resummation at next-to-next-to leading pole. *Phys. Rev.*, D74:074004, 2006.

[16] Richard D. Ball et al. A first unbiased global NLO determination of parton distributions and their uncertainties. *Nucl. Phys.*, B838:136–206, 2010.

[17] Andrea Banfi, Mrinal Dasgupta, and Yazid Delenda. Azimuthal decorrelations between QCD jets at all orders. *Phys.Lett.*, B665:86–91, 2008.

[18] Christian W. Bauer, Cheng-Wei Chiang, Sean Fleming, Adam K. Leibovich, and Ian Low. Resumming the color-octet contribution to radiative Upsilon decay. *Phys. Rev.*, D64:114014, 2001.

[19] Christian W. Bauer, Nicholas Daniel Dunn, and Andrew Hornig. Factorization of Boosted Multijet Processes for Threshold Resummation. *Phys. Rev.*, D82:054012, 2010.

[20] Christian W. Bauer, Nicholas Daniel Dunn, and Andrew Hornig. On the effectiveness of threshold resummation away from hadronic endpoint. 2010.

[21] Christian W. Bauer, Nicholas Daniel Dunn, and Andrew Hornig. Subtractions for SCET Soft Functions. 2011.

[22] Christian W. Bauer, Sean Fleming, Christopher Lee, and George Sterman. Factorization of e+e- Event Shape Distributions with Hadronic Final States in Soft Collinear Effective Theory. *Phys. Rev.*, D78:034027, 2008.

[23] Christian W. Bauer, Sean Fleming, and Michael E. Luke. Summing Sudakov logarithms in $B \to X_s$ gamma in effective field theory. *Phys. Rev.*, D63:014006, 2000.

[24] Christian W. Bauer, Sean Fleming, Dan Pirjol, Ira Z. Rothstein, and Iain W. Stewart. Hard scattering factorization from effective field theory. *Phys. Rev.*, D66:014017, 2002.

[25] Christian W. Bauer, Sean Fleming, Dan Pirjol, and Iain W. Stewart. An effective field theory for collinear and soft gluons: Heavy to light decays. *Phys. Rev.*, D63:114020, 2001.

[26] Christian W. Bauer, Andrew Hornig, and Frank J. Tackmann. Factorization for generic jet production. *Phys. Rev.*, D79:114013, 2009.

[27] Christian W. Bauer, Christopher Lee, Aneesh V. Manohar, and Mark B. Wise. Enhanced nonperturbative effects in Z decays to hadrons. *Phys. Rev.*, D70:034014, 2004.

[28] Christian W. Bauer and Aneesh V. Manohar. Shape function effects in $B \to X_s\gamma$ and $B \to X_u l\bar{\nu}$ decays. *Phys. Rev.*, D70:034024, 2004.

[29] Christian W. Bauer, Aneesh V. Manohar, and Mark B. Wise. Enhanced nonperturbative effects in jet distributions. *Phys. Rev. Lett.*, 91:122001, 2003.

[30] Christian W. Bauer, Dan Pirjol, and Iain W. Stewart. Soft-collinear factorization in effective field theory. *Phys. Rev.*, D65:054022, 2002.

[31] Christian W. Bauer and Iain W. Stewart. Invariant operators in collinear effective theory. *Phys. Lett.*, B516:134–142, 2001.

[32] Thomas Becher and Matthias Neubert. Infrared singularities of scattering amplitudes in perturbative QCD. *Phys.Rev.Lett.*, 102:162001, 2009.

[33] Thomas Becher and Matthias Neubert. On the Structure of Infrared Singularities of Gauge-Theory Amplitudes. *JHEP*, 0906:081, 2009.

[34] Thomas Becher, Matthias Neubert, and Ben D. Pecjak. Factorization and momentum-space resummation in deep-inelastic scattering. *JHEP*, 01:076, 2007.

[35] Thomas Becher, Matthias Neubert, and Gang Xu. Dynamical Threshold Enhancement and Resummation in Drell-Yan Production. *JHEP*, 07:030, 2008.

[36] Thomas Becher and Matthew D. Schwartz. A Precise determination of α_s from LEP thrust data using effective field theory. *JHEP*, 07:034, 2008.

[37] Thomas Becher and Matthew D. Schwartz. Direct photon production with effective field theory. 2009.

[38] C. F. Berger et al. Next-to-Leading Order QCD Predictions for W+3-Jet Distributions at Hadron Colliders. *Phys. Rev.*, D80:074036, 2009.

[39] Carola F. Berger, Tibor Kucs, and George Sterman. Event shape / energy flow correlations. *Phys. Rev.*, D68:014012, 2003.

[40] Edmond L. Berger and Harry Contopanagos. Perturbative gluon resummation of the top quark production cross-section. *Phys. Lett.*, B361:115–120, 1995.

[41] Ikaros I. Y. Bigi, Mikhail A. Shifman, N. G. Uraltsev, and A. I. Vainshtein. On the motion of heavy quarks inside hadrons: Universal distributions and inclusive decays. *Int. J. Mod. Phys.*, A9:2467–2504, 1994.

[42] Roberto Bonciani, Stefano Catani, Michelangelo L. Mangano, and Paolo Nason. Sudakov resummation of multiparton QCD cross sections. *Phys. Lett.*, B575:268–278, 2003.

[43] S. W. Bosch, B. O. Lange, M. Neubert, and Gil Paz. Factorization and shape-function effects in inclusive B-meson decays. *Nucl. Phys.*, B699:335–386, 2004.

[44] Oliver Brein, Abdelhak Djouadi, and Robert Harlander. NNLO QCD corrections to the Higgs-strahlung processes at hadron colliders. *Phys. Lett.*, B579:149–156, 2004.

[45] John M. Campbell, R. Keith Ellis, and David L. Rainwater. Next-to-leading order QCD predictions for W + 2jet and Z + 2jet production at the CERN LHC. *Phys. Rev.*, D68:094021, 2003.

[46] S. Catani, Yuri L. Dokshitzer, M. Olsson, G. Turnock, and B. R. Webber. New clustering algorithm for multi - jet cross-sections in e+ e- annihilation. *Phys. Lett.*, B269:432–438, 1991.

[47] S. Catani and M. H. Seymour. A general algorithm for calculating jet cross sections in NLO QCD. *Nucl. Phys.*, B485:291–419, 1997.

[48] S. Catani and L. Trentadue. Resummation of the QCD Perturbative Series for Hard Processes. *Nucl. Phys.*, B327:323, 1989.

[49] S. Catani and L. Trentadue. Comment on QCD exponentiation at large x. *Nucl. Phys.*, B353:183–186, 1991.

[50] Stefano Catani, Leandro Cieri, Giancarlo Ferrera, Daniel de Florian, and Massimiliano Grazzini. Vector boson production at hadron colliders: a fully exclusive QCD calculation at NNLO. *Phys. Rev. Lett.*, 103:082001, 2009.

[51] Stefano Catani, Michelangelo L. Mangano, and Paolo Nason. Sudakov resummation for prompt photon production in hadron collisions. *JHEP*, 07:024, 1998.

[52] Stefano Catani, Michelangelo L. Mangano, Paolo Nason, and Luca Trentadue. The Resummation of Soft Gluon in Hadronic Collisions. *Nucl. Phys.*, B478:273–310, 1996.

[53] Pan-ying Chen, Ahmad Idilbi, and Xiang-dong Ji. QCD factorization for deep-inelastic scattering at large Bjorken x(B) approx. 1-O(Lambda(QCD)/Q). *Nucl. Phys.*, B763:183–197, 2007.

[54] William Man-Yin Cheung, Michael Luke, and Saba Zuberi. Phase Space and Jet Definitions in SCET. 2009.

[55] Jui-yu Chiu, Andreas Fuhrer, Randall Kelley, and Aneesh V. Manohar. Factorization Structure of Gauge Theory Amplitudes and Application to Hard Scattering Processes at the LHC. 2009.

[56] John C. Collins and Davison E. Soper. Back-To-Back Jets in QCD. *Nucl. Phys.*, B193:381, 1981.

[57] John C. Collins and Davison E. Soper. The Theorems of Perturbative QCD. *Ann. Rev. Nucl. Part. Sci.*, 37:383–409, 1987.

[58] John C. Collins, Davison E. Soper, and George Sterman. Factorization of Hard Processes in QCD. *Adv. Ser. Direct. High Energy Phys.*, 5:1–91, 1988.

[59] John C. Collins, Davison E. Soper, and George F. Sterman. ALL ORDER FACTORIZATION FOR DRELL-YAN CROSS-SECTIONS. *Phys.Lett.*, B134:263, 1984.

[60] John C. Collins and George Sterman. Soft partons in qcd. *Nucl. Phys.*, B185:172, 1981.

[61] H. Contopanagos and G. Sterman. Normalization of the Drell-Yan cross-section in QCD. *Nucl. Phys.*, B400:211–224, 1993.

[62] M. Dasgupta and G. P. Salam. Resummation of non-global qcd observables. *Phys. Lett.*, B512:323–330, 2001.

[63] S. Dittmaier, S. Kallweit, and P. Uwer. NLO QCD corrections to WW+jet production at hadron colliders. *Phys. Rev. Lett.*, 100:062003, 2008.

[64] Yu. L. Dokshitzer and G. Marchesini. Hadron collisions and the fifth form factor. *Phys. Lett.*, B631:118–125, 2005.

[65] Stephen D. Ellis, Andrew Hornig, Christopher Lee, Christopher K. Vermilion, and Jonathan R. Walsh. Consistent Factorization of Jet Observables in Exclusive Multijet Cross-Sections. 2009.

[66] Stephen D. Ellis, Andrew Hornig, Christopher Lee, Christopher K. Vermilion, and Jonathan R. Walsh. Jet Shapes and Jet Algorithms in SCET. 2010.

[67] Stephen D. Ellis, Zoltan Kunszt, and Davison E. Soper. Jets in hadron colliders at order alpha-s**3. *Conf. Proc.*, C910725V1:417–418, 1991.

[68] Stephen D. Ellis, Zoltan Kunszt, and Davison E. Soper. Jets at hadron colliders at order $\alpha - s^{3:}$ A Look inside. *Phys. Rev. Lett.*, 69:3615–3618, 1992.

[69] Adam F. Falk, Elizabeth Ellen Jenkins, Aneesh V. Manohar, and Mark B. Wise. QCD Corrections and the Endpoint of the Lepton Spectrum in Semileptonic B Decays. *Phys. Rev.*, D49:4553–4559, 1994.

[70] Sean Fleming, Andre H. Hoang, Sonny Mantry, and Iain W. Stewart. Jets from Massive Unstable Particles: Top-Mass Determination. *Phys. Rev.*, D77:074010, 2008.

[71] Sean Fleming, Andre H. Hoang, Sonny Mantry, and Iain W. Stewart. Top Jets in the Peak Region: Factorization Analysis with NLL Resummation. *Phys. Rev.*, D77:114003, 2008.

[72] Jason Gallicchio and Matthew D. Schwartz. Seeing in Color: Jet Superstructure. *Phys.Rev.Lett.*, 105:022001, 2010.

[73] Einan Gardi and Lorenzo Magnea. Factorization constraints for soft anomalous dimensions in QCD scattering amplitudes. *JHEP*, 0903:079, 2009.

[74] S.L. Glashow. Partial Symmetries of Weak Interactions. *Nucl.Phys.*, 22:579–588, 1961.

[75] Massimiliano Grazzini. NNLO predictions for the Higgs boson signal in the H-¿WW- ¿lnu lnu and H-¿ZZ-¿4l decay channels. *JHEP*, 02:043, 2008.

[76] D.J. Gross and Frank Wilczek. Ultraviolet Behavior of Nonabelian Gauge Theories. *Phys.Rev.Lett.*, 30:1343–1346, 1973.

[77] B. Guberina, R.D. Peccei, and R. Ruckl. DIMENSIONAL REGULARIZATION TECHNIQUES AND THEIR USES IN CALCULATING INFRARED SAFE WEAK DECAY PROCESSES. *Nucl.Phys.*, B171:333, 1980.

[78] Robert V. Harlander and William B. Kilgore. Next-to-next-to-leading order Higgs production at hadron colliders. *Phys. Rev. Lett.*, 88:201801, 2002.

[79] Anson Hook, Martin Jankowiak, and Jay G. Wacker. Jet Dipolarity: Top Tagging with Color Flow. 2011.

[80] Andrew Hornig, Christopher Lee, and Grigory Ovanesyan. Effective Predictions of Event Shapes: Factorized, Resummed, and Gapped Angularity Distributions. *JHEP*, 05:122, 2009.

[81] Andrew Hornig, Christopher Lee, and Grigory Ovanesyan. Infrared Safety in Factorized Hard Scattering Cross- Sections. *Phys. Lett.*, B677:272–277, 2009.

[82] Ahmad Idilbi and Xiang-dong Ji. Threshold resummation for Drell-Yan process in soft- collinear effective theory. *Phys. Rev.*, D72:054016, 2005.

[83] Ahmad Idilbi, Xiang-dong Ji, Jian-Ping Ma, and Feng Yuan. Threshold resummation for Higgs production in effective field theory. *Phys. Rev.*, D73:077501, 2006.

[84] Ambar Jain, Massimiliano Procura, and Wouter J. Waalewijn. Fully-Unintegrated Parton Distribution and Fragmentation Functions at Perturbative k_T. 2011.

[85] Nikolaos Kidonakis, Gianluca Oderda, and George Sterman. Evolution of color exchange in QCD hard scattering. *Nucl. Phys.*, B531:365–402, 1998.

[86] Nikolaos Kidonakis, Gianluca Oderda, and George Sterman. Threshold resummation for dijet cross sections. *Nucl. Phys.*, B525:299–332, 1998.

[87] Nikolaos Kidonakis and George Sterman. Resummation for QCD hard scattering. *Nucl. Phys.*, B505:321–348, 1997.

[88] Gregory P. Korchemsky and George Sterman. Infrared factorization in inclusive B meson decays. *Phys. Lett.*, B340:96–108, 1994.

[89] Eric Laenen and Lorenzo Magnea. Threshold resummation for electroweak annihilation from DIS data. *Phys. Lett.*, B632:270–276, 2006.

[90] Eric Laenen, J. Smith, and W. L. van Neerven. All order resummation of soft gluon contributions to heavy quark production in hadron hadron collisions. *Nucl. Phys.*, B369:543–599, 1992.

[91] Eric Laenen, J. Smith, and W. L. van Neerven. Top quark production cross-section. *Phys. Lett.*, B321:254–258, 1994.

[92] Christopher Lee and George Sterman. Universality of nonperturbative effects in event shapes. 2006.

[93] Christopher Lee and George Sterman. Momentum flow correlations from event shapes: Factorized soft gluons and soft-collinear effective theory. *Phys. Rev.*, D75:014022, 2007.

[94] Adam K. Leibovich and I.Z. Rothstein. The Resummed rate for B –¿ X(s) gamma. *Phys.Rev.*, D61:074006, 2000.

[95] Aneesh V. Manohar. Deep inelastic scattering as $x \to 1$ using soft-collinear effective theory. *Phys. Rev.*, D68:114019, 2003.

[96] A. D. Martin, W. J. Stirling, R. S. Thorne, and G. Watt. Parton distributions for the LHC. *Eur. Phys. J.*, C63:189–285, 2009.

[97] S. Moch and A. Vogt. Higher-order soft corrections to lepton pair and Higgs boson production. *Phys. Lett.*, B631:48–57, 2005.

[98] K. Nakamura et al. Review of particle physics. *J.Phys.G*, G37:075021, 2010.

[99] H. David Politzer. Asymptotic Freedom: An Approach to Strong Interactions. *Phys.Rept.*, 14:129–180, 1974.

[100] J. Pumplin et al. New generation of parton distributions with uncertainties from global QCD analysis. *JHEP*, 07:012, 2002.

[101] V. Ravindran, J. Smith, and W. L. van Neerven. NNLO corrections to the total cross section for Higgs boson production in hadron hadron collisions. *Nucl. Phys.*, B665:325–366, 2003.

[102] Varun Sahni. Dark matter and dark energy. *Lect.Notes Phys.*, 653:141–180, 2004.

[103] Abdus Salam. Weak and Electromagnetic Interactions. *Conf.Proc.*, C680519:367–377, 1968.

[104] Gavin P. Salam. Towards Jetography. 2009.

[105] Matthew D. Schwartz. Resummation and NLO Matching of Event Shapes with Effective Field Theory. *Phys. Rev.*, D77:014026, 2008.

[106] Malin Sjodahl. Color evolution of $2 \to 3$ processes. *JHEP*, 12:083, 2008.

[107] Malin Sjodahl. Color structure for soft gluon resummation — a general recipe. *JHEP*, 09:087, 2009.

[108] Peter Zeiler Skands. Tuning Monte Carlo Generators: The Perugia Tunes. *Phys.Rev.*, D82:074018, 2010.

[109] George Sterman. SOFT GLUON CORRECTIONS TO SHORT DISTANCE HADRONIC CROSS- SECTIONS. *Phys. Lett.*, B179:281, 1986.

[110] George Sterman. Summation of Large Corrections to Short Distance Hadronic Cross-Sections. *Nucl. Phys.*, B281:310, 1987.

[111] George Sterman. Partons, factorization and resummation. . 1995.

[112] Iain W. Stewart and Frank J. Tackmann. Theory Uncertainties for Higgs and Other Searches Using Jet Bins. *Phys.Rev.*, D85:034011, 2012. 13 pages, 4 figures/ v2: journal version.

[113] Iain W. Stewart, Frank J. Tackmann, and Wouter J. Waalewijn. Factorization at the LHC: From PDFs to Initial State Jets. 2009.

[114] Gerard 't Hooft and M.J.G. Veltman. Regularization and Renormalization of Gauge Fields. *Nucl.Phys.*, B44:189–213, 1972.

[115] Michael Trott. Jets in effective theory: Summing phase space logs. *Phys. Rev.*, D75:054011, 2007.

[116] Steven Weinberg. A Model of Leptons. *Phys.Rev.Lett.*, 19:1264–1266, 1967.

[117] Steven Weinberg. Implications of Dynamical Symmetry Breaking. *Phys.Rev.*, D13:974–996, 1976.